Supporting Information for:

A Modular, Low Footprint and Scalable Flow Platform for the Expedient α-Aminohydroxylation of Enolizable Ketones

Victor-Emmanuel H. Kassin,[a] Romain Morodo,[a] Thomas Toupy,[a] Isaline Jacquemin,[a] Kristof Van Hecke,[b] Raphael Robiette[c] and Jean-Christophe M. Monbaliu[*,a]

[a] Center for Integrated Technology and Organic Synthesis, MolSys Research Unit, University of Liège, B-4000 Liège (Sart Tilman), Belgium

[b] XStruct, Departement of Chemistry, Ghent University, Krijgslaan 281 - S3, B-9000 Ghent, Belgium

[c] Institute of Condensed Matter and Nanosciences, Université catholique de Louvain, Place Louis Pasteur 1, 1348 Louvain-la-Neuve, Belgium

Table of Contents

1. Continuous flow setups

1.1 Microfluidic setups and parts

All microfluidic setups were assembled with commercially available parts.

1.1.1 Pumps

ThalesNano micro HPLC pumps (wetted parts: SS 316, ruby and sapphire) or Chemyx Fusion 6000 High Force syringe pumps equipped with stainless steel syringes (6 or 20 mL) with Dupont Kalrez Spectrum AS-568 O-rings (0.549 x 0.103”) were utilized to handle the liquid feeds.

1.1.2 PFA tubing and coils

PFA coil reactors and collection lines were constructed from PFA tubing (high purity PFA; 1.58 mm outer diameter, 750 µm internal diameter).

1.1.3 Connectors, ferrules and mixers

PEEK connectors, ferrules, static mixers and unions were purchased from IDEX/Upchurch (details in Table S1).

1.1.4 Check-valves

The check-valves inserted between the pumps and the reactors were purchased from IDEX/Upchurch Scientific (PEEK check-valve holder).

1.1.5 Back-pressure regulators

Spring loaded BPRs were purchased from IDEX/Upchurch Scientific (PEEK holder). Dome-type BPRs were purchased from Zaiput Flow Technologies (BPR-10). The dome-type BPR was connected to a compressed gas cylinder (nitrogen) to set the working pressure.

1.1.6 Liquid-liquid membrane separator

The in-line liquid-liquid separator was obtained from Zaiput Flow Technologies (SEP-10) and equipped with a hydrophobic membrane (1 µm pores).

1.1.7 Thermoregulatory devices

PFA coils reactors were thermoregulated in oil baths (Heidolph MR Hei-Tec equipped with Pt-1000 temperature sensors).

1.2 Mesofluidic scale setup (Corning® Advanced-Flow™ Low Flow reactor)

1.2.1 Pumps

The liquid feeds were handled with either ThalesNano micro HPLC or FLOM piston pumps.

1.2.2 Mesofluidic reactor

The lab scale setup was manufactured by Corning SAS (Corning® Advanced-Flow™ Low Flow reactor) and equipped with several fluidic modules connected in series (glass fluidic modules: 0.5 mL internal volume). See manuscript for detailed configuration.

1.2.3 Thermoregulatory devices

The reactor was maintained at reaction temperature with a LAUDA Integral XT 280 thermostat (THERM 180 thermofluid).

1.2.4 Back-pressure regulators

A dome-type BPR from Zaiput Flow Technologies (BPR-10) connected to a compressed gas cylinder (nitrogen) was utilized to set the working pressure.

1.2.5 Liquid-liquid membrane separator

The in-line liquid-liquid separator was obtained from Zaiput Flow Technologies (SEP-10) and equipped with a hydrophobic membrane (1 µm pores).

1.3 Pilot scale setup

1.3.1 Pumps

The liquid feeds were handled with a Corning® dosing line (HNP Mikrosysteme gear pumps).

1.3.2 Mesofluidic reactor

The pilot scale setup were manufactured by Corning SAS (Corning® Advanced-Flow™ G1 reactor and Corning® Advanced-Flow™ G1 SiC reactor) and equipped with several fluidic modules connected in series (glass fluidic modules: 8 mL internal volume; SiC fluidic modules: 8 mL internal volume). See manuscript for detailed configuration.

1.3.3 Thermoregulatory devices

The reactor was maintained at reaction temperature with a LAUDA Integral XT 280 thermostat (THERM 180 thermofluid).

1.3.4 Back-pressure regulators

A dome-type BPR from Zaiput Flow Technologies (BPR-1000) connected to a compressed gas cylinder (nitrogen) was utilized to set the working pressure.

1.3.5 Liquid-liquid membrane separator

The in-line liquid-liquid separator was obtained from Zaiput Flow Technologies (SEP-200) and equipped with a hydrophobic membrane (1 µm pores).

1.4 Part numbers & vendors

Standard fluidic elements and connectors were purchased from IDEX/Upchurch Scientific, Valco Instruments Co. Inc and Zaiput Flow Technologies (Table S1).

Table S1. Connectors, ferrules and unions

Item	Details	Vendor	Reference
Connectors	One-Piece Fingertight, PEEK, 10-32 Coned, for 1/16” OD	IDEX/ Upchurch Scientific	F-120X
	Super Flangeless Nuts, natural PEEK 1/4-28 thread for 1/16” OD tubing	IDEX/ Upchurch Scientific	P-255X
	Super Flangeless Ferrule Tefzel (ETFE) and SS ring 1/4-28 thread for 1/16” OD tubing	IDEX/ Upchurch Scientific	P-259X
Union	Natural polypropylene standard low pressure union 1/4-28	IDEX/ Upchurch Scientific	P-620
Mixer	T-mixer, natural PEEK 1/4-28 thread for 1/16" o.d. tubing, 0.02" through hole	IDEX/ Upchurch Scientific	P-712
Check-valve	Check-valve inline cartridge 1.5 psi	IDEX/ Upchurch Scientific	CV-3001
Spring-loaded BPR	BPR cartridge with gold coating (various set points)	IDEX/ Upchurch Scientific	P-763
Dome-type BPR	Dome-type BPR, metal-free, with adjustable set point	Zaiput Flow Techn.	BPR-10 BPR-1000
Membrane separator	Liquid-liquid membrane separator	Zaiput Flow Techn.	SEP-10 SEP-200
Tubing	High-purity PFA tubing, 1.58 mm outer diameter, 750 µm internal diameter	VICI (Valco Ins. Co. Inc.)	JR-T-4002-M25
	High-purity 1/8” and 1/4” PFA tubing, including appropriate PFA connections	Swagelok	PFA-T2-030-100 PFA-T4-047-100,

1.5 Detailed continuous flow setups

1.5.1 Continuous flow setup for the preparation of *tert*-butyl hypochlorite (***t*BuOCl**)

See manuscript for experimental details (Figure 4b).

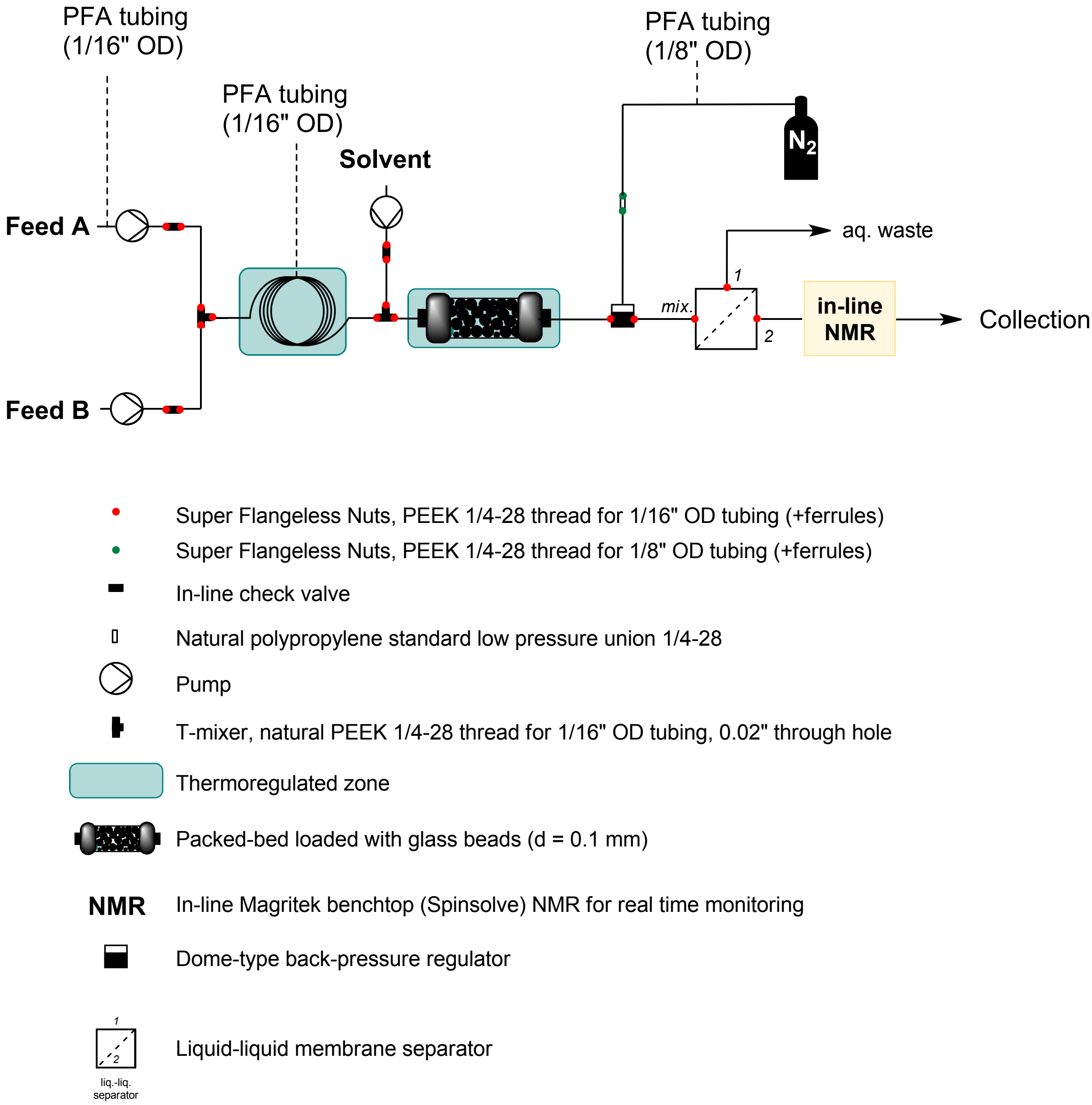

Figure S1. Detailed setup for the continuous flow preparation of ***t*BuOCl**

1.5.2 Continuous flow setup for the preparation of α-chloronitroso derivatives

See manuscript for experimental details (Figure 5b).

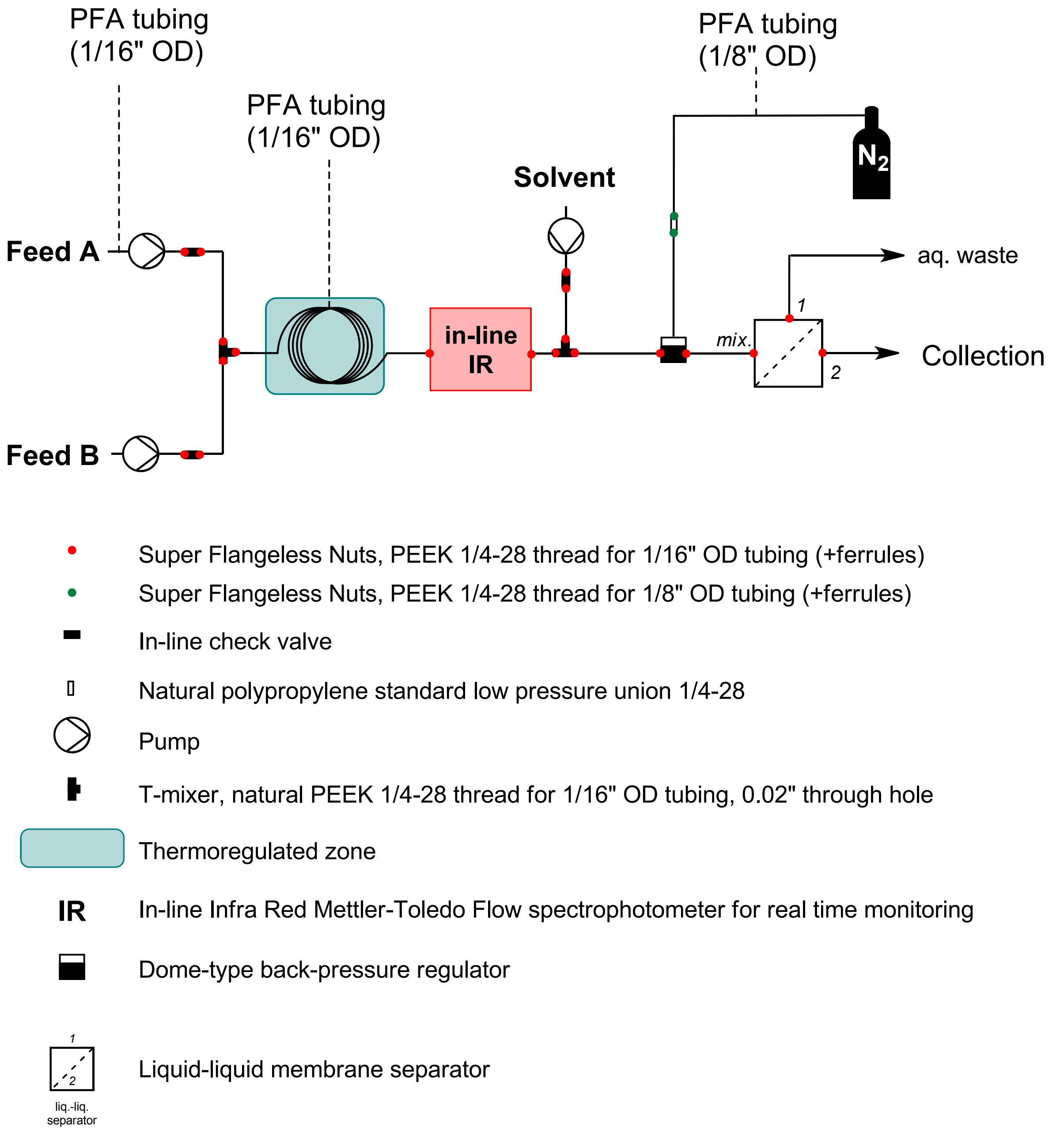

Figure S2. Detailed setup for the continuous flow preparation of α-chloronitroso derivatives

1.5.3 Concatenated continuous flow setup for the preparation of α-chloronitroso derivatives

See manuscript for experimental details (Figure 5b).

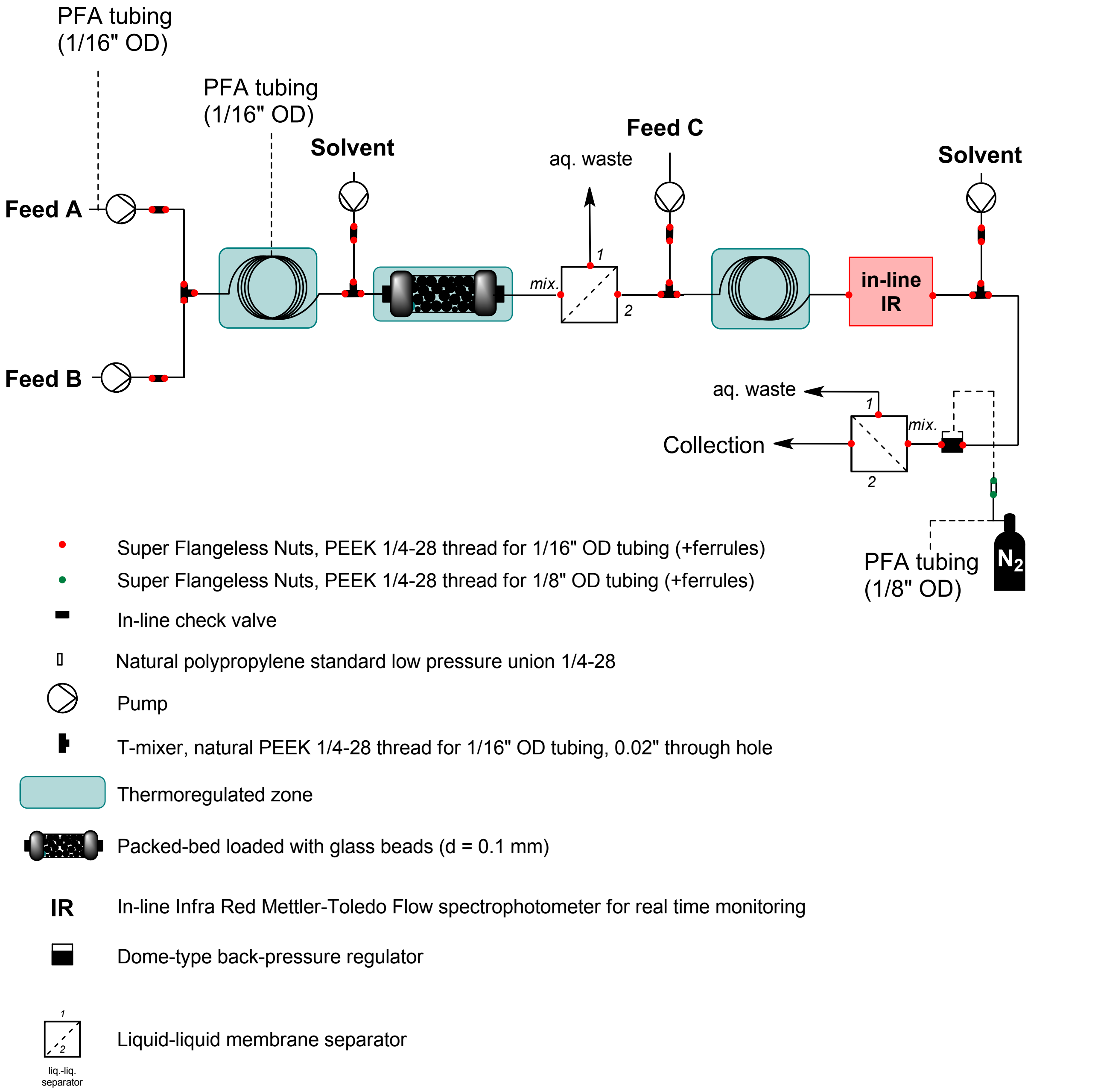

Figure S3. Detailed setup for the concatenated continuous flow preparation of α-chloronitroso derivatives

1.5.4 Continuous flow setup for the α-aminohydroxylation of enolizable ketones **2a-v**
See manuscript for experimental details (Figure 8a).

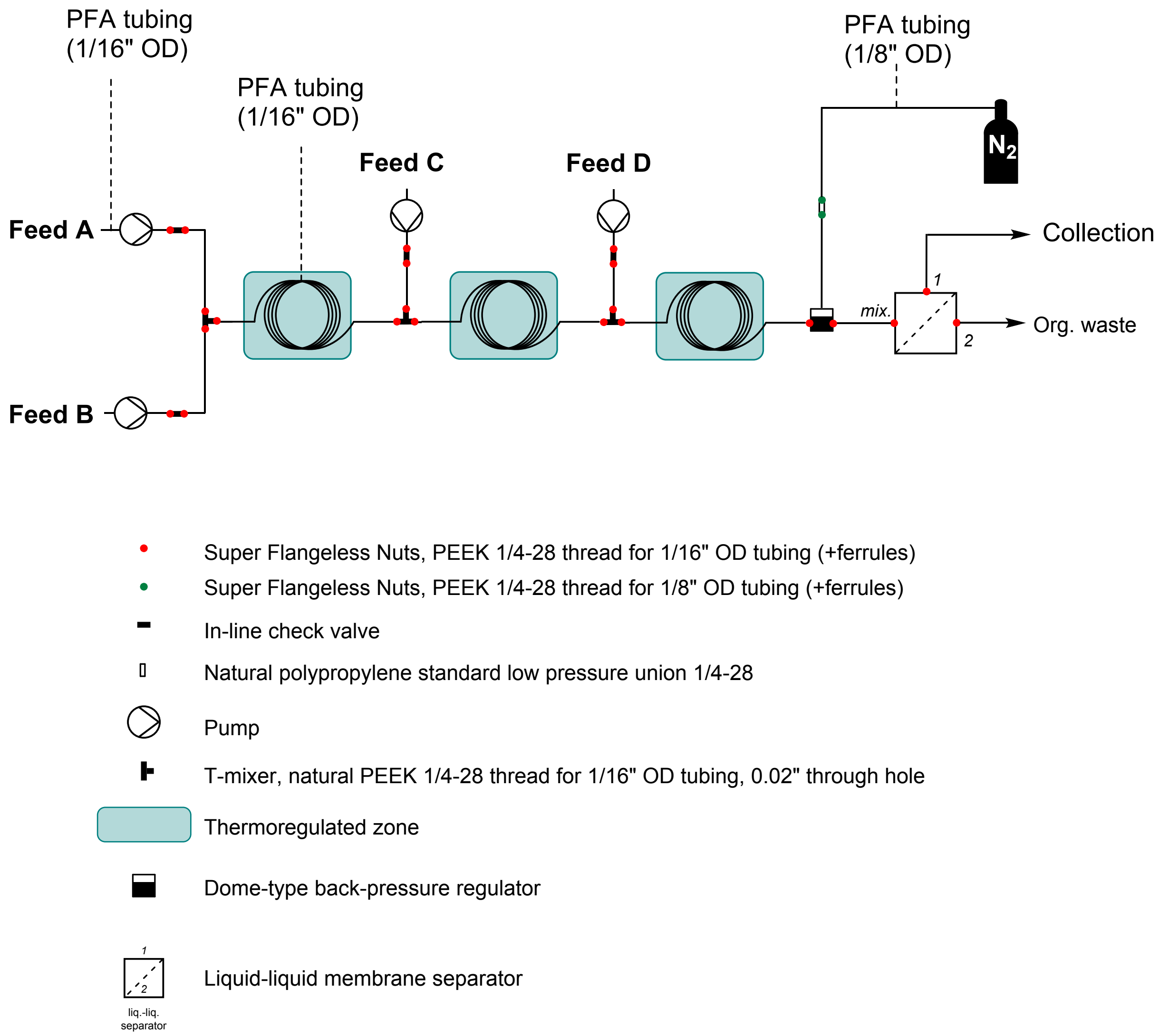

Figure S4. Detailed setup for the continuous flow α-aminohydroxylation of enolizable ketones

1.5.5 Fully concatenated continuous flow setup for the α-aminohydroxylation of enolizable ketones **2a-v**

See manuscript for experimental details (Figure 8a).

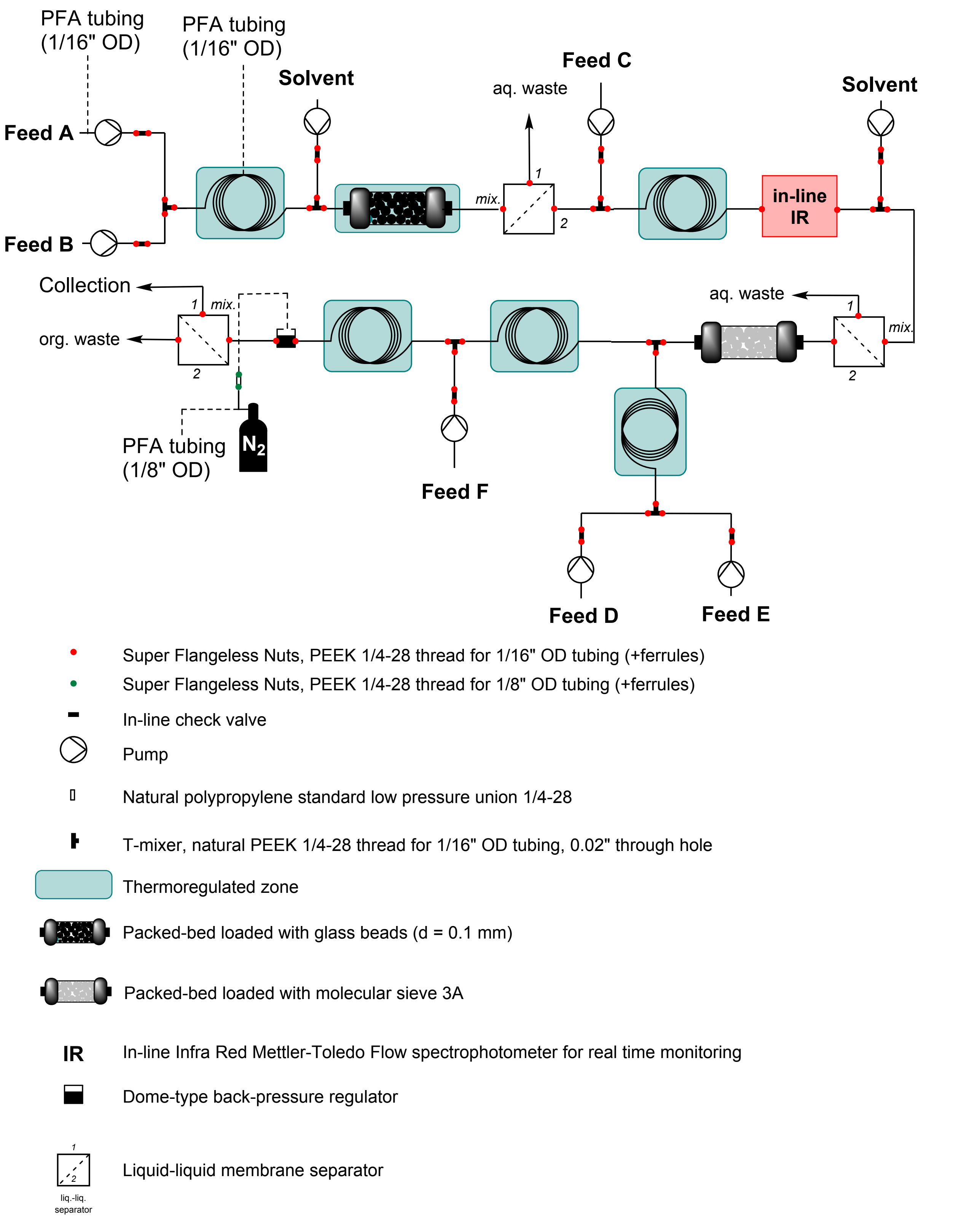

Figure S5. Detailed setup for the fully concatenated continuous flow α-aminohydroxylation of enolizable ketones

1.5.6 Mesofluidic preparation of α-chloronitroso derivatives (lab scale)

See manuscript for experimental details (Figure 6).

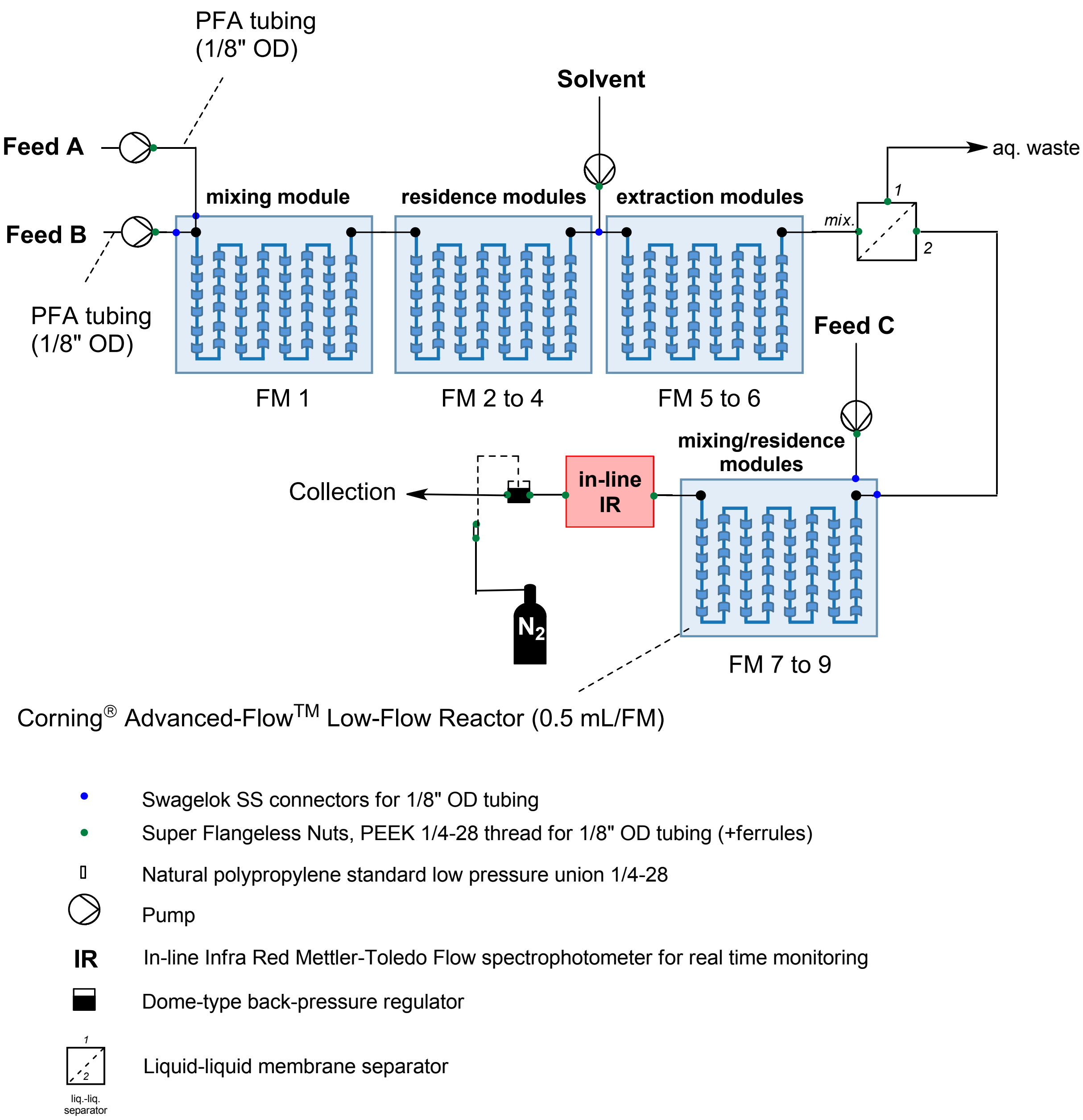

Figure S6. Detailed setup for the mesofluidic preparation of α-chloronitroso derivatives (lab scale)

1.5.7 Pilot scale preparation of α-chloronitroso compounds

See manuscript for experimental details (Figure 6).

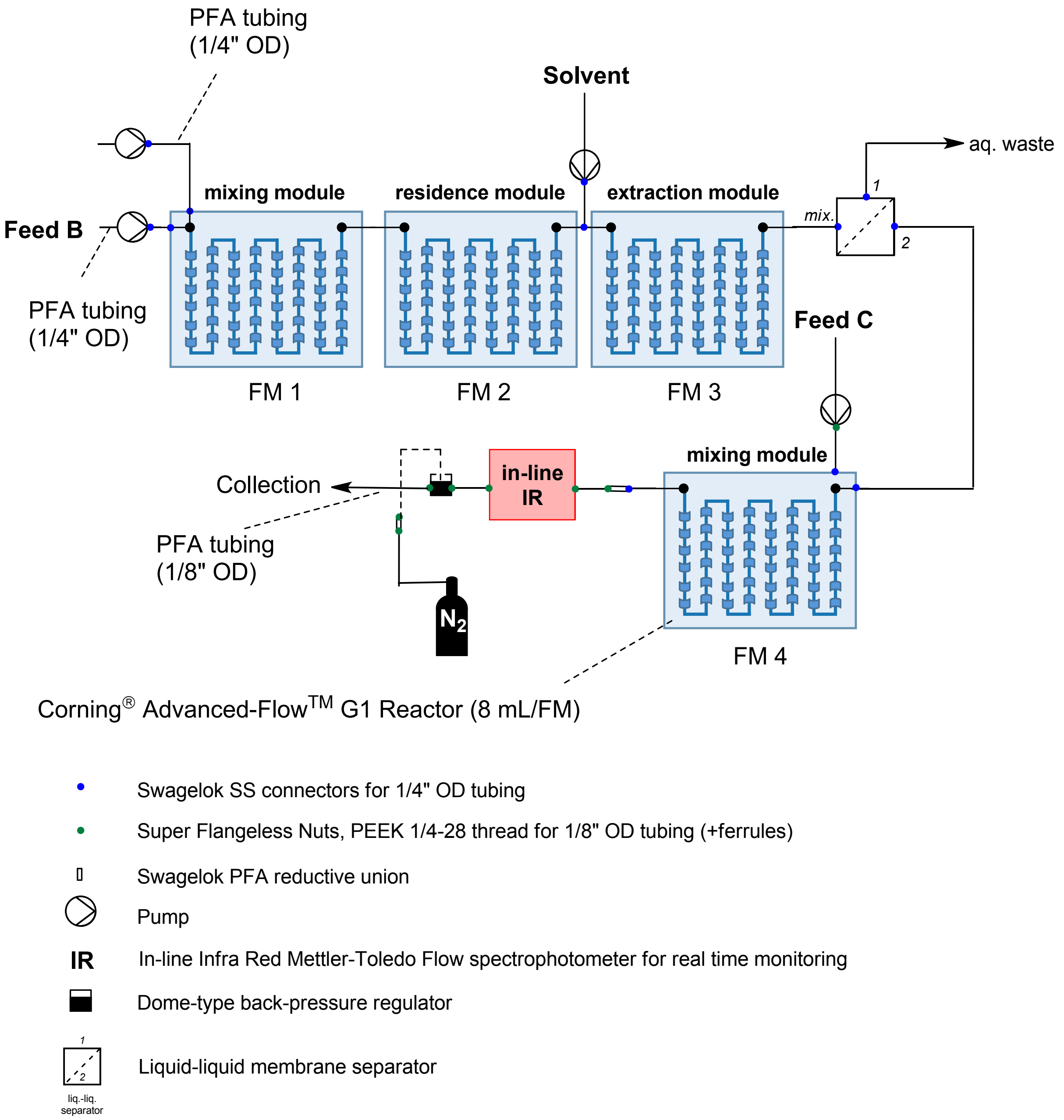

Figure S7. Detailed setup for the pilot scale production of α-chloronitroso derivatives

1.5.8 Pilot scale continuous flow α-aminohydroxylation of enolizable ketones **2b,k**

See manuscript for experimental details (see Figure S15).

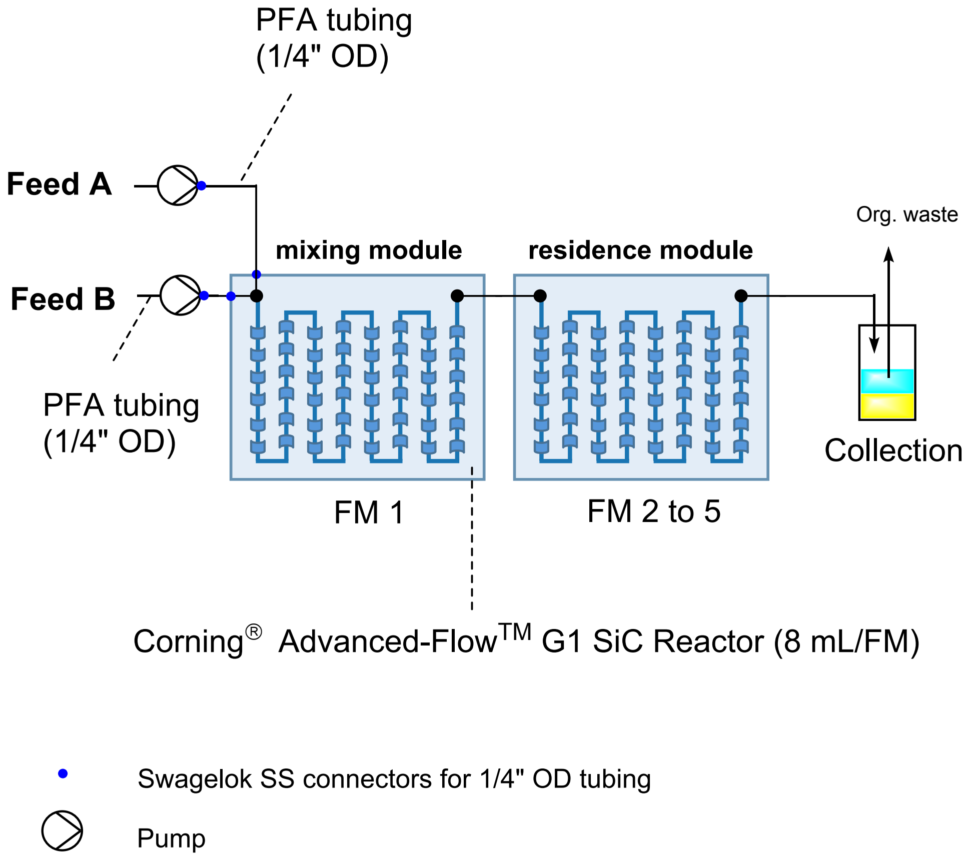

Figure S8. Detailed setup for the continuous flow α-aminohydroxylation of enolizable ketones (exemplified on ketones **2b** and **2k**)

2. Additional experimental details

2.1 Chemicals

Chemicals, purity, CAS numbers and suppliers are provided in Table S2.

Table S2. Solvents, chemicals and suppliers

Solvents	Purity (%)	CAS Number	Supplier
THF	99.8	109-99-9	Fischer
MTBE	>99	1634-04-4	VWR
Diethyl ether	>99	60-29-7	VWR
Ethanol (absolute)	>99	64-17-5	VWR
Hexane	98.5	110-54-3	VWR
Ethyl acetate	≥99.5	141-78-6	Aldrich
Methanol	>99	67-56-1	VWR
Petroleum ether (40-60)	>99	8032-32-4	VWR
Chemicals	**Purity (%)**	**CAS number**	**Supplier**
Sodium hypochlorite pentahydrate	N.A.	10022-70-5	TCI
tert-Butanol	99	75-65-0	ABCR
Acetic acid (glacial)	≥ 99	64-19-7	VWR
Acetoxime	≥ 98	127-06-0	TCI
2-Butanone oxime	≥ 99	96-29-7	TCI
Cyclopentanone oxime	98	1192-28-5	TCI
Cyclohexanone oxime	98	100-64-1	TCI
Cycloheptanone oxime	98	2158-31-8	TCI
(-)-Menthone	90	14073-97-3	TCI
(+)-Camphor	98	464-49-3	TCI
Propiophenone	99	93-55-0	Sigma Aldrich
4’-Methylpropiophenone	94	5337-93-9	ALFA AESAR
3’-Chloropropiophenone	98	34841-35-5	Sigma Aldrich
4’-Chloropropiophenone	98	936-59-4	Sigma Aldrich

4’-Fluoropropiophenone	98	456-03-1	Sigma Aldrich
4’-(Trifluoromethyl) propiophenone	99	711-33-1	Sigma Aldrich
2’-(Trifluoromethyl) propiophenone	97	16185-96-9	Sigma Aldrich
3’-(Trifluoromethyl) propiophenone	97	1533-03-5	Sigma Aldrich
3’-Nitropropiophenone	98	17408-16-1	Sigma Aldrich
4’-Methoxypropiophenone	≥ 99	121-97-1	Sigma Aldrich
Valerophenone	99	1009-14-9	Sigma Aldrich
Octanophenone	≥ 99	1674-37-9	Sigma Aldrich
1-(2-Thienyl)-1-propanone	98	13679-75-9	Sigma Aldrich
1,3-Diphenylpropan-1-one	98	1083-30-3	ALFA AESAR
1-(benzo[*d*][1,3]dioxol-5-yl)propan-1-one	98	28281-49-4	ALFA AESAR
Isobutyrophenone	98	611-70-1	TCI
1,2-Diphenylethan-1-one	98	451-40-1	TCI
Cyclobutyl phenyl ketone	>95	5407-98-7	TCI
Cyclopentyl phenyl ketone	96	5422-88-8	ALFA AESAR
2-Chlorophenyl cyclopentyl ketone	≥ 98	6740-85-8	TCI
Cyclohexyl phenyl ketone	>98	712-50-5	TCI
2-Phenylcyclohexanone	98	1444-85-1	Sigma Aldrich
Acetophenone	98	98-86-2	Sigma Aldrich
Lithium bis(trimethylsilyl)amide (26% in THF)	N.A.	4039-32-1	TCI
Hydroxylamine hydrochloride	97	5470-11-1	TCI
Sodium acetate trihydrate	99	6131-90-4	Sigma Aldrich
Pyridine	99	110-86-1	TCI
Zinc chloride (25% in 2-MTHF)	N.A.	7646-85-7	TCI
Zinc (II)	98	54010-75-2	TCI

trifluoromethanesulfonate			
Sodium bicarbonate	99	144-55-8	Sigma Aldrich
Potassium *tert*-butoxide	97	865-47-4	ALFA AESAR
Potassium hydroxide	85	1310-58-3	ACROS ORGANICS
Sodium borohydride	95	16940-66-2	TCI
Zinc dust	98	7440-66-6	Sigma Aldrich
Calcium chloride	96	10043-52-4	Sigma Aldrich
Potassium Iodide	>99	7681-11-0	Sigma Aldrich
Sodium thiosulfate	99	7772-98-7	Sigma Aldrich
Potassium Bichromate	>99	7778-50-9	Sigma Aldrich

2.2 Additional experimental data

2.2.1 Batch procedure for the synthesis of *tert*-butyl hypochlorite (***t*BuOCl**)

37 mL (0.162 mol, 1 equiv.) of *tert*-butanol and 25 mL (0.174 mol, 1.07 equiv.) of AcOH were added in one portion to 26.6 g (0.162 mol, 1 equiv.) of $NaOCl•5H_2O$ in 100 mL of water cooled in an ice/water bath. The mixture was vigorously stirred for 5 min at 0 °C and the whole setup was kept from light with aluminum foil. The resulting biphasic mixture was separated in a separatory funnel and the organic layer was washed with a 10% Na_2CO_3 aqueous solution (50 mL) and with deionized water (50 mL). The resulting yellow-green oil (14.5 g, 83%) was dried over calcium chloride ($CaCl_2$) and stored in brown glass bottle in a fridge at 4 °C.

2.2.2 Off-line titration of *tert*-butyl hypochlorite (***t*BuOCl**)

The concentration of ***t*BuOCl** was determined through a back titration using potassium iodide and sodium thiosulfate. A 0.1 M solution of sodium thiosulfate was prepared and back titrated with $K_2Cr_2O_7$ and KI in an aqueous solution of HCl. A solution of starch (1%) in water was used as titration indicator.

The concentration of the sodium thiosulfate solution was 0.0958 M. The titration of *tert*-butyl hypochlorite feed (collected from the reactor) was performed in biphasic conditions (water/MTBE) under vigorous stirring using potassium iodide, sodium thiosulfate and a solution of starch (1%) in water was used as titration indicator. The calculated molarity of ***t*BuOCl** was 0.9899 M.

2.2.3 Low field NMR monitoring for the preparation of ***t*BuOCl**

Low field NMR monitoring was carried out for the optimization of the preparation of ***t*BuOCl**. Downstream extraction (see manuscript; Figure 4b) with MTBE renders the interpretation cumbersome with an overlap of the ^1H NMR signals. The extraction with dichloromethane performed equally well with no overlap.

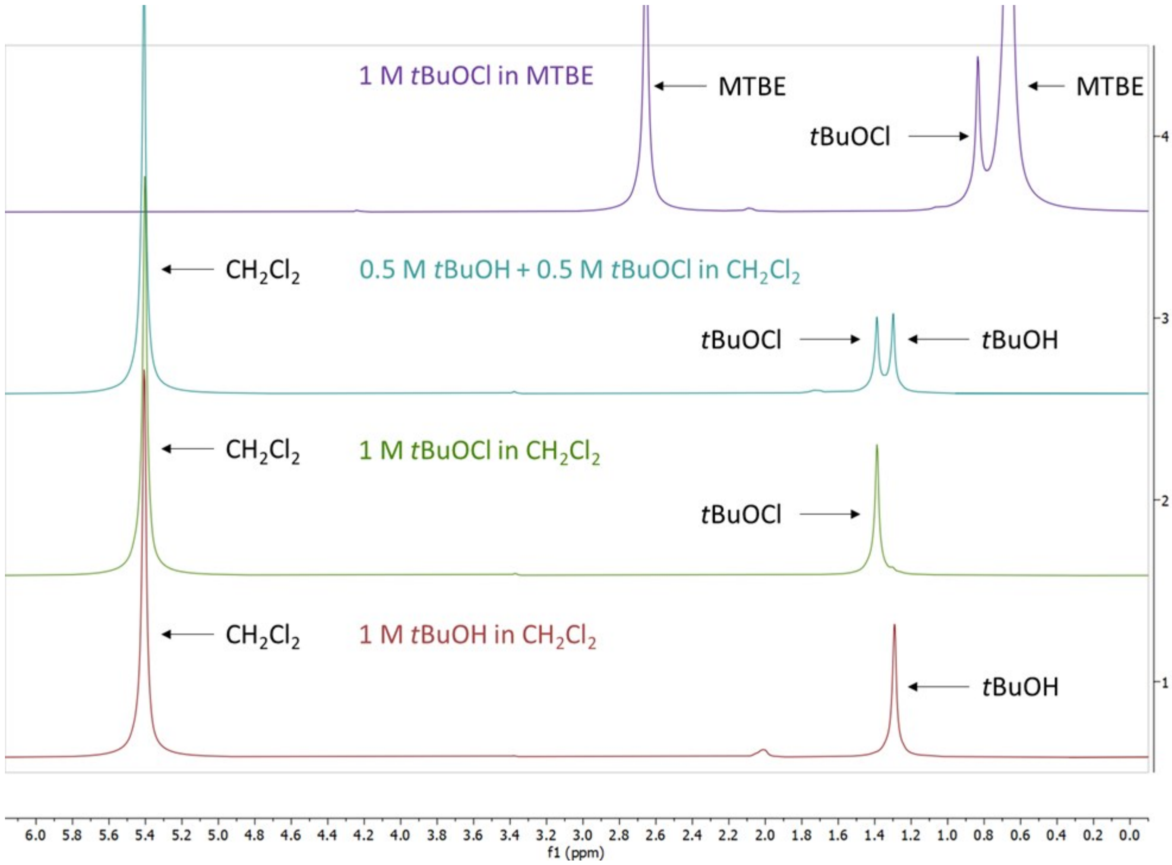

Figure S9. Low field NMR (43 MHz) reaction monitoring for the preparation of ***t*BuOCl**

2.2.4 Batch procedure for the synthesis of camphor oxime

15.6 g (0.115 mol, 1.25 equiv.) of hydroxylamine hydrochloride and 9.6 g of sodium acetate trihydrate (0.0138 mol, 0.15 equiv.) were dissolved in 60 mL of water. The resulting solution was added to a solution of camphor (14 g, 0.092 mol, 1 equiv.) dissolved in 60 mL of methanol. The reaction mixture was stirred for 12 h at 60 °C. Afterwards, methanol was removed under reduced pressure to give a white powder, which was washed with water (3 x 25 mL) over medium porosity ceramic filter to give the corresponding oxime as a white solid (14.8 g, 96% yield).

2.2.5 Batch procedure for the synthesis of menthone oxime

8.35 g (0.119 mol, 1.2 equiv.) of hydroxylamine hydrochloride were dissolved in 200 mL of methanol and stirred at room temperature. Then, 17.9 g (0.319 mol, 3.2 equiv.) of potassium hydroxide (KOH) were added to the solution and the mixture was stirred for 1 hour. The resulting milky solution was filtered off to recover a colorless solution. Afterwards, 15.4 g (0.1 mol, 1 equiv.) of menthone were added to the filtrate and the mixture was vigorously stirred under reflux for 3 hours. Then, the solvent was removed under reduced pressure and 500 mL of water was added to the resulting residue. The solution was left at room temperature overnight to slowly recrystallize the desired product. The crystals were filtered off and washed with 2 x 100 mL of cold water to give the corresponding oxime as white crystals (12 g, 71% yield).

2.2.6 Batch procedure for the synthesis of 1-chloro-1-nitrosocyclopentane (**1a**)

1.38 g (0.0127 mol, 1 equiv.) of *tert*-butyl hypochlorite (***t*BuOCl**) was slowly added to 1.44 g (0.0127 mol, 1 equiv.) of cyclopentanone oxime (**4a**) dissolved in 20 mL MTBE, and the mixture was stirred at 0 °C for 15 min. The setup was covered in aluminum foil to prevent light exposure. The resulting blue organic layer was washed with aqueous Na_2CO_3 (10 wt.-%, 2x 20 mL) and dried over MS 3Å or $CaCl_2$. Compound **1a** was stored under inert atmosphere (Argon) at low temperature (< 4 °C).

2.2.7 Batch procedure for the synthesis of 2-(hydroxyamino)-1-phenylpropan-1-one (*rac*-**3b**)

This reaction is water sensitive and has to be carried out with a dried glassware, dried solvent and under an inert atmosphere. 8.5 mL of LiHMDS 1.3 M (0.011 mol, 1.1 equiv.) were added slowly to 1.34 g (0.01 mol, 1 equiv) of propiophenone (**2b**) in 100 mL of dry THF at -78 °C. The mixture was stirred for 30 min at -78 °C. Next, 20 mL of 1-chloro-1-nitrosocyclopentane (**1a**) (0.5 M in MTBE, 0.01 mol, 1 equiv.) were slowly added, and the temperature was allowed to raise up to -30 °C. The reaction medium was then stirred for 1.5 h at -30 °C. 150 mL of HCl 1 M were next added to the mixture. The mixture was stirred for 12 h at room temperature. The organic solvent and the remaining 1-chloro-1-nitrosocyclopentane (**1a**) were removed under reduced pressure. Then, the extraction was performed in a separatory funnel with Et_2O/HCl 1 M (1:1) (2 x 50 mL) and Et_2O (1 x 50 mL). The pH of the combined aqueous phases was adjusted to 8 with the slow addition of solid Na_2CO_3. The white solid (*rac*-**3b**) was filtered off and the remaining *rac*-**3b** in the aqueous solution was extracted with Et_2O (3 x 50 mL). The combined organic phases were dried over Na_2SO_4 and concentrated under reduced pressure to give 2-(hydroxyamino)-1-phenylpropan-1-one (*rac*-**3b**) as a white solid (1.4 g, 90% yield).

2.2.8 Batch procedure for the synthesis of (*Z*)-*N*,*N*'-dihydroxy-2-oxo-2-phenylacetimidamide (**5**)

This reaction is water sensitive and has to be carried out with a dried glassware, dried solvent and under an inert atmosphere. 1.2 g (0.01 mol, 1 equiv.) of acetophenone (**2a**) dissolved in 50 mL of dry THF were added slowly to 8.5 mL of LiHMDS 1.3 M (0.011 mol, 1.1 equiv.) in 50 mL of dry THF at -78 °C. The mixture was stirred for 30 min at -78 °C. Next, 20 mL of 1-chloro-1-nitrosocyclopentane (**1a**) (0.5 M in MTBE, 0.01 mol, 1 equiv.) were slowly added, and the temperature was allowed to increase up to -30 °C. The reaction medium was then stirred for 1.5 h at -30 °C. 150 mL of HCl 1 M were next added to the mixture. The mixture was stirred for 12 h at room temperature. The organic solvent and the remaining 1-chloro-1-nitrosocyclopentane (**1a**) were removed under reduced pressure. Then, extraction was performed in a separatory funnel with Et_2O/HCl 1 M (1:1) (2 x 50 mL) and Et_2O (1 x 50 mL). The pH of the combined aqueous phases was adjusted to 8 with the slow addition of solid Na_2CO_3 and the aqueous phase became orange. The aqueous solution was extracted with Et_2O (3 x 50 mL). The combined organic phases were dried over Na_2SO_4 and concentrated under reduced pressure to give (*Z*)-*N*,*N*'-dihydroxy-2-oxo-2-phenylacetimidamide (**5**) as an orange solid (0.80 g, 46% yield).

2.2.9 Batch procedure for the synthesis of cyclopentanone oxime **4a** from crude cyclopentanone (recycling experiment)

The organic permeate of an α-aminohydroxylation experiment on propiophenone (**2b**) performed on a 0.01 mol scale was concentrated under reduced pressure. The crude residue was dissolved in 50 mL of MeOH. Afterwards, 0.82 g of hydroxylamine hydrochloride (0.12 mol, 1.2 equiv.) was added under stirring at room temperature. Then, 1.6 mL (0.2 mol, 2 equiv.) of pyridine were slowly added and the mixture was left stirring until the solid hydroxylamine hydrochloride was fully dissolved. Upon completion, the solvent was removed under vacuum and the residue was dissolved in 50 mL of Et_2O and washed with HCl 1 M (3x 30 mL). The resulting organic phase was dried over $MgSO_4$ and concentrated under reduced pressure to give cyclopentanone oxime (**4a**) as a white solid (0.82 g, 83% yield).

2.2.10 Optimization of the continuous flow preparation of ***t*BuOCl**

Different parameters were screened to assess their impact on the ***t*BuOCl** formation, and the organic stream after separation was directly analyzed with a Magritek Spinsolve 43 MHz NMR spectrometer (^{1}H NMR).

Table S3. Process optimization for the continuous flow synthesis of ***t*BuOCl** in H_2O with in-line liquid-liquid CH_2Cl_2 extraction (membrane separator).

Entry[a]	NaOCl (M)	*t*BuOH: AcOH (M)	Res. Time (min)	CH_2Cl_2 flow rate (mL min^{-1})	Conv. (%)[b]	Yield (%)[c]
1	1	1:1	5	0.1	90	60
2	1.2	1:1	5	0.1	94	61
3	1.5	1:1	5	0.1	>99	60
4	1.5	1:1	5	0.2	>99	65
5[d]	1.5	1:1	5	0.2	>99	98
6	1.5	1:1	2.5	0.2	55	50

[a] Typical conditions: P = 5 bar; liquid flow rate = 0.1 mL min^{-1} each. [b] Conversions was determined by ^{1}H NMR (Magritek Spinsolve 43 MHz NMR spectrometer). [c] Determined by weight after solvent removal. [d] Short packed-bed column (filled with glass beads d = 0.1 mm) inserted before the liquid-liquid extraction module.

2.2.11 Continuous flow preparation of ***t*BuOCl** (lab scale)

The pumps used to deliver an aqueous solution of sodium hypochlorite (1.5 M) and an aqueous mixture of *tert*-butanol and acetic acid (1 M, 1:1) were set to 0.1 mL min^{-1}. Both streams were mixed through a PEEK T-mixer and the resulting mixture was reacted in a PFA capillary coil (1 mL internal volume, 5 min residence time) at 25 °C. The pump used to deliver MTBE upstream the extraction module was set to 0.2 mL min^{-1}. tert-Butyl hypochlorite (***t*BuOCl**) was extracted through a short column loaded with glass beads (ϕ = 0.1 mm), followed with a back pressure regulator (5 bar) and a membrane separator. The organic permeate was collected at steady state and analyzed by 400 MHz ^{1}H NMR (99% conv.).

2.2.12 Continuous flow preparation of 1-chloro-1-nitrosocyclopentane **1a** (lab scale).

The pumps used to deliver cyclopentanone oxime **4a** (1 M in MTBE) and ***t*BuOCl** (1 M in MTBE) were both set to 0.1 mL min^{-1}. Both streams were mixed through a PEEK T-mixer and the resulting mixture was reacted in a PFA capillary coil (1 mL internal volume, 5 min residence time) at 25 °C. An in-line IR spectrometer was inserted downstream to monitor the appearance of **1a** (99% conv. at steady state). The reactor effluent was quenched with a stream of aqueous sodium carbonate (10 wt.-%, 0.2 mL min^{-1}) under 5 bar of counterpressure. The resulting biphasic mixture was processed through a hydrophobic membrane separator and the permeate organic effluent was collected and analyzed. The data matched those previously reported in the literature (see Supporting Information, Section 2.3). **CAUTION**: 1-chloro-1-nitrosocyclopentane (**1a**) is a reactive and unstable species with a pungent smell that decomposes under heat or UV irradiation. It must be handled with great care under a fume hood in the absence of direct light. Storage over $CaCl_2$ at -8 °C in a brown glass bottle.

2.2.13 Transposition of Generator I and Generator II to pilot scale

Table S4. Process optimization for the continuous flow generation of ***t*BuOCl** under mesofluidic lab scale conditions (Corning® Advanced-Flow™ Low Flow reactor)

Entry[a]	NaOCl (M)	Total Flow rates (mL min^{-1})	CH_2Cl_2 Flow rate (mL min^{-1})	Res. Time (s)	Conv. (%)[b]
1	1.5	1	0.5	67	50
2	1.5	1.3	0.6	51	50
3	1.5	1.7	0.8	39	70
4	1.5	2	1	33	90
5	1.5	2.5	1.3	27	80
6	1.5	3	1.5	22.5	80
7	2.25	2	1	33	95

[a] Typical conditions: concentration of the *t*BuOH:AcOH feed (1:1) = 1 M; the temperature was set at 25 °C; P = 5 bar ; total reactor internal volume = 2.5 mL. [b] Conversions were determined by in-line ^1H NMR (Magritek Spinsolve 43 MHz NMR spectrometer).

Table S5. Process optimization for the continuous flow generation of 1-chloro-1-nitrosocyclopentane (**1a**) under mesofluidic conditions (Corning® Advanced-Flow™ Low Flow reactor)

Entry[a]	***t*BuOCl** Flow rate (mL min^{-1})	**4a** Flow rate (mL min^{-1})	MTBE Flow rate (mL min^{-1})	Total Res. Time (s)	Conv. **1a** (%)[b]
1	2	2	2	51	99

[a] Typical conditions: concentration of ***t*BuOCl** and **4a** = 1 M; the temperature was set at 25 °C for the fluidic modules used for the generation of ***t*BuOCl** and 10 °C for the formation of nitroso compounds **1a,b**; P = 5 bar; total reactor internal volume = 2 mL (Generator I) and 1.5 mL (Generator II). [b] Conversions were determined by in-line IR.

Table S6. Process optimization for the continuous flow generation of 1-chloro-1-nitrosocyclopentane (**1a**) under pilot scale conditions (Corning® Advanced-Flow™ G1 reactor)

Entry[a]	*t*BuOCl Flow rate (mL min^{-1})	**4a** Flow rate (mL min^{-1})	MTBE Flow rate (mL min^{-1})	**1a** Flow rate (mL min^{-1})	Total Res. Time (s)	Conv. **1a** (%)[b]
1	15	15	15	30	51	99

[a] Typical conditions: concentration of ***t*BuOCl** and **4a** = 1 M; the temperature was set at 25 °C for the modules used for the generation of ***t*BuOCl** (Generator I) and 10 °C generation of **1a** (Generator II); P = 5 bar; total reactor internal volume = 16 mL (Generator I) and 8 mL (Generator II). [b] Conversions were determined by in-line IR.

2.2.14 Optimization of the α-aminohydroxylation of propiophenone (**2b**) under continuous flow conditions

2.2.14.1 Optimization of the enolization step toward **en-2b**

Table S7. Process optimization for the continuous flow enolization of **2b** in THF with LiHMDS (T-mixer).

Entry[a]	Res. time (min)	T (°C)	Conv. **en-2b** (%)[b]
1	10	-78	96
2	5	-78	87
3	1	-78	70
4	0.75	-78	42
5	0.5	-78	40
6	0.25	-78	28
7	10	-60	93
8	5	-60	90
9	1	-60	87
10	0.75	-60	65
11	0.5	-60	47
12	0.25	-60	39
13	10	-30	97
14	5	-30	97
15	1	-30	97
16	0.75	-30	80
17	0.5	-30	51

18	0.25	-30	46
19	10	0	98
20	5	0	97
21	1	0	97
22	0.75	0	89
23	0.5	0	80
24	0.25	0	52
25[c]	10	r.t.	0
26[c]	5	r.t.	0
27[c]	1	r.t.	0

[a] Typical conditions: concentration of **2b** in the feed solution = 0.5 M; 1.1 equiv. of LiHMDS in THF; concentration of **1a** in the feed solution = 0.55 M; P = 5 bar; liquid flow rate = 0.1 mL min^{-1} each. [b] Conversion were determined by HPLC/DAD processed at 250 nm. [c] Reactive feed in module 2 turned black and clogged the PFA tubing.

2.2.14.2 Optimization of the hydrolysis step

Table S8. Process optimization for the continuous flow hydrolysis of **en-nit-2b** in THF with HCl (T-mixer).

Entry[a]	HCl (M)	T (°C)	Res. Time (min)	Conv. *rac*-**3b** (%)[b]
1	1	25	1	20
2	4	25	1	22
3	6	25	1	50
4	6	25	5	70
5	6	25	10	87
6	6	40	1	72
7	6	60	1	99

[a] Typical conditions: concentration of **2b** in the feed solution = 0.5 M; 1.1 equiv. of LiHMDS; concentration of **1a** in the feed solution = 0.55 M; P = 5 bar; liquid flow rate = 0.1 mL min^{-1} each. [b] Conversions were determined by HPLC/DAD processed at 250 nm.

2.2.15 Chemical neutralization of 1-chloro-1-nitrosocyclopentane (**1a**)

The neutralization of 1-chloro-1-nitrosocyclopentane (**1a**) was carried out according to a reported procedure (see manuscript for experimental details) in the presence of triphenylphosphine. The neutralization kinetic was monitored through the formation of triphenylphosphine oxide using HPLC/DAD data processed at 225 nm (Figure S10).

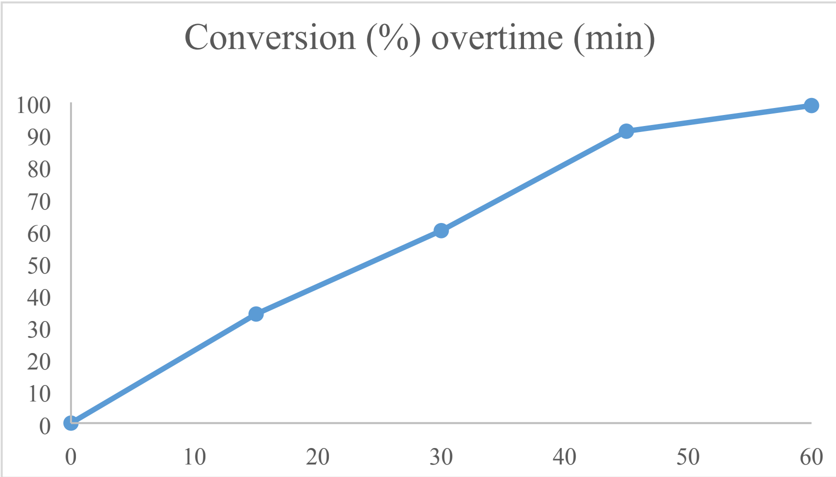

Figure S10. Monitoring of the conversion of triphenylphosphine into triphenylphosphine oxide for the chemical neutralization of 1-chloro-1-nitrosocyclopentane (**1a**).

2.2.16 Comparison of 1-chloro-1-nitrosocyclopentane (**1a**) and 1-chloro-1-nitrosocyclohexane (**1b**) for the α-aminohydroxylation on propiophenone (**2b**)

The preliminary trials performed on the enolate derived from propiophenone (**en-2b**) using α-chloronitroso derivative **1a** showed an extremely fast reaction. Therefore, measuring direct conversions into **3b** overtime was not possible. To the reactivity of both **1a**,**b**, we performed the α-aminohydroxylation on propiophenone (**2b**, see experimental details in section 2.2.7) in batch using both **1a**,**b**. After the successive addition of a given volume of **1a** and **1b** added (corresponding to 16.6 mol% in MTBE), the reaction mixture was sampled, hydrolyzed and diluted with MeOH prior to injection in an offline HPLC/DAD to monitor the respective conversions toward *rac*-**3b** (Figure S11).

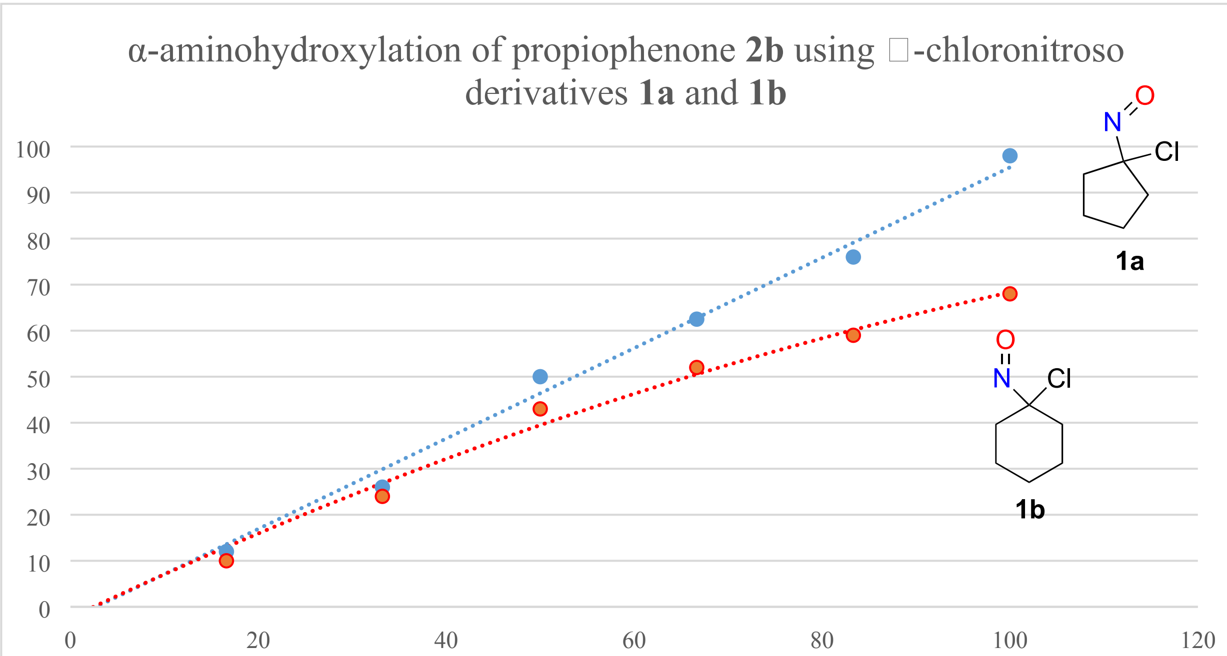

Figure S11. α-Aminohydroxylation on propiophenone (**2b**) using **1a** (blue dots) and **1b** (red dots). The data reported here show the conversion (%) of **en-2b** toward *rac*-**3b** as a function of the addition of **1a** or **1b** added (expressed in mol-%).

2.2.17 Continuous flow generation of various α-chloronitroso derivatives **1**

The concatenation of Generator I and Generator II was achieved (see manuscript for details, Figure 5b). Changing the oxime feed and adapting the reaction conditions enabled the preparation of a small library of various α-chloronitroso derivatives **1**, including chiral and biobased scaffolds (Figure S12 and Table S9).

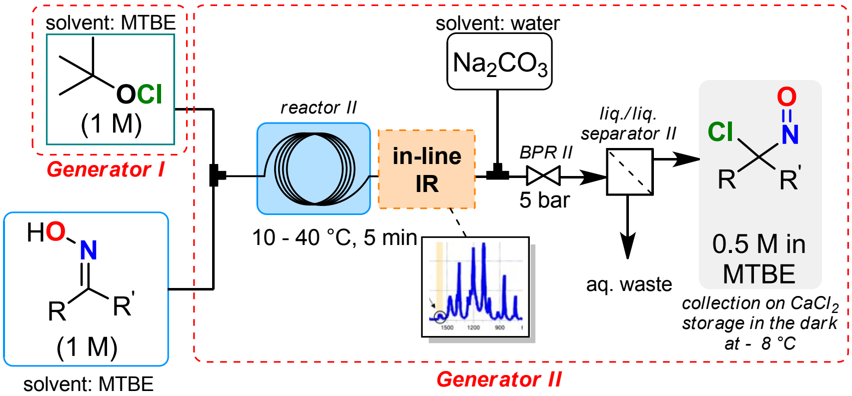

Figure S12. Simplified microfluidic flowchart for Generator II for the production of model α-chloronitroso species showcasing the in-line IR and the extraction module.

Table S9. Optimized conditions for the continuous flow generation of the α-chloronitroso library

Entry	Oximes	1-derivatives	Residence time (min)	Temperature (°C)	Conversion (%)[a]
1	R = R′ = CH_3	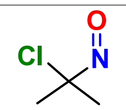	5	10	>99
2	R = CH_3, R′ = Et.	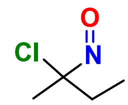	5	10	>99
3	R = R′ = cyclopentyl (**1a**)	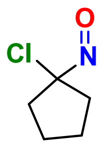	5	10	>99
4	R = R′ = cyclohexyl (**1b**)	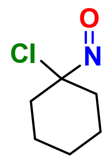	5	10	>99
5[b]	R = R′ = cycloheptyl*	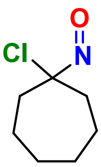	5	40	>99
6[b]	R = R′ = camphor*	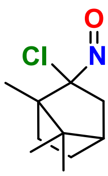	5	40	>99

7	R = R′ = menthone	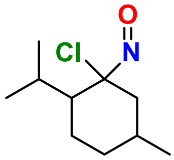	5	40	>99

[a]Determined by in-line IR spectroscopy

[b]Reactor coupled with an ultrasonic transducer

*Precipitate formed during the reaction

2.2.18 In-line IR spectroscopy for real-time monitoring (generation of α-chloronitroso compounds)

An in-line IR spectrometer was utilized to monitor the formation of α-chloronitroso compounds. The areas of interest for the specific vibration bands for α-chloronitroso compounds (υ_{NO}= 1621-1539 cm^{-1}) and oximes (υ_{OH} = 3600-3550 cm^{-1}, υ_{CN}= 1720-1665 cm^{-1}) can be easily monitored over time (Figure S13).

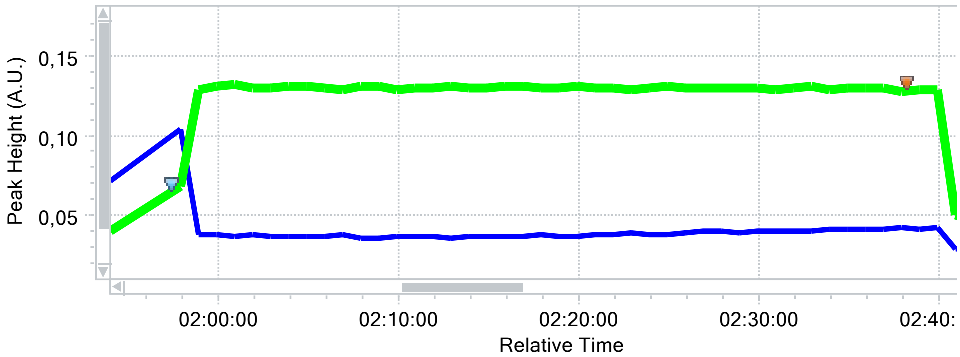

Figure S13. Representative example of in-line IR monitoring for the preparation of nitroso compounds **1**. The blue data points are the relative intensity of the characteristic vibration band of the oxime (υ_{OH} = 3600-3550 cm^{-1}) and the green data points are the relative intensity of the characteristic vibration band of the corresponding nitroso compound (υ_{NO}= 1621-1539 cm^{-1}). The green triangle (left) indicates the injection of ***t*BuOCl**, while the orange triangle (right) indicates the interruption of both pumps for ***t*BuOCl** and the starting oxime **4a**. The reaction reached full conversion after a residence time of 5 min at 25 °C. As illustrated, the process was stable, and consistent results were obtained for long runs.

2.2.19 Karl Fischer titration of the MTBE permeate downstream Generator II

Since the α-aminohydroxylation requires strictly anhydrous conditions, the MTBE permeate downstream Generator II was analyzed by Karl Fisher titration. The efficiency of the membrane separator led to a residual 19 ppm moisture content (Table S10). Further drying was attempted, and the best results were obtained with MS 3Å. The addition of a column packed with MS 3Å downstream the membrane separator was therefore considered prior to full concatenation.

Table S10: Recapitulative of Karl-Fischer titration from 1-chloro-1-nitrosocyclopentane (**1a**) flow

Entry	Drying method	Drying time	[H_2O]
1	/	/	19 ppm
2	$CaCl_2$	20 min	8 ppm
3	MS 3 Å	180 min	3 ppm

2.2.20 Final liquid-liquid separation

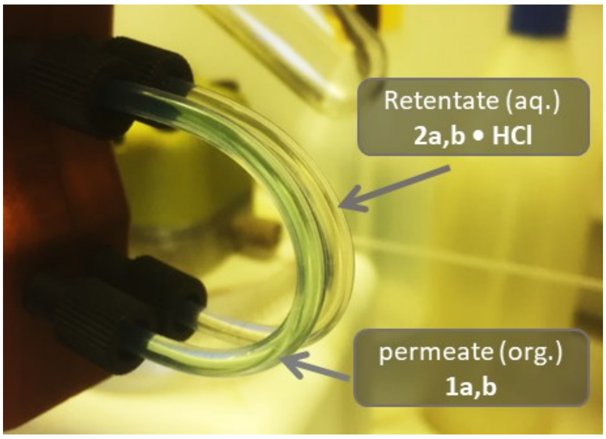

Figure S14. Close-up of the membrane separator (Zaiput Flow Technologies SEP-10) showing the retentate (aqueous) and permeate (organic) after membrane separation of the reactor effluent. The slight blue color of the permeate is due to residual nitroso **1a**.

2.2.21 Pilot scale electrophilic amination

See Figure S8 for detailed flow chart and setup.

Figure S15. Close-up of the pilot scale electrophilic α-aminohydroxylation setup relying on a 48 mL internal volume Corning® Advanced-Flow™ G1 SiC reactor (Courtesy of Corning®). The total residence time is 48 s. The reactor effluent was collected in aqueous HCl (1 M) to perform the hydrolysis of the intermediate nitrones **nit-2b,k** toward compounds *rac*-**3b,k**. **H**: inlet for thermofluid; **I1**: inlet for **1a** (0.5 M in MTBE); **I2**: inlet for preformed **en-2b,k** (0.5 M in THF).

2.3 Characterization of compounds

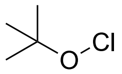

C_4H_9ClO
MW 108,03

***tert*-butyl hypochlorite (*t*BuOCl) ^{1}H NMR ($CDCl_3$, 400 MHz):** δ = 0.16 (s, 9H) ppm. **^{13}C ($CDCl_3$, 100.6 MHz):** δ = 84.0, 26.9 ppm.

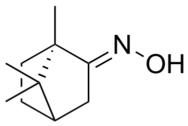

$C_{10}H_{17}NO$
MW 167,13

(1*R*,*E*)-1,7,7-trimethylbicyclo[2.2.1]heptan-2-one oxime. ^{1}H NMR ($CDCl_3$, 400 MHz): δ = 9.02 (s, 1H), 2.61 – 2.50 (m, 1H), 2.06 (d, *J* = 17.8 Hz, 1H), 1.92 (t, *J* = 4.4 Hz, 1H), 1.89 – 1.78 (m, 1H), 1.76 – 1.64 (m, 1H), 1.46 (ddd, *J* = 13.1, 9.4, 4.3 Hz, 1H), 1.24 (ddd, *J* = 12.2, 9.4, 4.2 Hz, 1H), 1.01 (s, 3H), 0.92 (s, 3H), 0.80 (s, 3H) ppm. **^{13}C ($CDCl_3$, 100.6 MHz):** δ = 170.1, 51.9, 48.4, 43.8, 33.2, 32.8, 27.4, 19.6, 18.7, 11.2 ppm. **ESI HRMS** *m/z* $C_{10}H_{17}NO^+$ $[M+H]^+$: calcd 168.1382; found 168.1390.

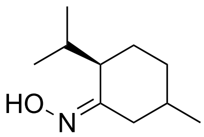

$C_{10}H_{19}NO$
MW 169,14

(2*R*,*Z*)-2-isopropyl-5-methylcyclohexan-1-one oxime. ^{1}H NMR ($CDCl_3$, 400 MHz): δ = 3.08 – 3.01 (m, 1H), 2.18 – 2.05 (m, J = 6.8 Hz, 1H), 1.92 – 1.61 (m, 4H), 1.35 (dtd, J = 13.6, 10.9, 3.3 Hz, 1H), 1.20 – 1.07 (m, 1H), 1.03 – 0.78 (m, 10H).**^{13}C ($CDCl_3$, 100.6 MHz):** δ = 161.3, 48.9, 33.0, 32.5, 32.1, 26.9, 26.4, 21.9, 21.6, 19.1 ppm. **ESI HRMS** *m/z* $C_{10}H_{19}NO^+$ $[M+H]^+$: calcd 170.1539; found 170.1538.

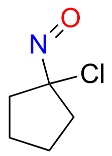

C_5H_8ClNO
MW 133,02

1-chloro-1-nitrosocyclopentane (1a). ^{1}H NMR ($CDCl_3$, 400 MHz): δ = 3.04 – 2.91 (m, 2H), 2.25 – 2.06 (m, 4H), 2.01 – 1.87 (m, 2H) ppm. **^{13}C ($CDCl_3$, 100.6 MHz):** δ = 123.0, 38.2, 25.6 ppm. The NMR data matched those reported in the literature.[S1]

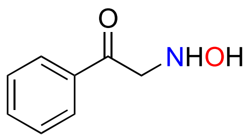

$C_8H_9NO_2$
MW 151,17

2-(hydroxyamino)-1-phenylethan-1-one (3a). ^{1}H NMR (D_2O, 400 MHz): δ = 8.05 – 7.99 (m, 2H), 7.82 – 7.76 (m, 1H), 7.65 – 7.59 (m, 2H), 5.08 (s, 2H) ppm. **^{13}C NMR (D_2O, 100.6 MHz):** δ = 192.6, 135.5, 133.0, 129.2, 128.3, 56.6 ppm. **ESI HRMS** *m/z* $C_8H_9NO_2^+$ $[M+H]^+$: calcd 152.0706; found 152.0718.

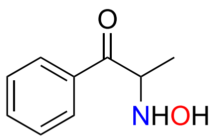

$C_9H_{11}NO_2$
MW 165,1920

2-(hydroxyamino)-1-phenylpropan-1-one (*rac*-3b). ^{1}H NMR (D_2O, 400 MHz): δ = 7.98-7.94 (m, 2H), 7.77-7.70 (m, 1H), 7.60-7.54 (m, 2H), 5.36 (q, *J* = 7.3 Hz, 1H), 1.59 (d, *J* = 7.3 Hz, 3H) ppm. **^{13}C NMR (D_2O, 100.6 MHz):** δ = 196.7, 135.7, 132.2, 129.4, 129.0, 62.2, 13.6 ppm. **ESI HRMS** *m/z* $C_9H_{11}NO_2^+$ $[M+H]^+$: calcd 166.0862; found 166.0862.

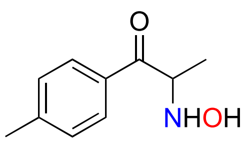

$C_{10}H_{13}NO_2$
MW 179,21

2-(hydroxyamino)-1-(*p*-tolyl)propan-1-one (*rac*-3c). ^{1}H NMR ($CDCl_3$, 400 MHz): δ = 7.89 (d, *J* = 8.3 Hz, 2H), 7.29 (d, *J* = 8.0 Hz, 2H), 5.48 (s, 2H), 4.73 (q, *J* = 7.2 Hz, 1H), 2.43 (s, 3H), 1.25 (d, *J* = 7.2 Hz, 3H) ppm. **^{13}C NMR ($CDCl_3$, 100.6 MHz):** δ = 201.3, 144.8, 132.8, 129.6, 128.7, 61.5, 21.9, 15.9 ppm. **ESI HRMS** *m/z* $C_{10}H_{13}NO_2^+$ $[M+H]^+$: calcd 180.1019; found 180.1030.

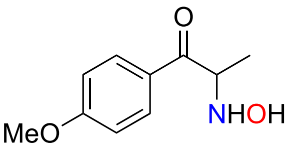

$C_{10}H_{13}NO_3$
MW 195,22

2-(hydroxyamino)-1-(4-methoxyphenyl)propan-1-one (*rac*-3d). **^{1}H NMR (D_2O, 400 MHz):** δ = 7.88 (d, J = 9.0 Hz, 2H), 6.98 (d, J = 9.0 Hz, 2H), 5.20 (q, J = 7.2 Hz, 1H), 3.80 (s, 3H), 1.53 (d, J = 7.3 Hz, 3H) ppm. **^{13}C NMR (D_2O, 100.6 MHz):** δ = 194.9, 164.8, 131.5, 125.2, 114.5, 61.6, 55.7, 13.6 ppm. **ESI HRMS** *m/z* $C_{10}H_{13}NO_3^+$ $[M+H]^+$: calcd 196.0968; found 196.0955.

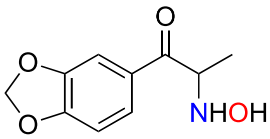

$C_{10}H_{11}NO_4$
MW 209,20

1-(benzo[*d*][1,3]dioxol-5-yl)-2-(hydroxyamino)propan-1-one (*rac*-3e). **^{1}H NMR (D_2O, 400 MHz):** δ = 7.68 (dd, J = 8.3, 1.8 Hz, 1H), 7.44 (d, J = 1.8 Hz, 1H), 7.01 (d, J = 8.3 Hz, 1H), 6.12 (d, J = 2.0 Hz, 2H), 5.27 (q, J = 7.2 Hz, 1H), 1.62 (d, J = 7.3 Hz, 3H) ppm. **^{13}C NMR (D_2O, 100.6 MHz):** δ = 194.6, 153.6, 148.4, 126.8, 126.7, 108.6, 107.8, 102.7, 61.9, 13.8 ppm. **ESI HRMS** *m/z* $C_{10}H_{11}NO_4^+$ $[M+Na]^+$: calcd 232.0580; found 232.0582.

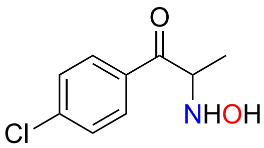

$C_9H_{10}ClNO_2$
MW 199,63

1-(4-chlorophenyl)-2-(hydroxyamino)propan-1-one (*rac*-3f). **^{1}H NMR ($CDCl_3$, 400 MHz):** δ = 7.93 (d, J = 8.7 Hz, 2H), 7.50 (d, J = 8.7 Hz, 2H), 5.30 (q, J = 7.3 Hz, 1H), 1.59 (d, J = 7.3 Hz, 3H) ppm. **^{13}C NMR ($CDCl_3$, 100.6 MHz):** δ = 195.5, 141.3, 130.7, 130.4, 129.5, 62.1, 13.5 ppm. **ESI HRMS** *m/z* $C_9H_{10}ClNO_2^+$ $[M+H]^+$: calcd 200.0472; found 200.0472.

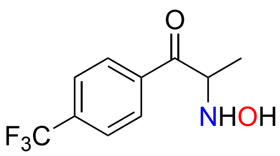

$C_{10}H_{10}F_3NO_2$
MW 233,19

2-(hydroxyamino)-1-(4-(trifluoromethyl)phenyl)propan-1-one (*rac*-3g). **^{1}H NMR (D_2O, 400 MHz):** δ = 8.17 (d, J = 8.1 Hz, 2H), 7.93 (d, J = 8.3 Hz, 2H), 5.40 (q, J = 7.3 Hz, 1H), 1.63 (d, J = 7.4 Hz, 3H) ppm. **^{13}C NMR (D_2O, 100.6 MHz):** δ = 196.2, 135.4, 135.1, 129.5, 126.4, 126.3, 62.5, 13.2 ppm. **ESI HRMS** *m/z* $C_{10}H_{10}F_3NO_2^+$ $[M+H]^+$: calcd 234.0736; found 234.0766.

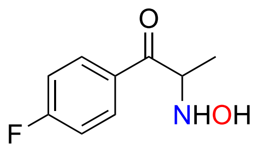

$C_9H_{10}FNO_2$
MW 183,18

1-(4-fluorophenyl)-2-(hydroxyamino)propan-1-one (*rac*-3h). **^{1}H NMR (D_2O, 400 MHz):** δ = 8.01 (dd, J = 8.7, 5.5 Hz, 2H), 7.22 (t, J = 8.8 Hz, 2H), 5.33 (q, J = 7.3 Hz, 1H), 1.59 (d, J = 7.3 Hz, 3H) ppm. **^{13}C NMR (D_2O, 100.6 MHz):** δ = 195.1, 167.9, 165.4, 132.1, 132.0, 128.8, 116.6, 116.4, 62.1, 13.6 ppm. **ESI HRMS** *m/z* $C_9H_{10}FNO_2^+$ $[M+H]^+$: calcd 184.0768; found 184.0744.

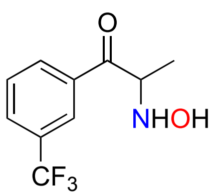

$C_{10}H_{10}F_3NO_2$
MW 233,19

2-(hydroxyamino)-1-(3-(trifluoromethyl)phenyl)propan-1-one (*rac*-3i). **^{1}H NMR (D_2O, 400 MHz):** δ = 8.18-8.10 (m, 2H), 7.84 (d, J = 7.8 Hz, 1H), 7.64 (t, J = 7.8 Hz, 1H), 5.36 (q, J = 7.3 Hz, 1H), 1.56 (d, J = 7.3 Hz, 3H) ppm. **^{13}C NMR (D_2O, 100.6 MHz):** δ = 195.3, 132.9, 132.3, 131.4, 131.3, 130.9, 130.6, 130.3, 130.1, 127.4, 125.4, 125.3, 124.7, 122.0, 119.3, 62.1, 13.2 ppm. **ESI HRMS** *m/z* $C_{10}H_{10}F_3NO_2^+$ $[M+H]^+$: calcd 234.0736; found 234.0766.

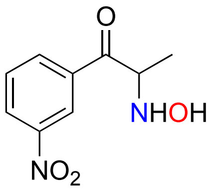

$C_9H_{10}N_2O_4$
MW 210,18

2-(hydroxyamino)-1-(3-nitrophenyl)propan-1-one (*rac*-3j). ^{1}H NMR (D_2O, 400 MHz): δ = 8.75-8.70 (m, 1H), 8.51-8.46 (m, 1H), 8.37-8.32 (m, 1H), 7.83-7.76 (m, 1H) 5.42 (q, *J* = 7.3 Hz, 1H), 1.63 (d, *J* = 7.3 Hz, 3H) ppm. **^{13}C NMR (D_2O, 100.6 MHz):** δ = 194.8, 148.2, 134.9, 133.6, 130.8, 129.3, 123.6, 62.3, 13.1 ppm. **ESI HRMS** *m/z* $C_9H_{10}N_2O_4^+$ [M+H]$^+$: calcd 211.0713; found 211.0700

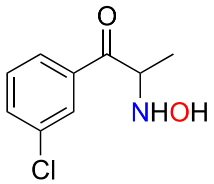

$C_9H_{10}ClNO_2$
MW 199,63

1-(3-chlorophenyl)-2-(hydroxyamino)propan-1-one (*rac*-3k). ^{1}H NMR (D_2O, 400 MHz): δ = 7.80 – 7.72 (m, 2H), 7.48 – 7.41 (m, 1H), 7.36 (t, *J* = 7.9 Hz, 1H), 5.25 (q, *J* = 7.3 Hz, 1H), 1.52 (d, *J* = 7.3 Hz, 3H) ppm. **^{13}C NMR (D_2O, 100.6 MHz):** δ = 195.0, 134.9, 134.7, 133.7, 130.7, 128.3, 127.3, 62.1, 13.5 ppm. **ESI HRMS** *m/z* $C_9H_{10}ClNO_2^+$ [M+Na]$^+$: calcd 222.0292; found 222.0290.

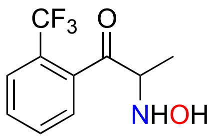

$C_{10}H_{10}F_3NO_2$
MW 233,19

2-(hydroxyamino)-1-(2-(trifluoromethyl)phenyl)propan-1-one (*rac*-3l). ^{1}H NMR (MeOD/ D_2O, 400 MHz): δ = 7.89 – 7.80 (m, 1H), 7.80 – 7.65 (m, 3H), 5.10 (q, *J* = 7.3 Hz, 1H), 1.35 (d, *J* = 7.3 Hz, 3H) ppm. **^{13}C NMR (MeOD/D_2O, 100.6 MHz):** δ = 198.3, 135.6, 135.5, 133.9, 130.7, 130.1, 129.8, 129.6, 129.5, 129.2, 128.8, 128.7, 128.6, 126.0, 123.3, 120.6, 65.2, 12.7 ppm. **ESI HRMS** *m/z* $C_{10}H_{10}F_3NO_2^+$ [M+H]$^+$: calcd 234.0736; found 234.0766.

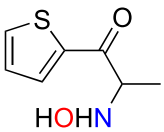

$C_7H_9NO_2S$
MW 171,21

2-(hydroxyamino)-1-(thiophen-2-yl)propan-1-one (*rac*-3m). ^{1}H NMR ($CDCl_3$, 400 MHz): δ = 7.84 (d, *J* = 3.8 Hz, 1H), 7.71 (d, *J* = 4.9 Hz, 1H), 7.17 (t, *J* = 4.4 Hz, 1H), 4.56 (q, *J* = 7.2 Hz, 1H), 1.29 (d, *J* = 7.2 Hz, 3H) ppm. **^{13}C NMR ($CDCl_3$, 100.6 MHz):** δ = 194.6, 142.6, 134.8, 132.8, 128.5, 63.1, 16.1 ppm. **ESI HRMS** *m/z* $C_7H_9NO_2S^+$ [M+H]$^+$: calcd 172.0426; found 172.0420.

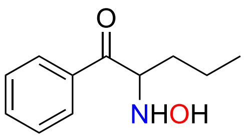

$C_{11}H_{15}NO_2$
MW 193,25

2-(hydroxyamino)-1-phenylpentan-1-one (*rac*-3n). ^{1}H NMR ($CDCl_3$, 400 MHz): δ = 8.06 – 7.94 (m, 2H), 7.69 – 7.56 (m, 1H), 7.54 – 7.45 (m, 2H), 4.70 (dd, *J* = 7.5, 4.9 Hz, 1H), 1.68 – 1.55 (m, 1H), 1.54 – 1.27 (m, 3H), 0.88 (t, *J* = 7.1 Hz, 3H) ppm. **^{13}C NMR ($CDCl_3$, 100.6 MHz):** δ = 201.9, 136.0, 133.7, 128.9, 128.5, 66.0, 32.6, 19.6, 14.1 ppm. **ESI HRMS** *m/z* $C_{11}H_{15}NO_2^+$ [M+H]$^+$: calcd 194.1175; found 194.1172.

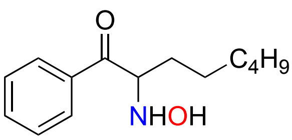

$C_{14}H_{21}NO_2$
MW 235,33

2-(hydroxyamino)-1-phenyloctan-1-one (*rac*-3o). ^{1}H NMR ($CDCl_3$, 400 MHz): δ = δ 8.05 – 7.98 (m, 2H), 7.67 – 7.58 (m, 1H), 7.52 – 7.44 (m, 2H), 4.66 (dd, *J* = 7.8, 4.8 Hz, 1H), 1.67 - 1.61 (m, 1H), 1.55 – 1.13 (m, 10H), 0.83 (t, *J* = 6.8 Hz, 3H) ppm. **^{13}C NMR ($CDCl_3$, 100.6 MHz):** δ = 202.0, 136.0, 133.7, 128.9, 128.5, 66.3, 31.6, 30.5, 29.4, 26.3, 22.6, 14.1 ppm. **ESI HRMS** *m/z* $C_{14}H_{21}NO_2^+$ [M+H]$^+$: calcd 236.1645; found 236.1633.

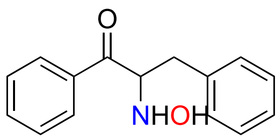

$C_{15}H_{15}NO_2$
MW 241,29

2-(hydroxyamino)-1,3-diphenylpropan-1-one (*rac*-3p). ^{1}H NMR (CDCl$_3$, 400 MHz): δ = 7.95 (d, J = 7.7 Hz, 2H), 7.58 (t, J = 7.4 Hz, 1H), 7.46 (t, J = 7.6 Hz, 2H), 7.28 – 7.11 (m, 5H), 5.90 (s, 2H), 4.84 (dd, J = 8.3, 5.2 Hz, 1H), 2.99 (dd, J = 14.1, 5.2 Hz, 1H), 2.81 (dd, J = 14.1, 8.3 Hz, 1H) ppm. **^{13}C NMR (CDCl$_3$, 100.6 MHz):** δ = 200.8, 136.8, 136.0, 133.7, 129.3, 128.9, 128.7, 128.6, 127.0, 67.2, 36.2 ppm. **ESI HRMS** *m/z* $C_{15}H_{15}NO_2^+$ [M+H]$^+$: calcd 242.1175; found 242.1155.

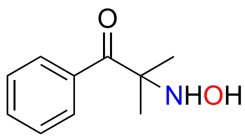

$C_{10}H_{13}NO_2$
MW 179,22

2-(hydroxyamino)-2-methyl-1-phenylpropan-1-one (3q). ^{1}H NMR (CDCl$_3$, 400 MHz): δ = 7.91 – 7.84 (m, 2H), 7.54 – 7.45 (m, 1H), 7.44-7.37 (m, 2H), 5.83 (s, 2H), 1.46 (s, 6H) ppm. **^{13}C NMR (CDCl$_3$, 100.6 MHz):** δ = 206.0, 137.2, 131.9, 128.4, 67.4, 23.5 ppm. **ESI HRMS** *m/z* $C_{10}H_{13}NO_2^+$ [M+H]$^+$: calcd 180.1019; found 180.0993.

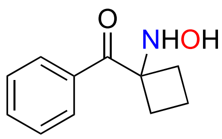

$C_{11}H_{13}NO_2$
MW 191,23

(1-(hydroxyamino)cyclobutyl)(phenyl)methanone (3r). ^{1}H NMR (CDCl$_3$, 400 MHz): δ = 7.95 – 7.88 (m, 2H), 7.53 (t, J = 7.5 Hz, 1H), 7.42 (t, J = 7.6 Hz, 2H), 5.65 (s, 1H), 5.33 (s, 1H), 2.79 – 2.63 (m, 2H), 2.26 – 2.14 (m, 2H), 2.12 – 1.97 (m, 1H), 1.94 – 1.79 (m, 1H) ppm. **^{13}C NMR (CDCl$_3$, 100.6 MHz):** δ = 201.2, 135.0, 132.7, 129.2, 128.5, 70.7, 29.1, 14.9 ppm. **ESI HRMS** *m/z* $C_{11}H_{13}NO_2^+$ [M+H]$^+$: calcd 192.1019; found 192.1003.

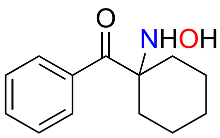

$C_{13}H_{17}NO_2$
MW 219,28

(1-(hydroxyamino)cyclohexyl)(phenyl)methanone (3s). ^{1}H NMR (CDCl$_3$, 400 MHz): δ = 7.94 – 7.86 (m, 2H), 7.51 – 7.36 (m, 3H), 5.26 (s, 2H), 1.99 (ddd, J = 13.8, 9.6, 5.1 Hz, 2H), 1.80 (dt, J = 13.6, 4.8 Hz, 2H), 1.68 – 1.46 (m, 5H), 1.38 (dtt, J = 13.9, 9.8, 5.3 Hz, 1H) ppm. **^{13}C NMR (CDCl$_3$, 100.6 MHz):** δ = 206.7, 138.3, 131.3, 128.3, 128.1, 70.0, 30.9, 25.6, 21.8 ppm. **ESI HRMS** *m/z* $C_{13}H_{17}NO_2^+$ [M+H]$^+$: calcd 220.1332; found 220.1340.

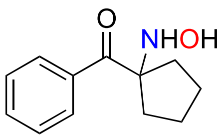

$C_{12}H_{15}NO_2$
MW 205,26

(1-(hydroxyamino)cyclopentyl)(phenyl)methanone (3t). ^{1}H NMR (D$_2$O, 400 MHz): δ = 7.72 – 7.65 (m, 2H), 7.57 (t, J = 7.5 Hz, 1H), 7.42 (t, J = 7.8 Hz, 2H), 2.47 – 2.33 (m, 2H), 2.28 – 2.12 (m, 2H), 2.07 – 1.86 (m, 4H) ppm. **^{13}C NMR (D$_2$O, 100.6 MHz):** δ = 200.1, 134.0, 132.7, 128.8, 128.5, 80.8, 33.5, 25.6 ppm. **ESI HRMS** *m/z* $C_{12}H_{15}NO_2^+$ [M+H]$^+$: calcd 206.1175; found 206.1200.

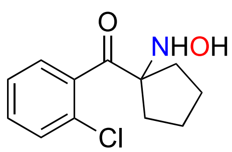

$C_{12}H_{14}ClNO_2$
MW 239,69

(2-chlorophenyl)(1-(hydroxyamino)cyclopentyl)methanone (3u). ^{1}H NMR (CDCl$_3$, 400 MHz): δ = 7.42 - 7.26 (m, 4H), 5.84 (s, 2H), 2.12 – 1.83 (m, 2H), 1.81 – 1.66 (m, 6H) ppm. **^{13}C NMR (CDCl$_3$, 100.6 MHz):** δ = 209.0, 139.4, 130.5, 130.2, 130.0, 127.0, 126.5, 79.2, 33.8, 24.9 ppm. **ESI HRMS** *m/z* $C_{12}H_{14}ClNO_2^+$ [M+H]$^+$: calcd 240.0785; found 240.0770.

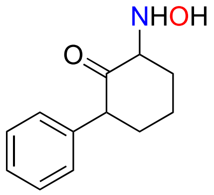

$C_{12}H_{15}NO_2$
MW 205,26

2-(hydroxyamino)-6-phenylcyclohexan-1-one (3v-1). ^{1}H NMR ($CDCl_3$, 400 MHz): δ = 7.44 – 7.18 (m, 4H), 7.16 – 7.10 (m, 2H), 3.81 (dd, J = 12.8, 5.9 Hz, 1H), 3.65 (dd, J = 12.4, 5.4 Hz, 1H), 2.47 – 2.36 (m, 1H), 2.35 – 2.26 (m, 1H), 2.12 – 1.88 (m, 3H), 1.77 – 1.61 (m, 1H) ppm. **^{13}C NMR ($CDCl_3$, 100.6 MHz):** δ = 209.4, 137.4, 128.8, 128.5, 127.4, 69.8, 57.0, 35.9, 32.4, 24.2 ppm. **ESI HRMS** *m/z* $C_{12}H_{15}NO_2^+$ [M+H]$^+$: calcd 206.1175; found 206.1163.

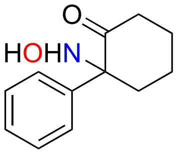

$C_{12}H_{15}NO_2$
MW 205,26

2-(hydroxyamino)-2-phenylcyclohexan-1-one (3v-2). ^{1}H NMR ($CDCl_3$, 400 MHz): δ = 7.50 – 7.24 (m, 5H), 5.48 (s, 2H), 2.73 (dq, J = 14.0, 2.9 Hz, 1H), 2.48 (dp, J = 14.4, 2.1 Hz, 1H), 2.43 – 2.26 (m, 2H), 2.03 – 1.63 (m, 4H) ppm. **^{13}C NMR ($CDCl_3$, 100.6 MHz):** δ = 212.0, 136.2, 129.3, 128.8, 127.6, 74.3, 40.8, 32.4, 27.2, 22.0 ppm. **ESI HRMS** *m/z* $C_{12}H_{15}NO_2^+$ [M+H]$^+$: calcd 206.1175; found 206.1168.

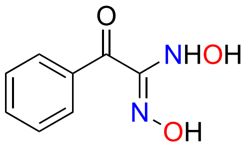

$C_8H_8N_2O_3$
MW 180,05

(*Z*)-*N*,*N*'-dihydroxy-2-oxo-2-phenylacetimidamide (5). ^{1}H NMR ($CDCl_3$, 400 MHz): δ = 8.03 – 7.94 (m, 2H), 7.61 – 7.51 (m, 1H), 7.47 – 7.39 (m, 2H), 5.23 (s, 2H) ppm. **^{13}C NMR ($CDCl_3$, 100.6 MHz):** δ = 187.5, 150.3, 135.5, 133.2, 130.5, 128.2 ppm. **ESI HRMS** *m/z* $C_8H_8N_2O_3^+$ [M+H]$^+$: calcd 181.0607; found 181.0600.

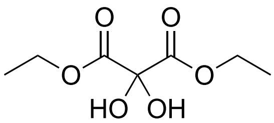

$C_7H_{12}O_6$
MW 192,06

Diethyl 2,2-dihydroxymalonate (6). ^{1}H NMR ($CDCl_3$, 400 MHz): δ = 4.97 (s, 2H), 4.30 (q, J = 7.2 Hz, 4H), 1.28 (t, J = 7.2 Hz, 6H) ppm. **^{13}C NMR ($CDCl_3$, 100.6 MHz):** δ = ^{13}C NMR (101 MHz, $CDCl_3$) δ 168.4, 90.3, 63.5, 13.9 ppm. The NMR data matched those reported in the literature.[S2]

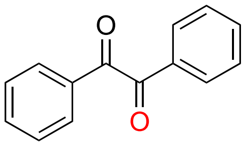

$C_{14}H_{10}O_2$
MW 210,23

Benzil (7). ^{1}H NMR ($CDCl_3$, 400 MHz): δ = 8.01 – 7.94 (m, 4H), 7.70 – 7.61 (m, 2H), 7.55 - 7.45 (m, 4H) ppm. **^{13}C NMR ($CDCl_3$, 100.6 MHz):** δ = 194.7, 135.0, 133.1, 130.0, 129.2 ppm. **ESI HRMS** *m/z* $C_{14}H_{10}O_2^+$ [M+Na]$^+$: calcd 233.0573; found 233.0570.

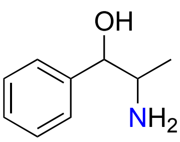

$C_9H_{13}NO$
MW 151,20

2-amino-1-phenylpropan-1-ol. ^{1}H NMR ($CDCl_3$, 400 MHz): δ = 7.36 – 7.21 (m, 5H), 4.46 (d, J = 4.8 Hz, 1H), 3.09 (dt, J = 11.2, 5.6 Hz, 1H), 2.20 (s, 3H), 0.94 (d, J = 6.6 Hz, 3H) ppm. **^{13}C NMR ($CDCl_3$, 100.6 MHz):** δ = 141.7, 128.2, 127.5, 126.7, 77.6, 52.1, 18.3 ppm. **ESI HRMS** *m/z* $C_9H_{13}NO^+$ [M+H]$^+$: calcd 152.1069; found 152.1070.

2.4 LC analysis

2.4.1 Analytical Method

Eluent: A: Water + 0.1% Formic acid (v:v)
B: Acetonitrile

Gradient Table:

Time [min]	A [%]	B [%]
0	100	0
20	20	80
23	20	80
23.01	100	0
26	100	0

Flow : 1 mL min^{-1}
Injection Volume : 5-10 µL
Column : C18, 100 × 4.6 mm, 3 µm
Oven Temperature : 40 °C
Diode Array Detector : 180-800 nm

2.4.2 Copies of representative LC traces

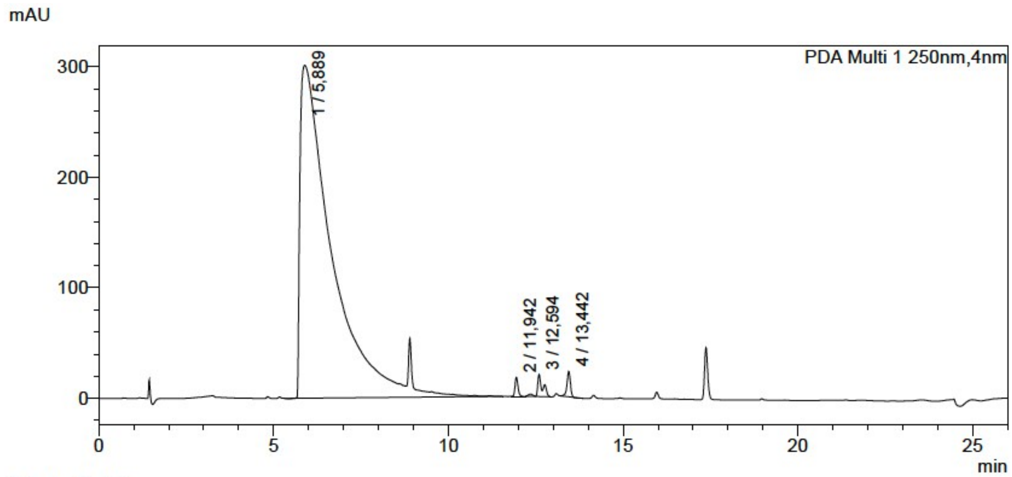

Peak Table

PDA Ch1 250nm

Peak#	Ret. Time	Area	Area%
1	5,889	19070479	97,628
2	11,942	101891	0,522
3	12,594	206368	1,056
4	13,442	155165	0,794
Total		19533903	100,000

Figure S16. LC trace of crude 2-(hydroxyamino)-1-phenylpropan-1-one (*rac*-**3b**). Pilot scale α-aminohydroxylation of propiophenone (**2b**) with nitroso **1a**. Peak identification was conducted using purified substances analyzed by either NMR and/or HRMS. Peak #1 (5.889 min) = compound *rac*-**3b**, peak #2 (11.942 min) = residual **2b**, peak #3 (12.594 min) = unidentified compound and peak #4 (13.442 min) = unidentified compound.

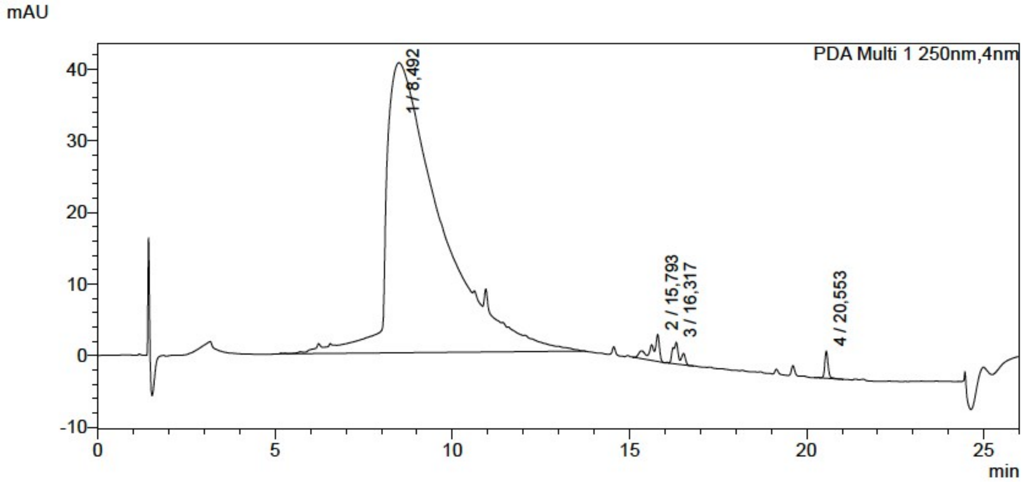

Peak Table

PDA Ch1 250nm

Peak#	Ret. Time	Area	Area%
1	8,450	4948160	88,339
2	15,792	218141	3,894
3	16,319	198918	3,551
4	20,549	236083	4,215
Total		5601303	100,000

Figure S17. LC trace of crude 1-(3-chlorophenyl)-2-(hydroxyamino)propan-1-one (*rac*-**3k**). Pilot scale α-aminohydroxylation of **2k** with **1a**. Peak identification was conducted using purified substances analyzed by either NMR and/or HRMS. Peak #1 (8.450 min) = compound *rac*-**3k**, peak #2 (15.792 min) = residual **2k**, peak #3 (16.319 min) = unidentified compound and peak #4 (20.549 min) = unidentified compound

2.5 Copies of ^{1}H and ^{13}C NMR spectra

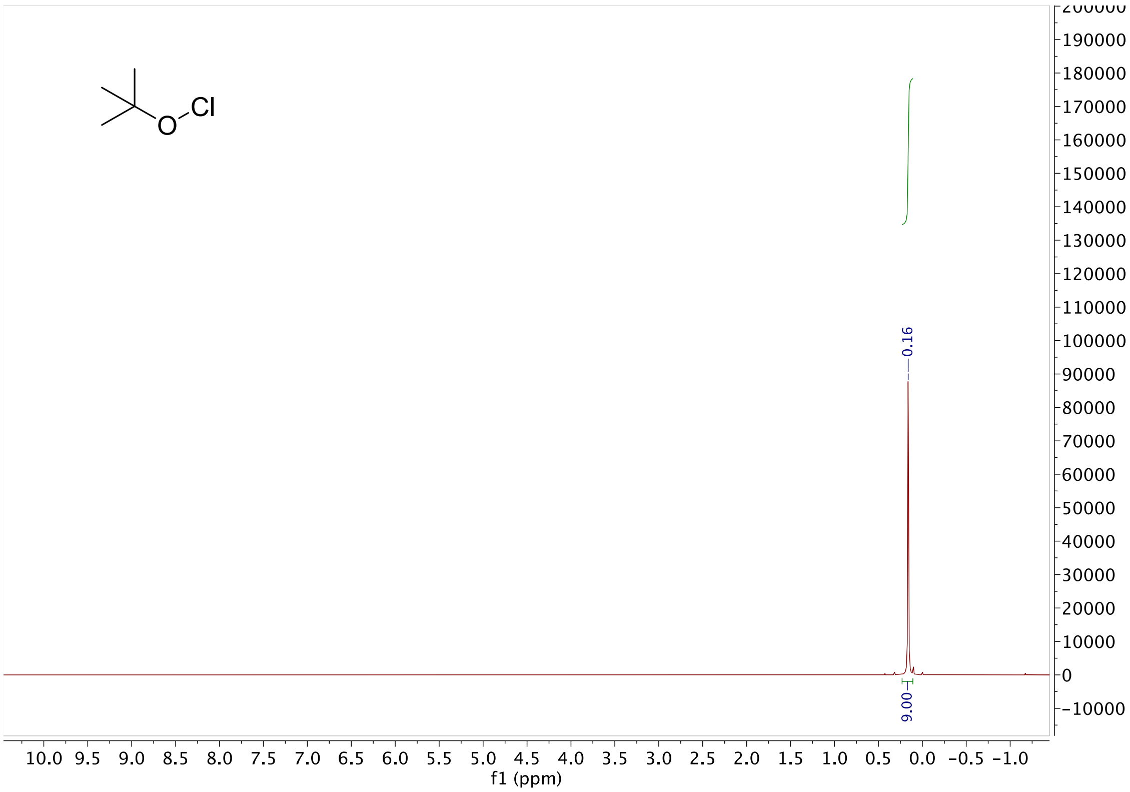

Figure S18. ^{1}H NMR spectrum (400 MHz) of *tert*-butyl hypochlorite (***t*BuOCl**) in $CDCl_3$.

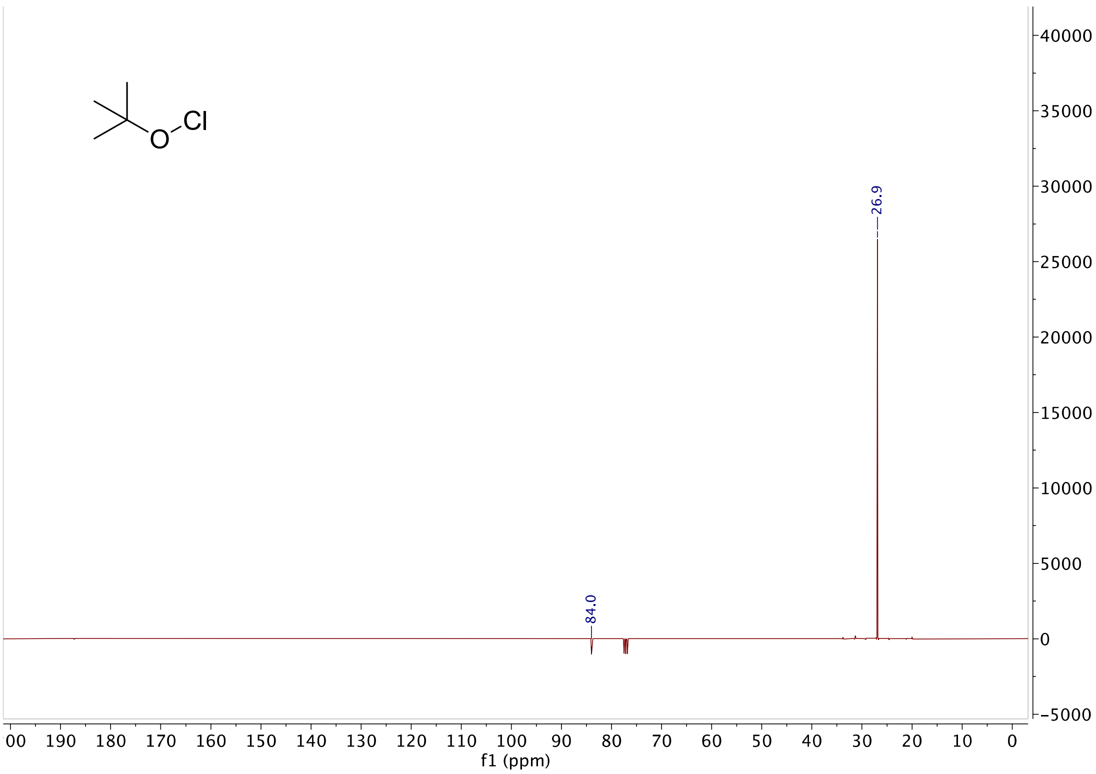

Figure S19. ^{13}C APT NMR spectrum (100.6 MHz) of *tert*-butyl hypochlorite (***t*BuOCl**) in $CDCl_3$.

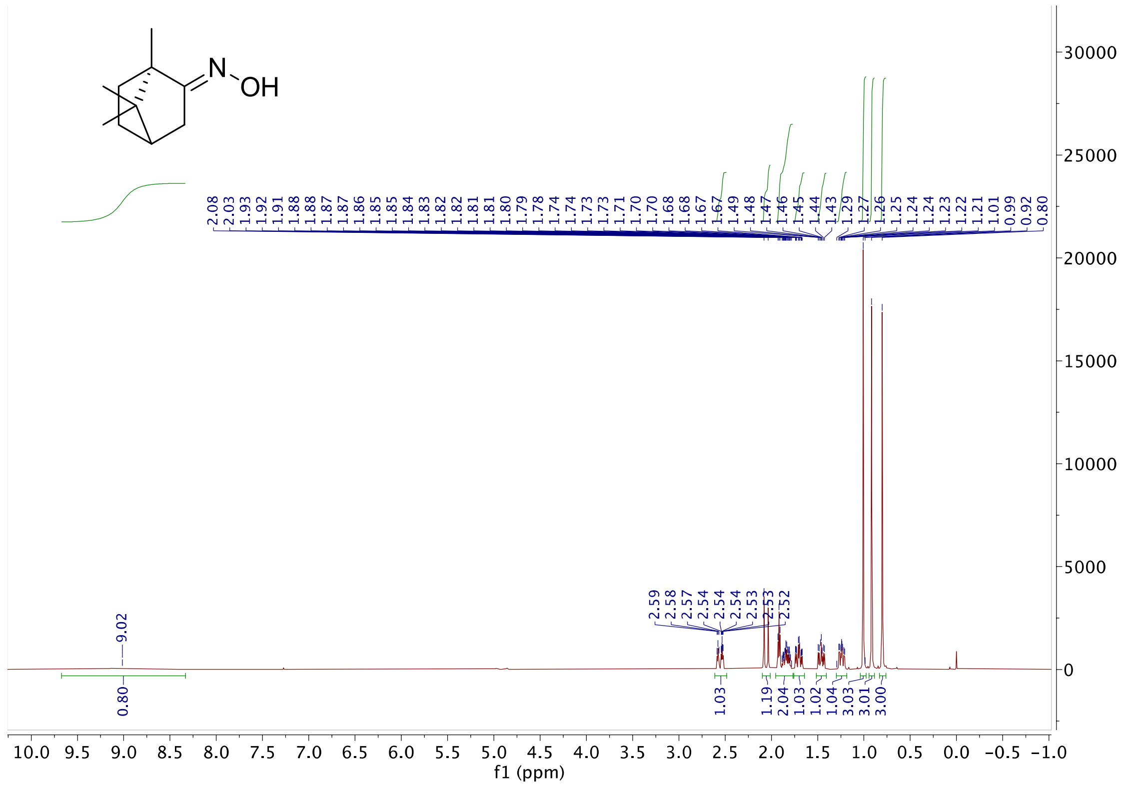

Figure S20. ^{1}H NMR spectrum (400 MHz) of (1*R*,*E*)-1,7,7-trimethylbicyclo[2.2.1]heptan-2-one oxime in $CDCl_3$.

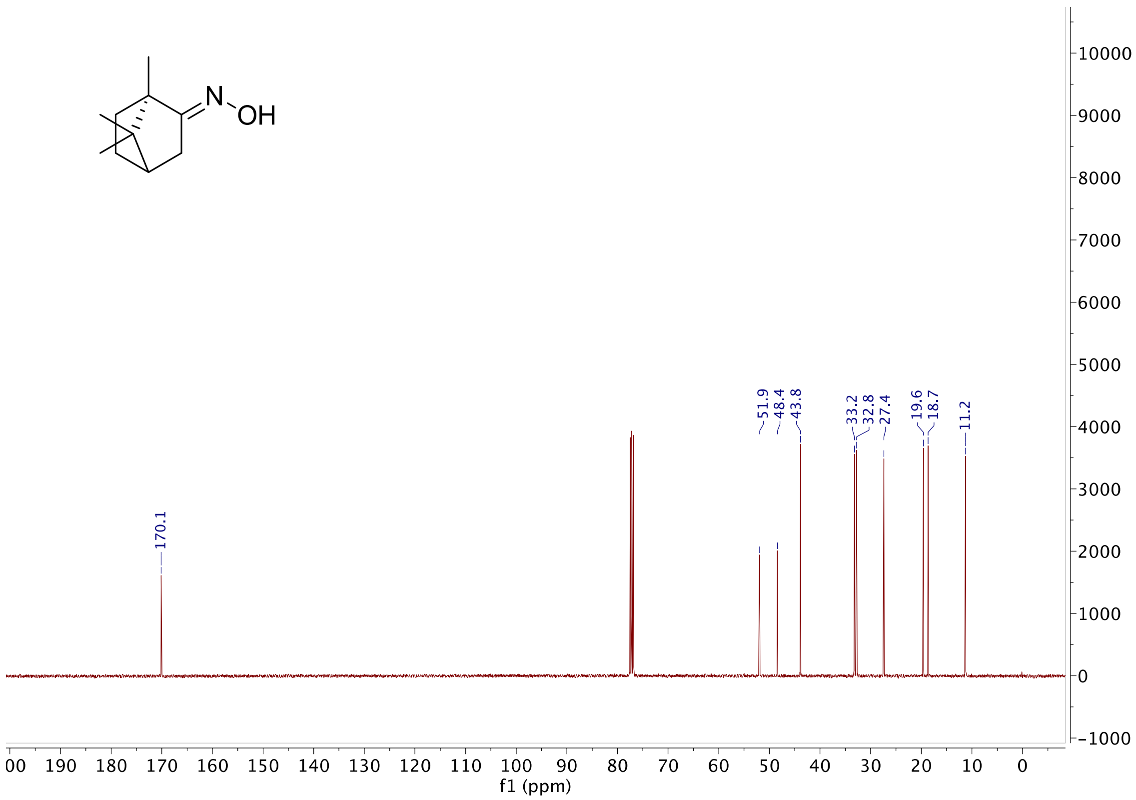

Figure S21. ^{13}C NMR spectrum (100.6 MHz) of (1*R*,*E*)-1,7,7-trimethylbicyclo[2.2.1]heptan-2-one oxime in $CDCl_3$.

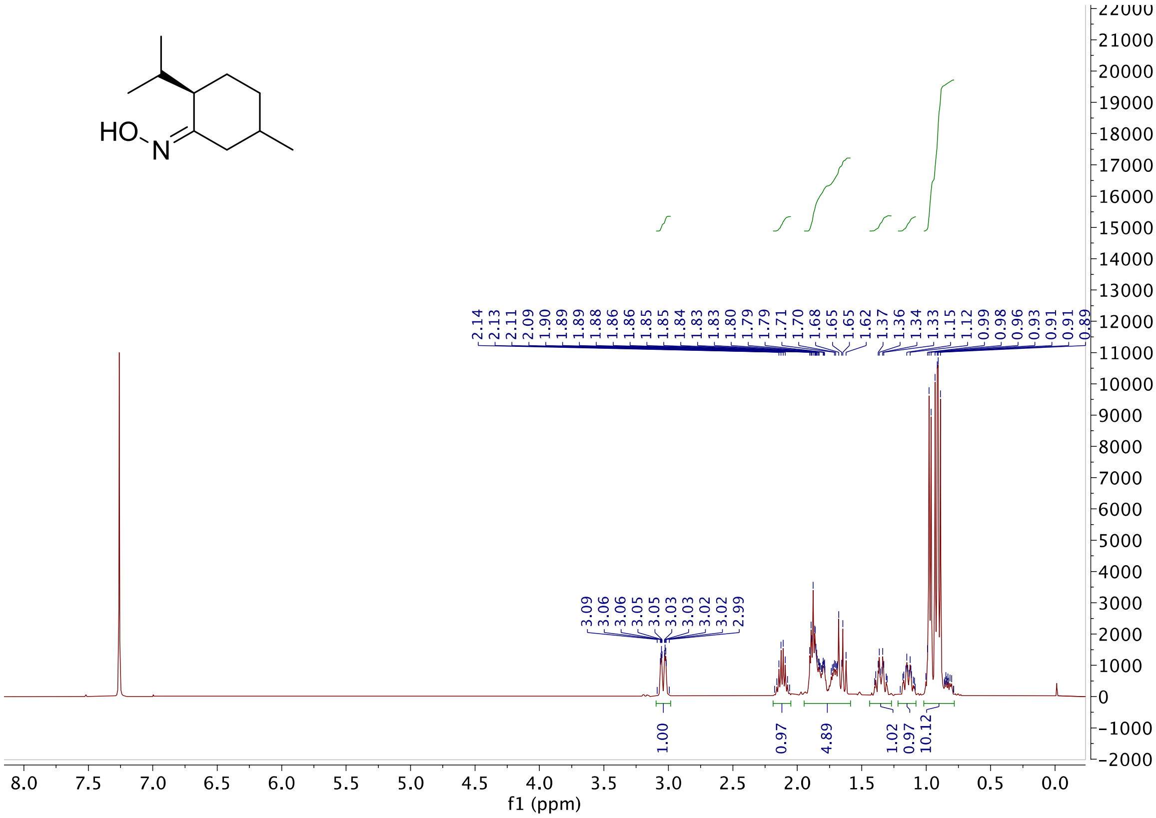

Figure S22. ^{1}H NMR spectrum (400 MHz) of (2*R*,*Z*)-2-isopropyl-5-methylcyclohexan-1-one oxime in $CDCl_3$.

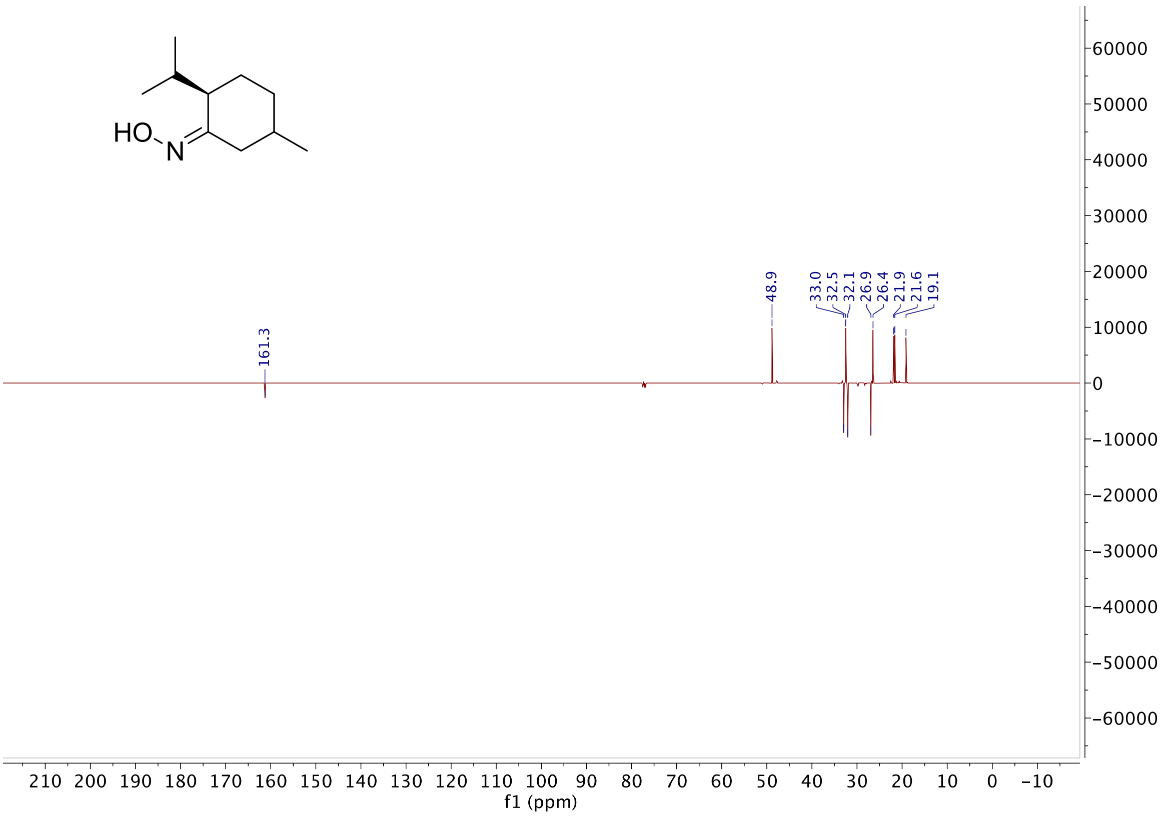

Figure S23. ^{13}C APT NMR spectrum (100.6 MHz) of (2*R*,*Z*)-2-isopropyl-5-methylcyclohexan-1-one oxime in $CDCl_3$.

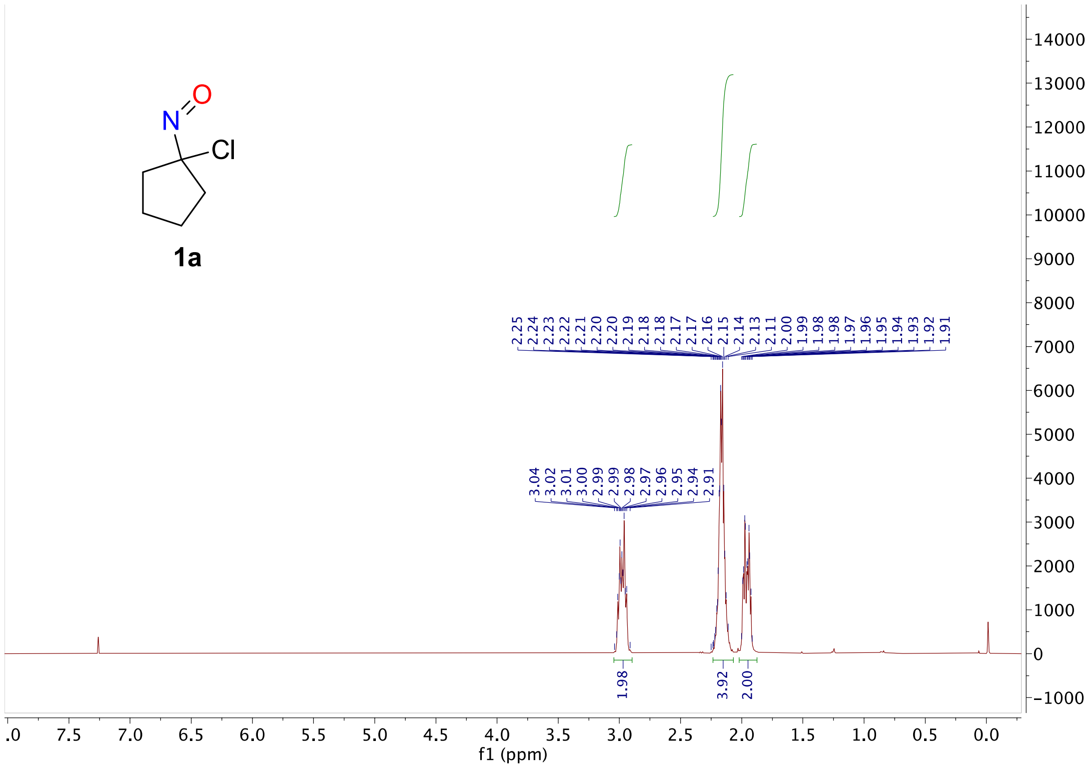

Figure S24. ^{1}H NMR spectrum (400 MHz) of 1-chloro-1-nitrosocyclopentane (**1a**) in $CDCl_3$.

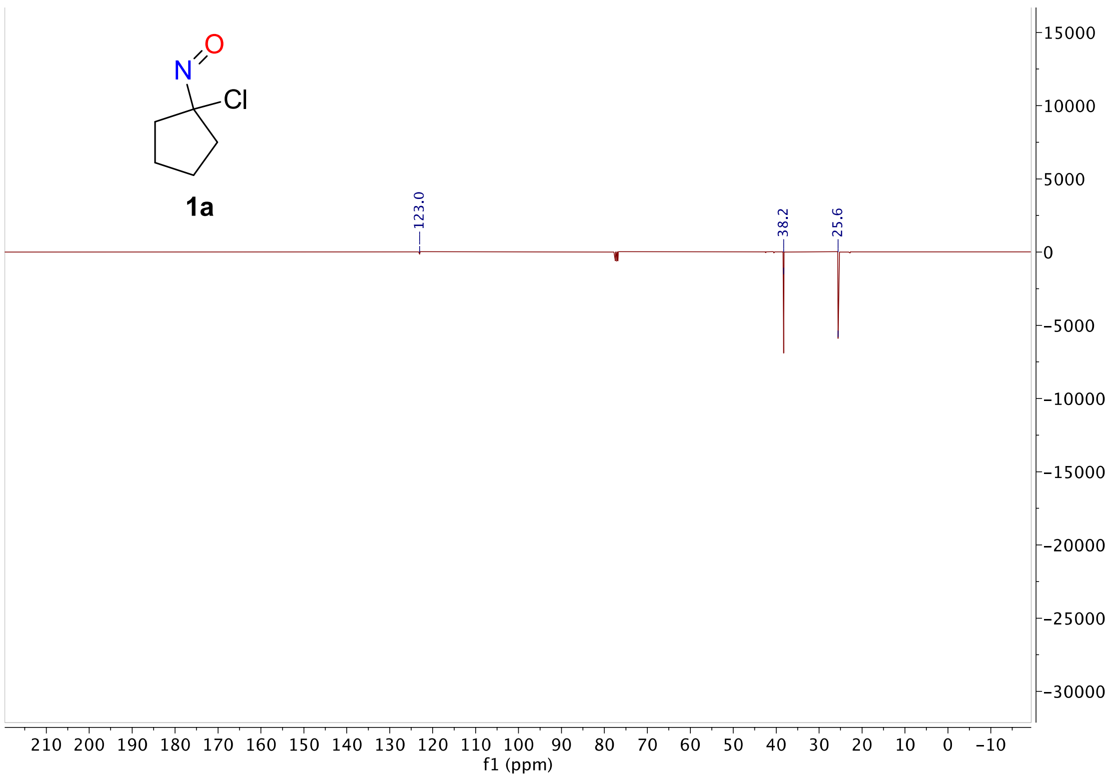

Figure S25. ^{13}C APT NMR spectrum (100.6 MHz) of 1-chloro-1-nitrosocyclopentane (**1a**) in $CDCl_3$.

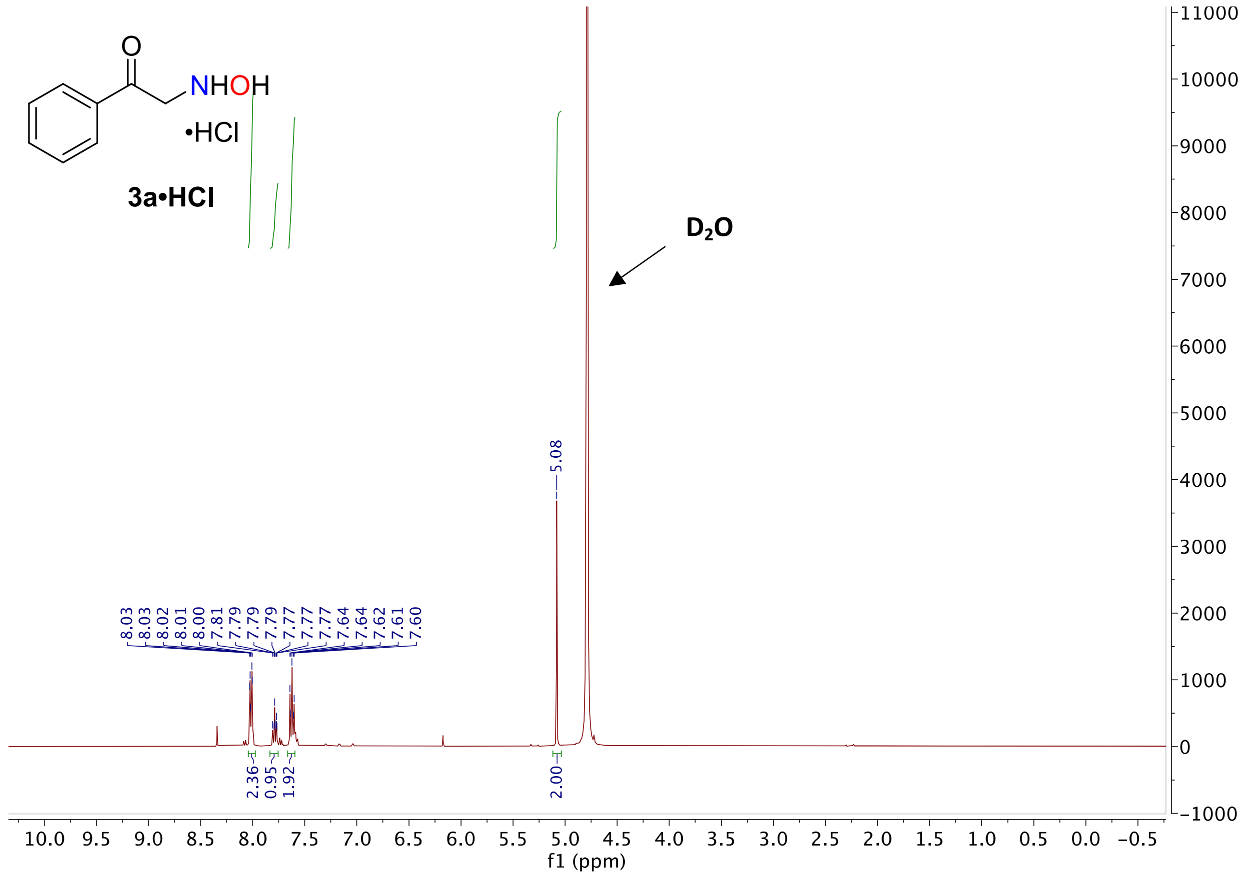

Figure S26. ^{1}H NMR spectrum (400 MHz) of 2-(hydroxyamino)-1-phenylethan-1-one hydrochloride (**3a•HCl**) in D_2O.

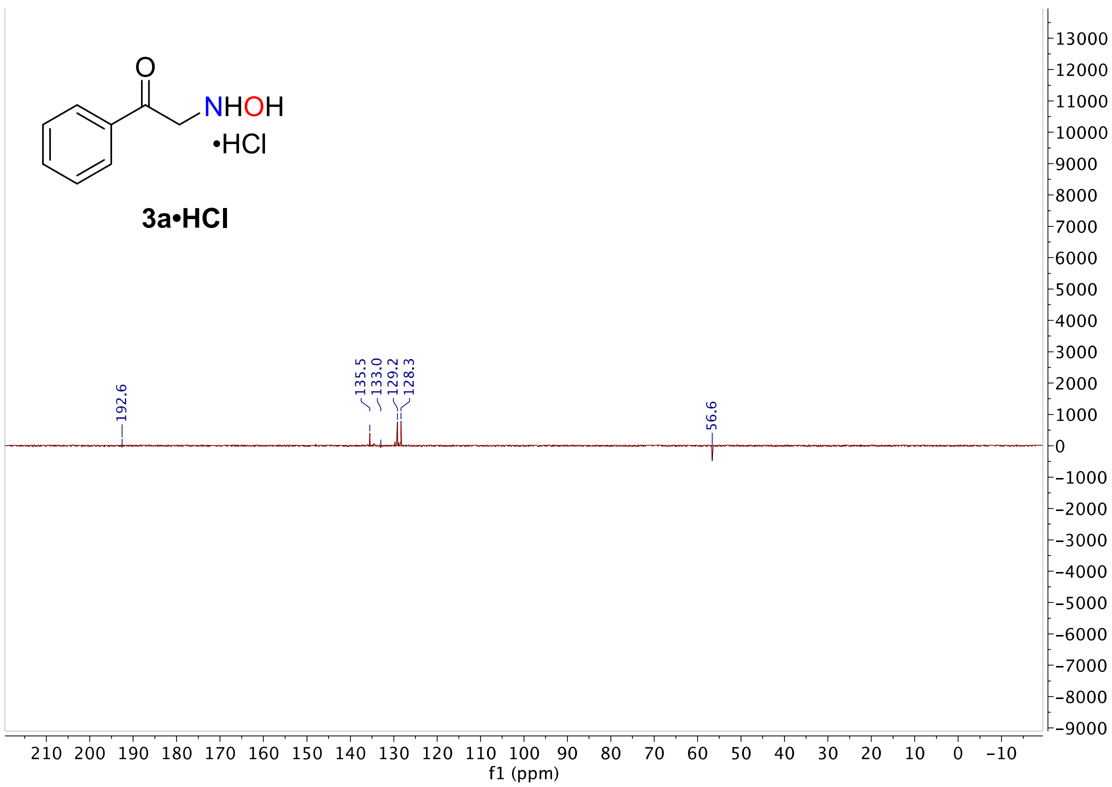

Figure S27. ^{13}C APT NMR spectrum (100.6 MHz) of 2-(hydroxyamino)-1-phenylethan-1-one hydrochloride (**3a•HCl**) in D_2O.

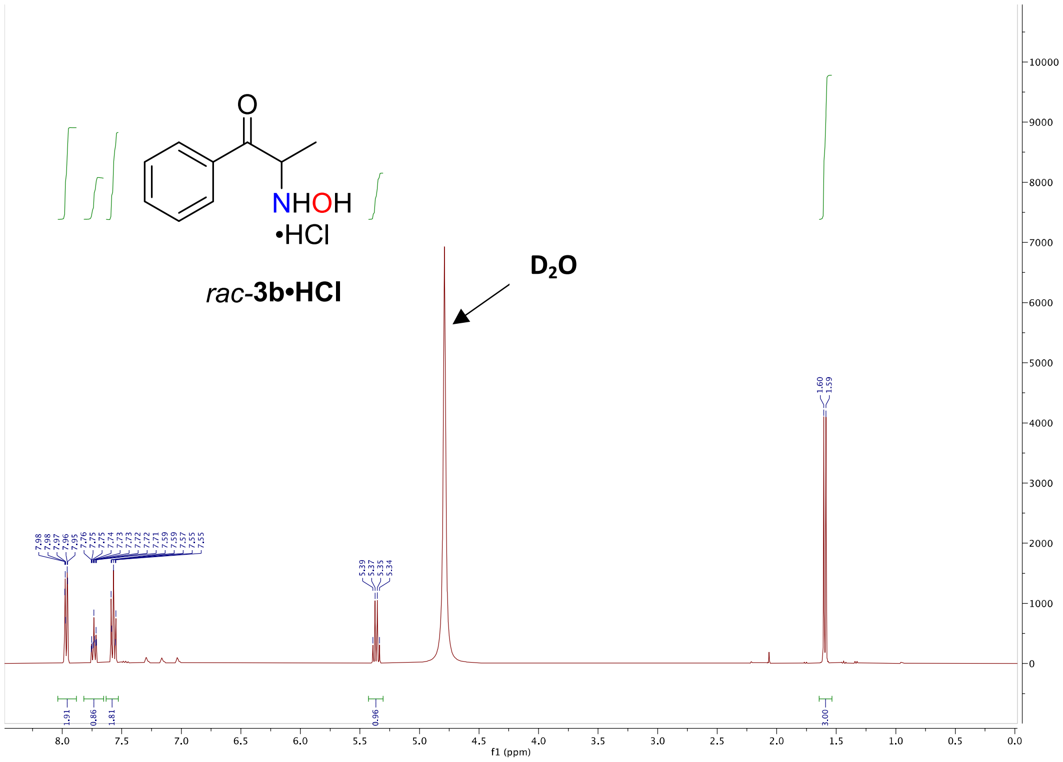

Figure S28. ^{1}H NMR spectrum (400 MHz) of 2-(hydroxyamino)-1-phenylpropan-1-one hydrochloride (*rac*-**3b•HCl**) in D_2O.

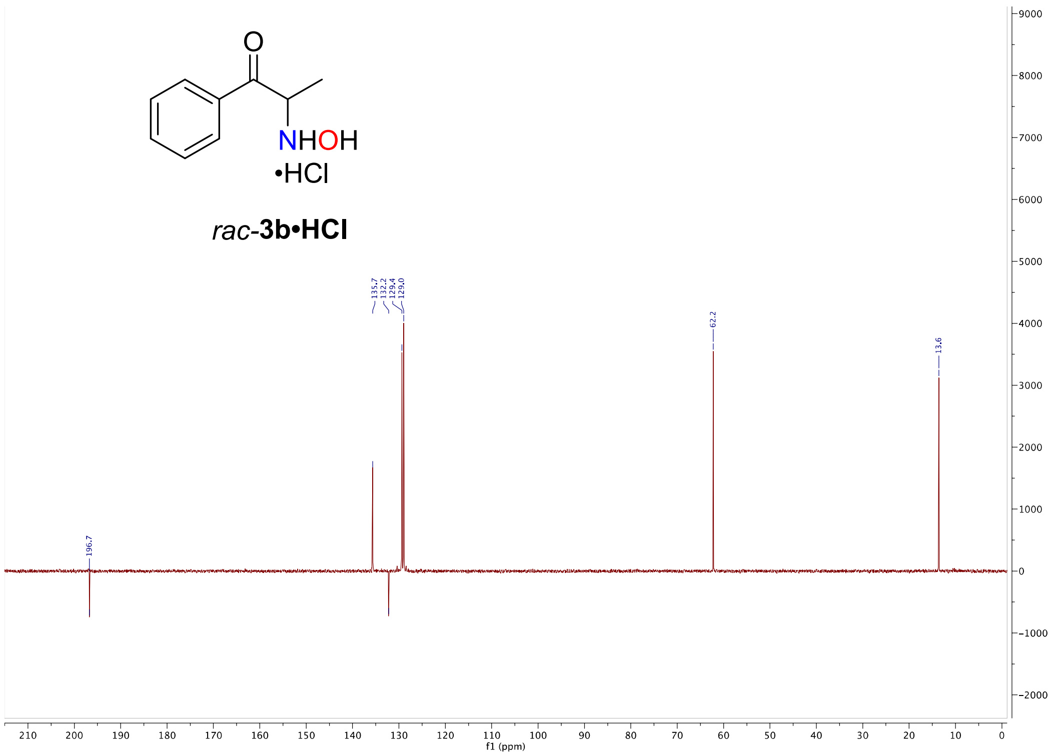

Figure S29. ^{13}C APT NMR spectrum (100.6 MHz) of (2-(hydroxyamino)-1-phenylpropan-1-one hydrochloride (*rac*-**3b•HCl**) in D_2O.

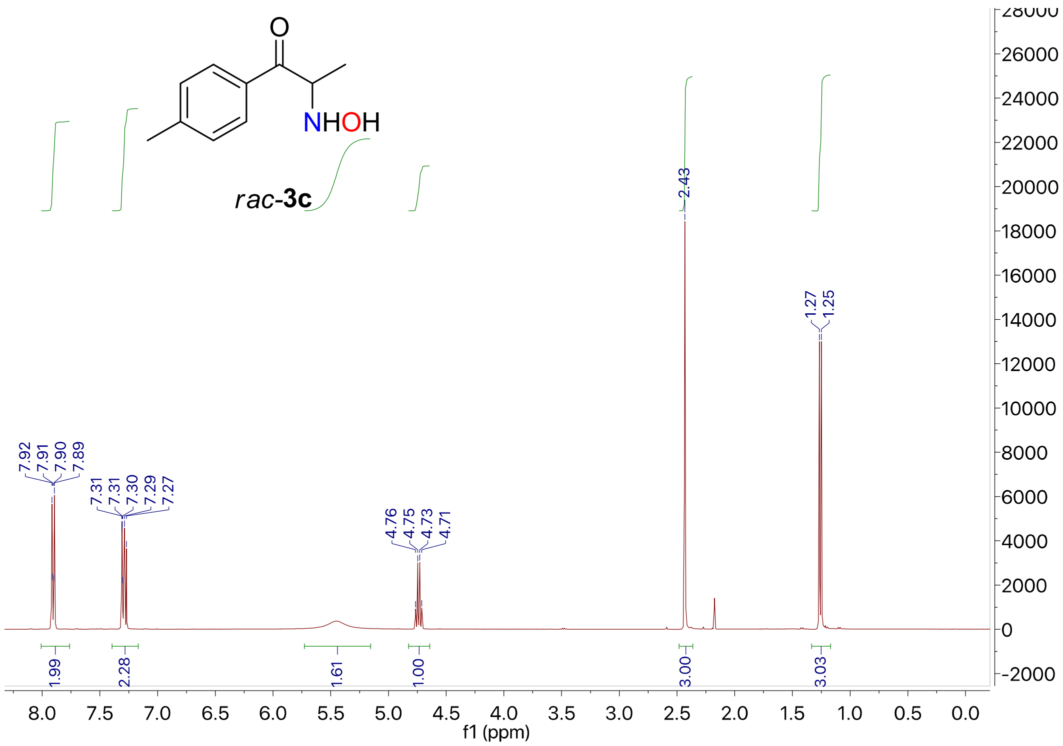

Figure S30. [1]H NMR spectrum (400 MHz) of 2-(hydroxyamino)-1-(*p*-tolyl)propan-1-one (*rac*-**3c**) in $CDCl_3$.

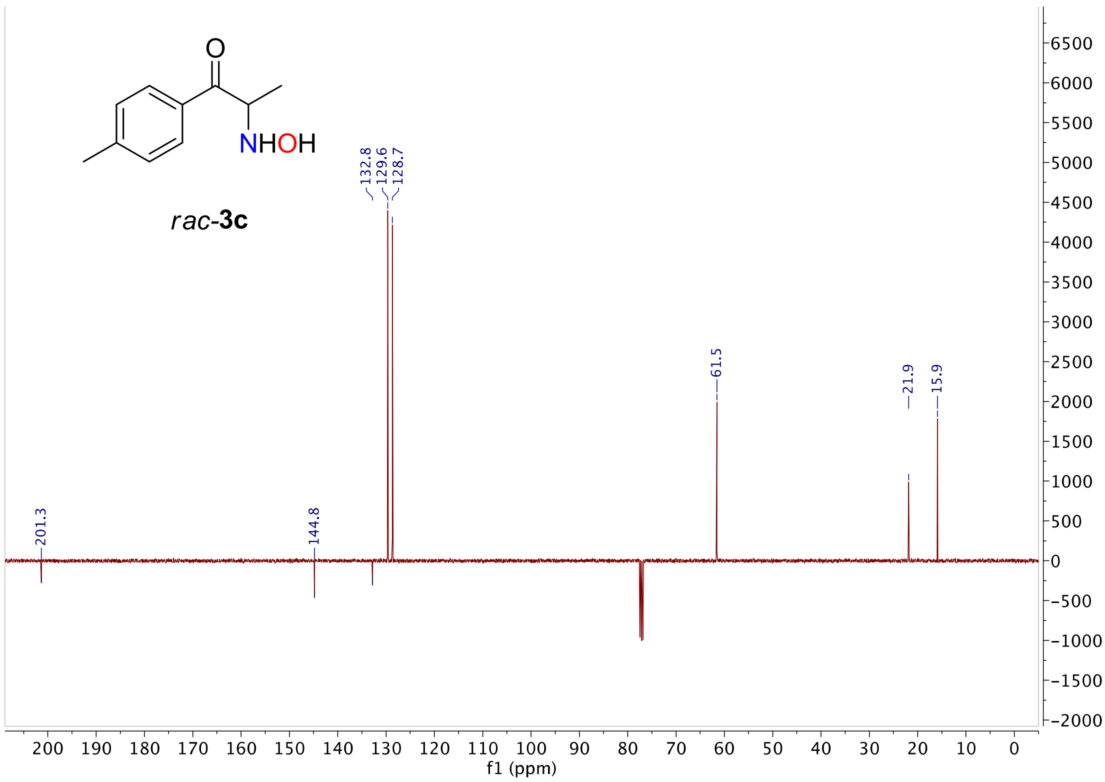

Figure S31. [13]C APT NMR spectrum (100.6 MHz) of 2-(hydroxyamino)-1-(*p*-tolyl)propan-1-one (*rac*-**3c**) in $CDCl_3$.

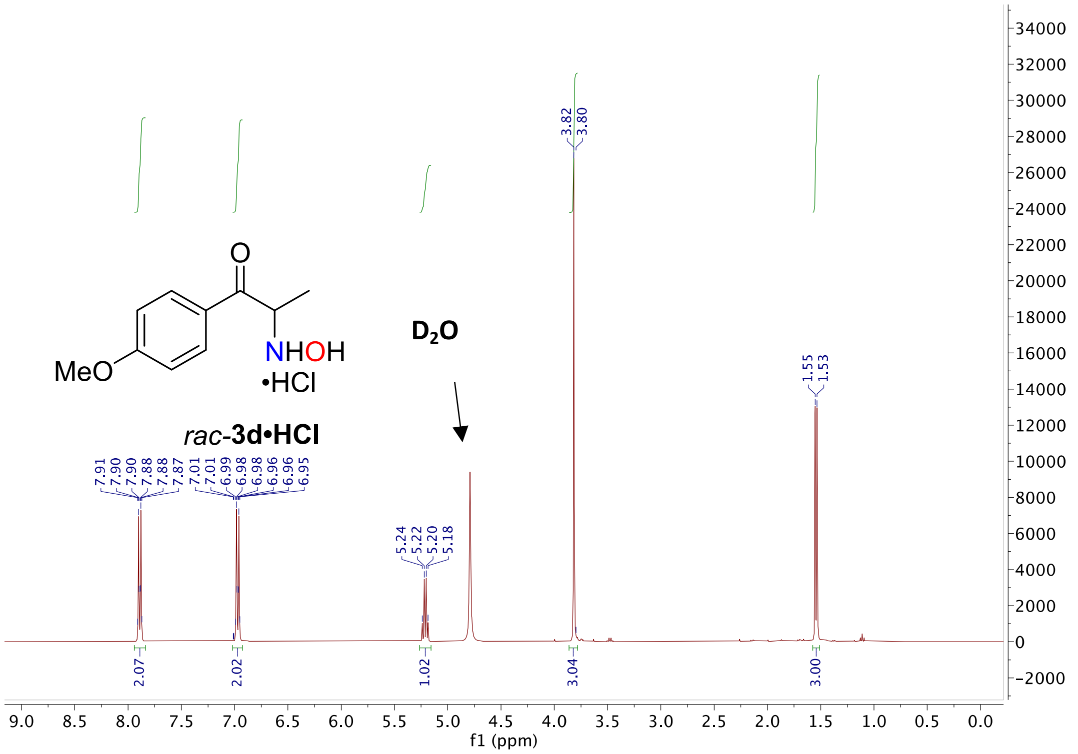

Figure S32. ^{1}H NMR spectrum (400 MHz) of 2-(hydroxyamino)-1-(4-methoxyphenyl)propan-1-one hydrochloride (*rac*-**3d•HCl**) in D_2O.

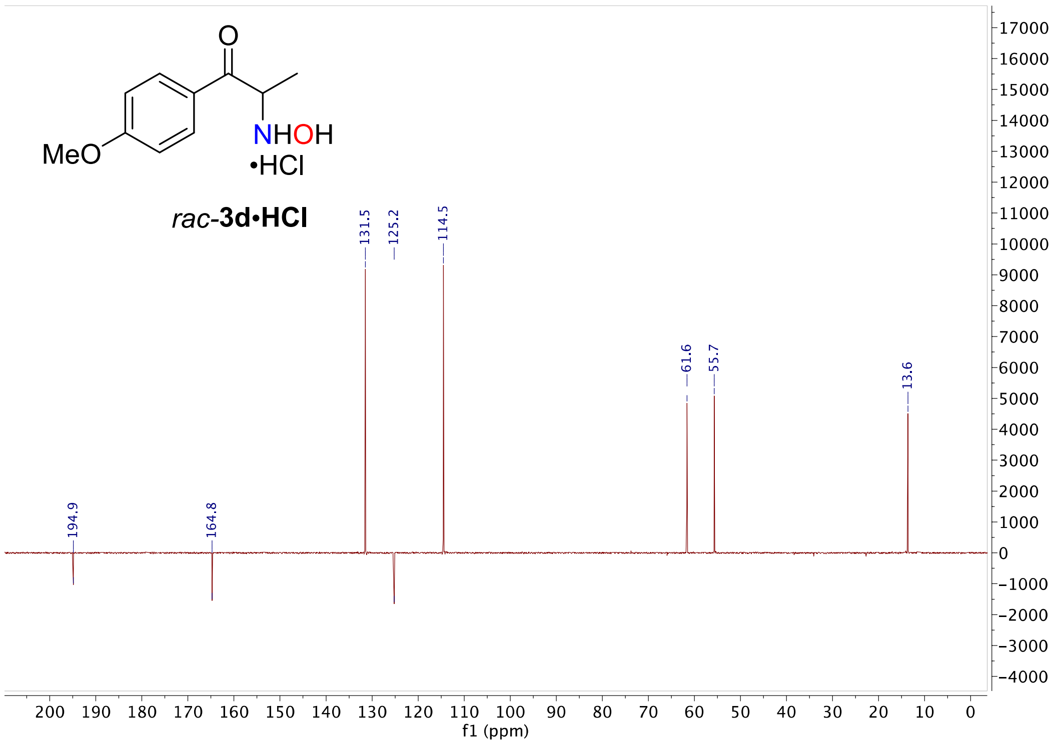

Figure S33. ^{13}C APT NMR spectrum (100.6 MHz) of 2-(hydroxyamino)-1-(4-methoxyphenyl)propan-1-one (*rac*-**3d•HCl**) hydrochloride in D_2O.

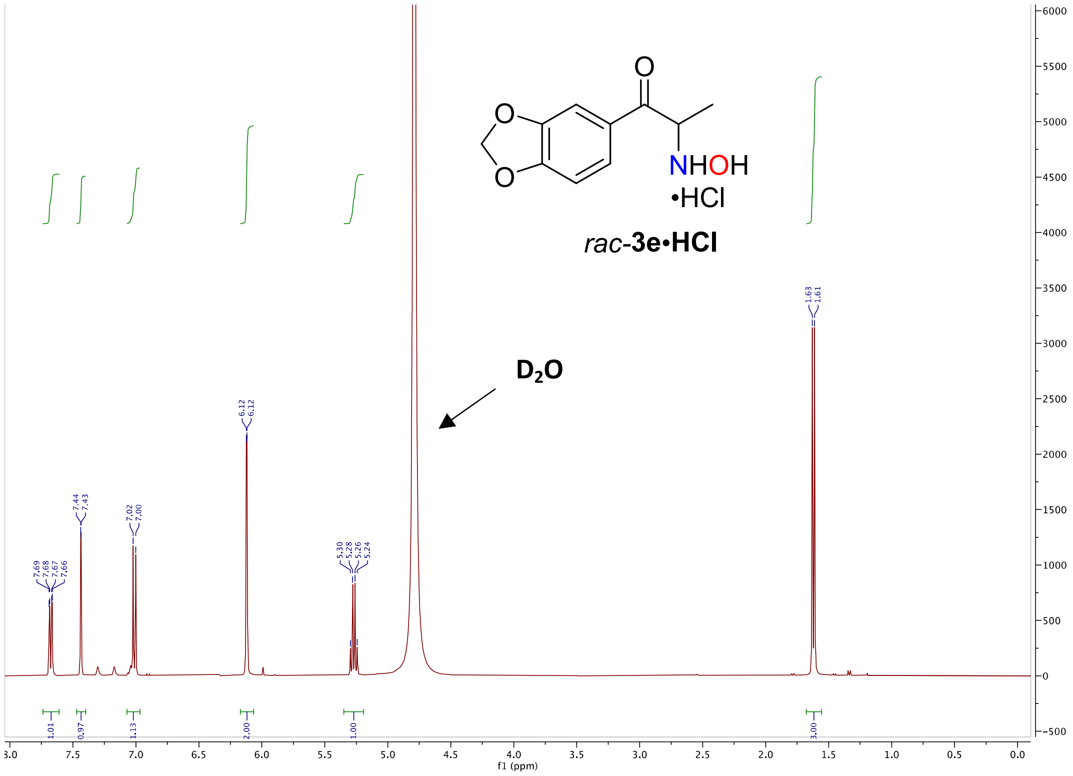

Figure S34. ¹H NMR spectrum (400 MHz) of 1-(benzo[*d*][1,3]dioxol-5-yl)-2-(hydroxyamino)propan-1-one hydrochloride (*rac*-**3e•HCl**) in D_2O.

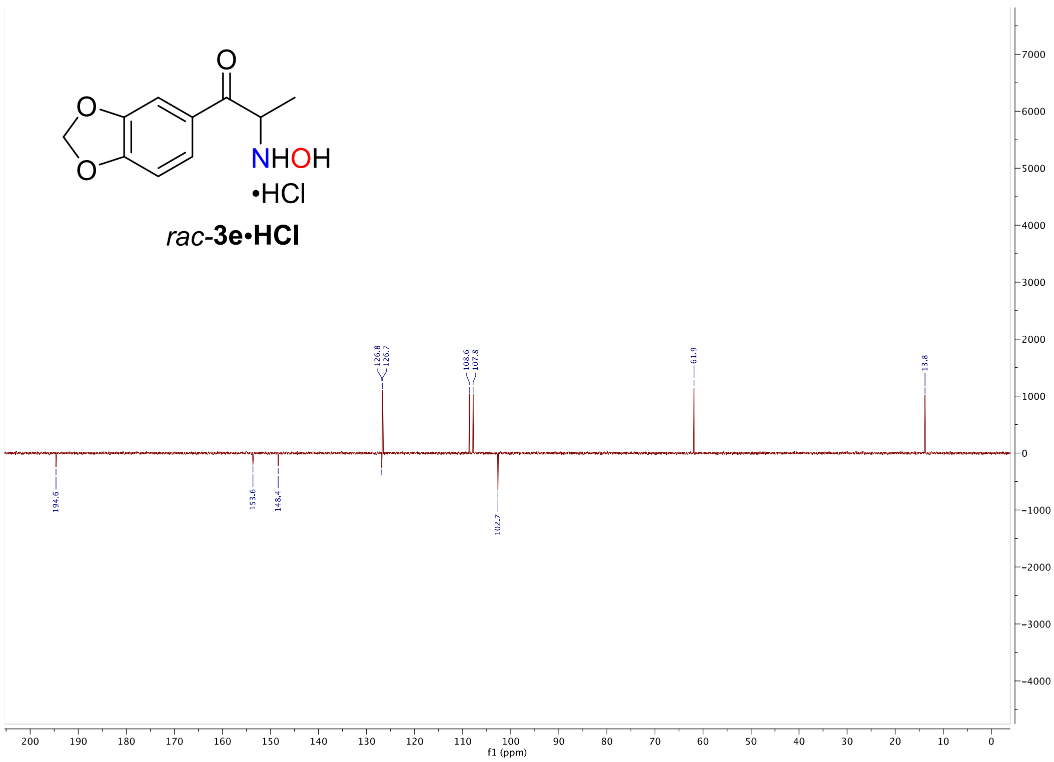

Figure S35. ^{13}C APT NMR spectrum (100.6 MHz) of 1-(benzo[*d*][1,3]dioxol-5-yl)-2-(hydroxyamino)propan-1-one hydrochloride (*rac*-**3e•HCl**) in D_2O.

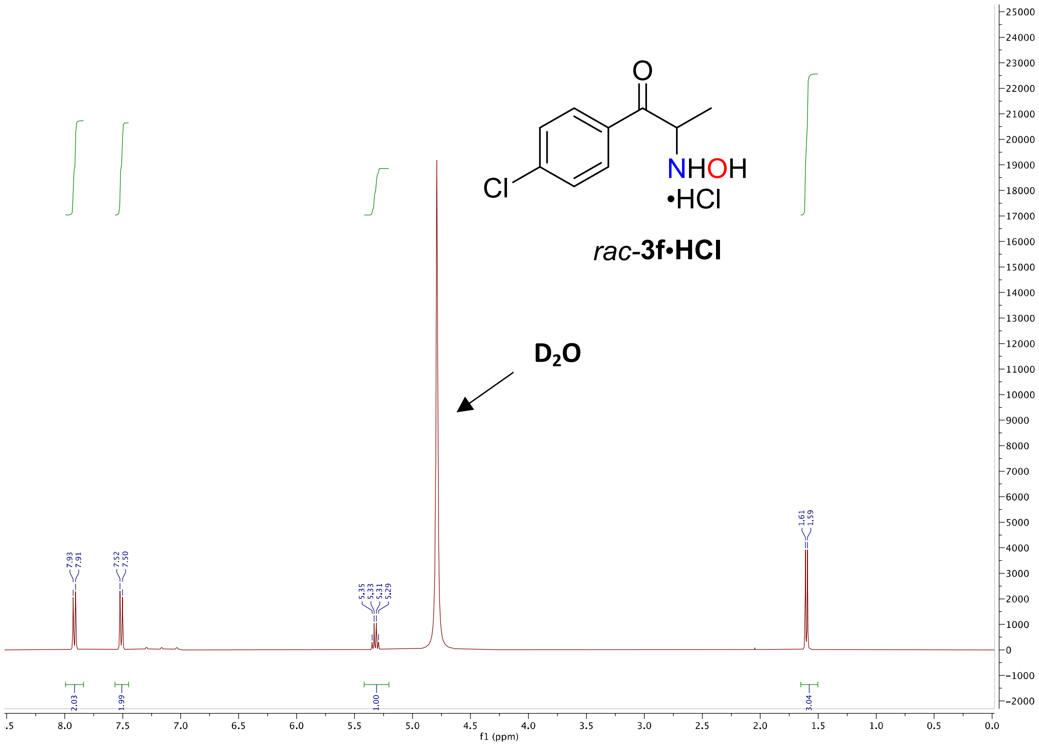

Figure S36. ^{1}H NMR spectrum (400 MHz) of 1-(4-chlorophenyl)-2-(hydroxyamino)propan-1-one hydrochloride (*rac*-**3f•HCl**) in D_2O.

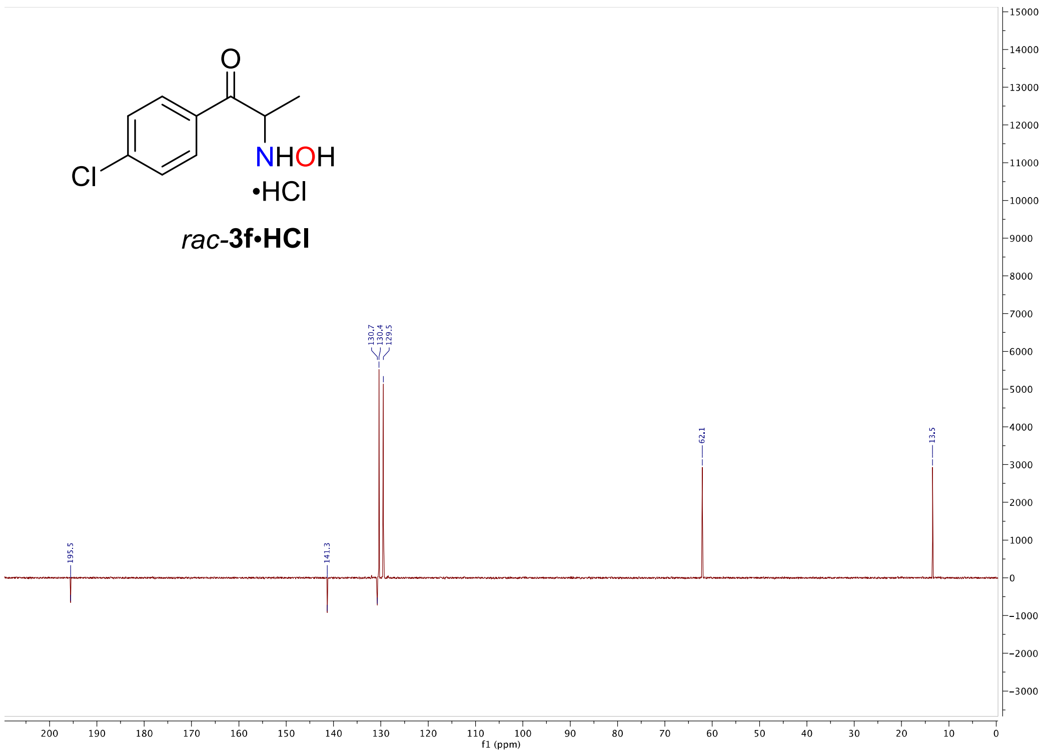

Figure S37. ^{13}C APT NMR spectrum (100.6 MHz) of 1-(4-chlorophenyl)-2-(hydroxyamino)propan-1-one hydrochloride (*rac*-**3f•HCl**) in D_2O.

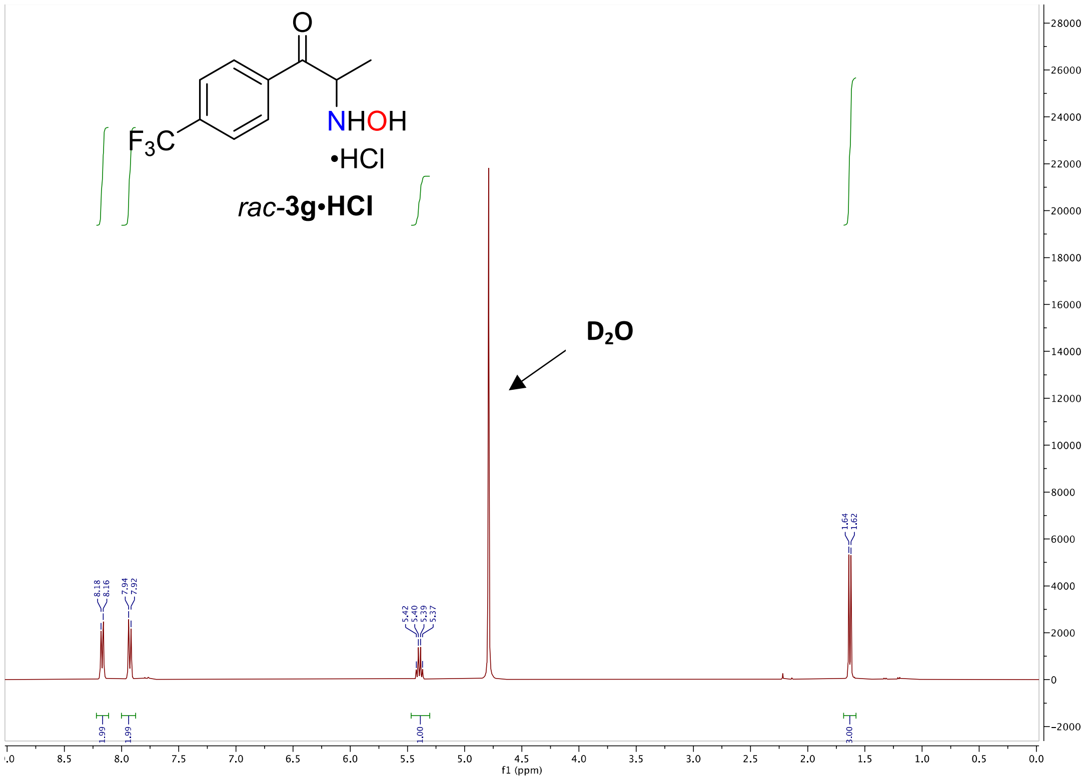

Figure S38. ^{1}H NMR spectrum (400 MHz) of 2-(hydroxyamino)-1-(4-(trifluoromethyl)phenyl)propan-1-one hydrochloride (*rac*-**3g•HCl**) in D_2O.

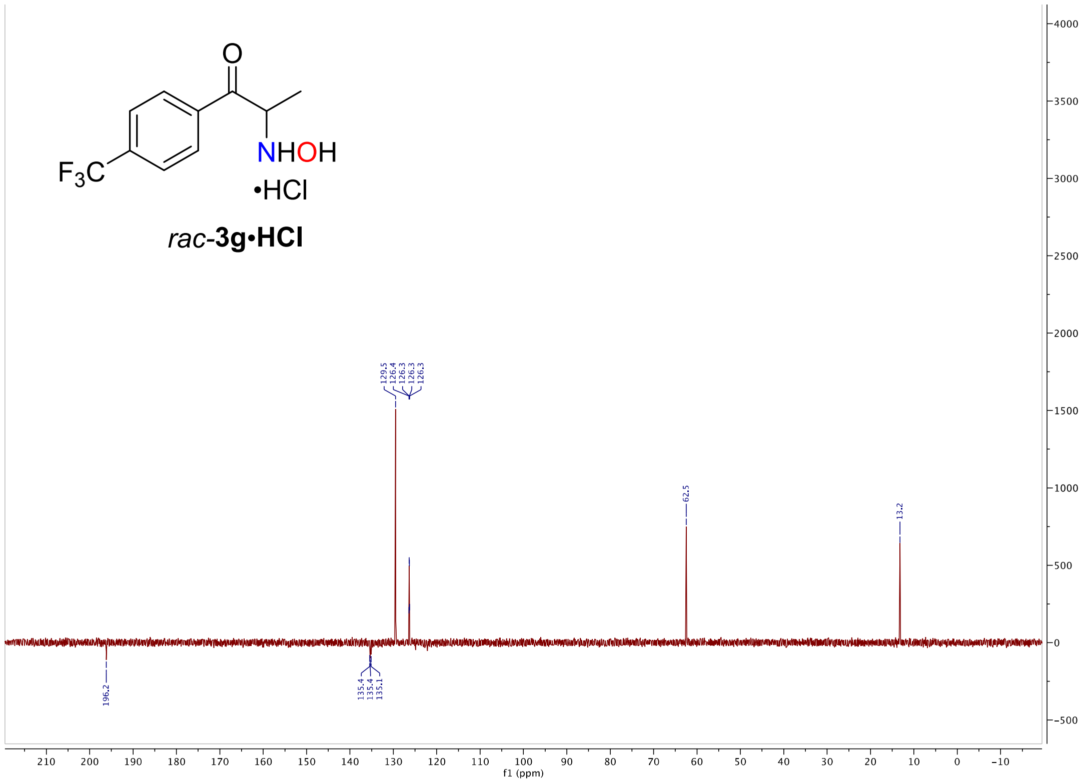

Figure S39. ^{13}C APT NMR spectrum (100.6 MHz) of 2-(hydroxyamino)-1-(4-(trifluoromethyl)phenyl)propan-1-one hydrochloride (*rac*-**3g•HCl**) in D_2O.

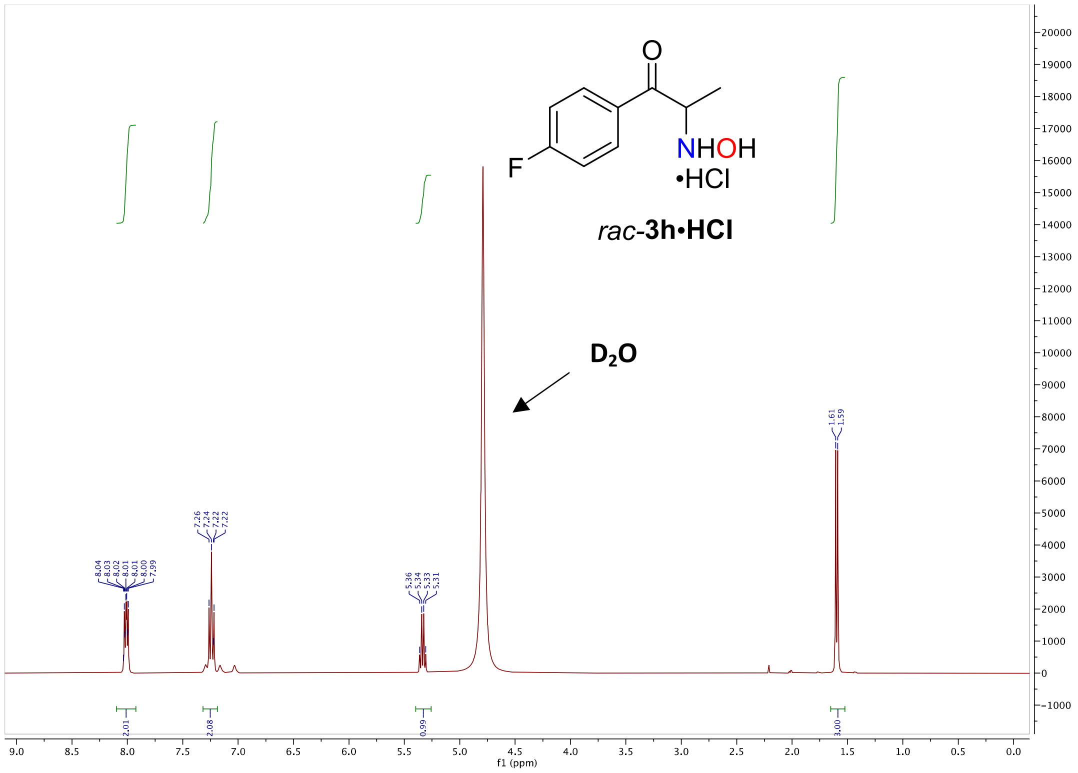

Figure S40. ^{1}H NMR spectrum (400 MHz) of 1-(4-fluorophenyl)-2-(hydroxyamino)propan-1-one hydrochloride (*rac*-**3h•HCl**) in D_2O.

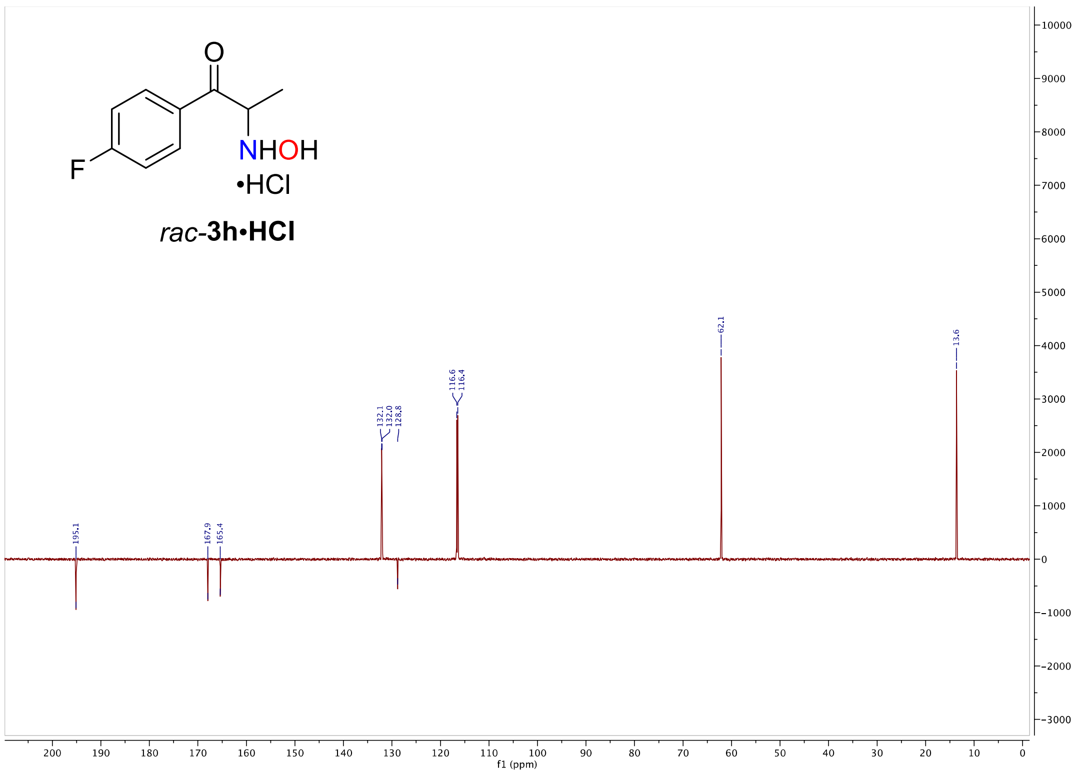

Figure S41. ^{13}C APT NMR spectrum (100.6 MHz) of 1-(4-fluorophenyl)-2-(hydroxyamino)propan-1-one hydrochloride (*rac*-**3h•HCl**) in D_2O.

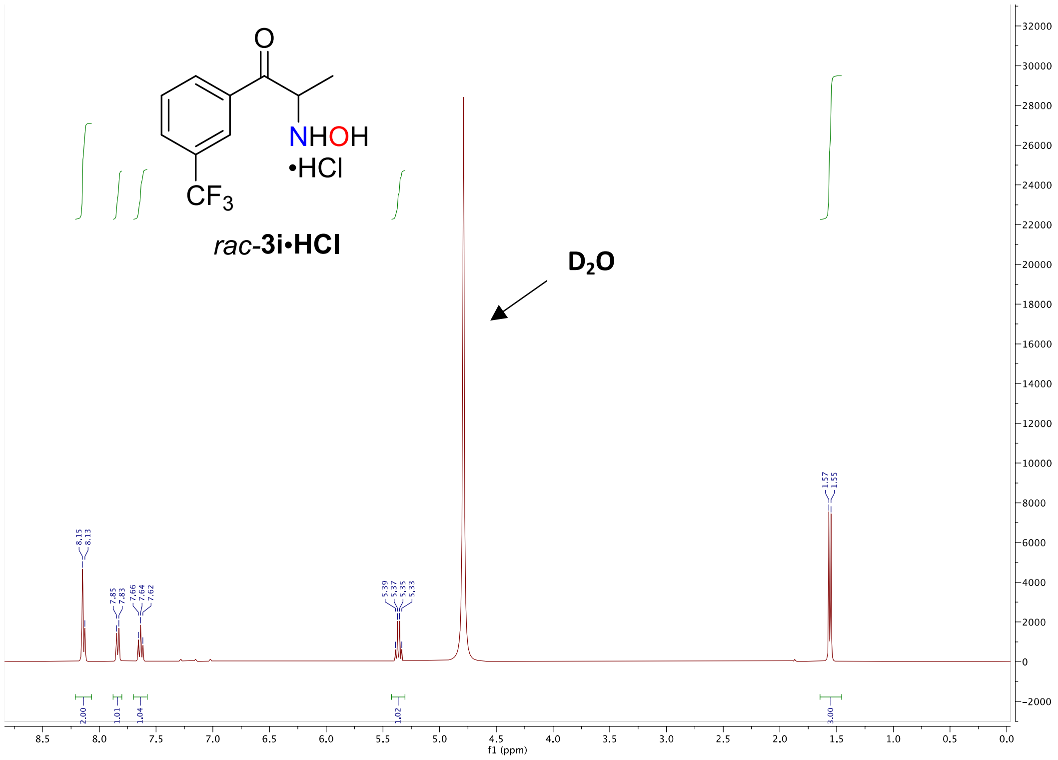

Figure S42 ^{1}H NMR spectrum (400 MHz) of 2-(hydroxyamino)-1-(3-(trifluoromethyl)phenyl)propan-1-one hydrochloride (**3i•HCl**) in D_2O.

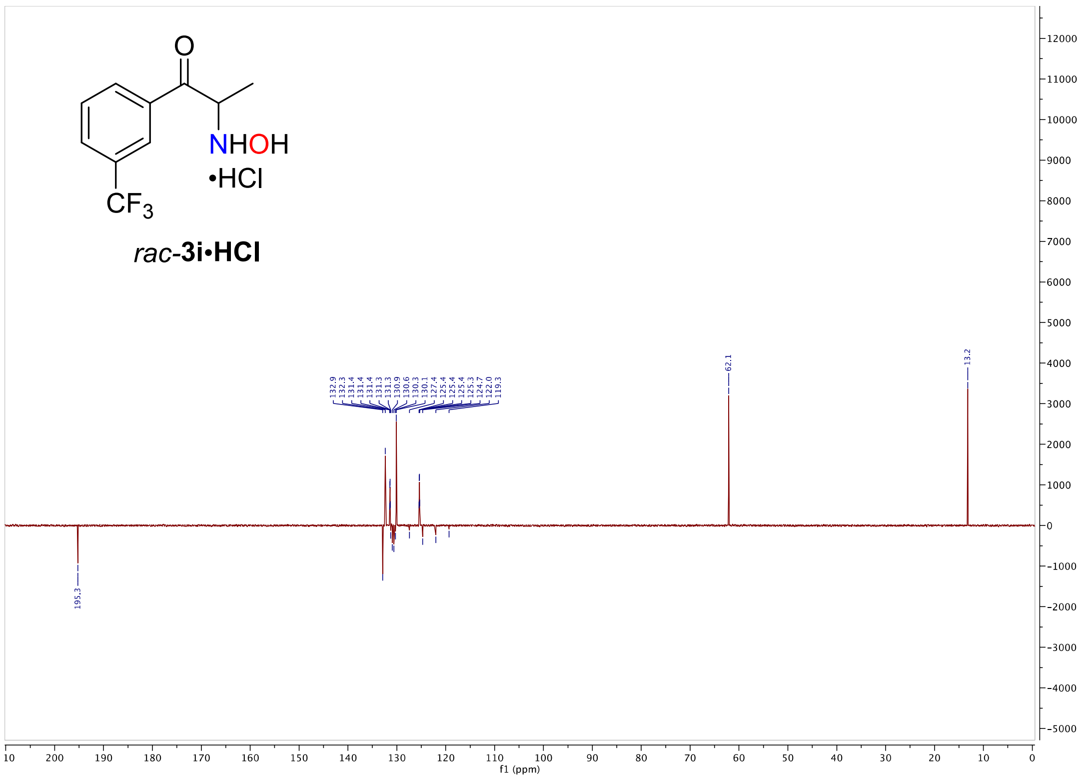

Figure S43. ^{13}C APT NMR spectrum (100.6 MHz) of 2-(hydroxyamino)-1-(3-(trifluoromethyl)phenyl)propan-1-one hydrochloride (*rac*-**3i•HCl**) in D_2O.

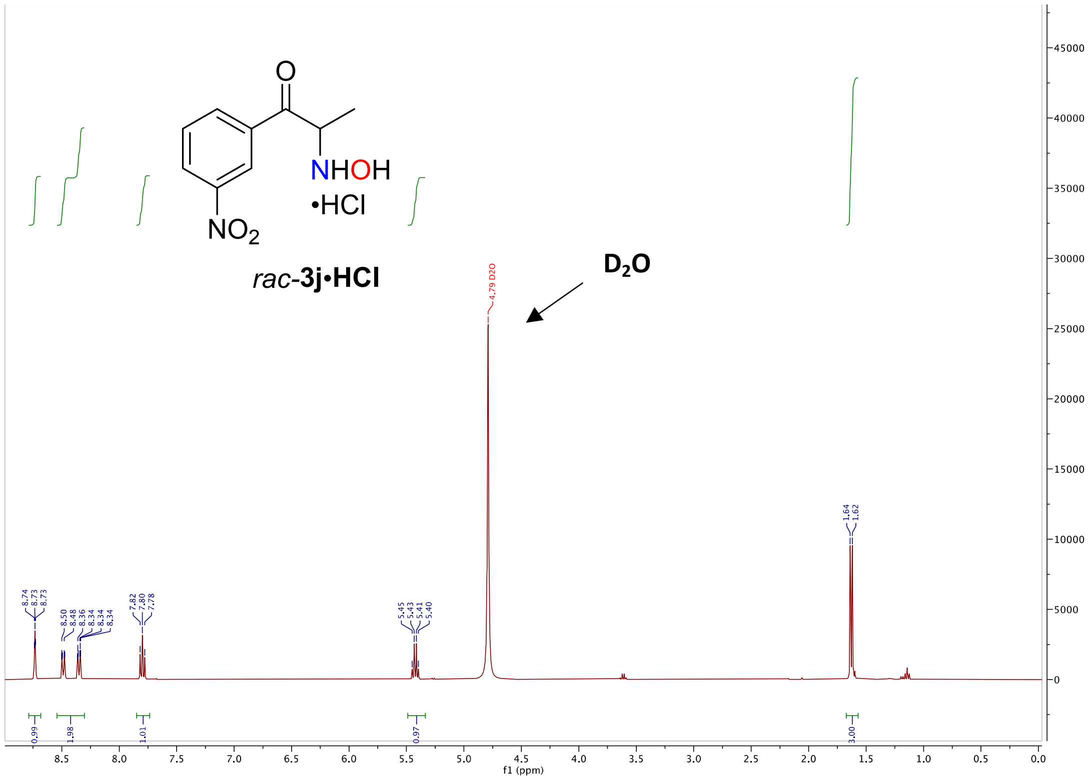

Figure S44. ^{1}H NMR spectrum (400 MHz) of 2-(hydroxyamino)-1-(3-nitrophenyl)propan-1-one hydrochloride (*rac*-**3j•HCl**) in D_2O.

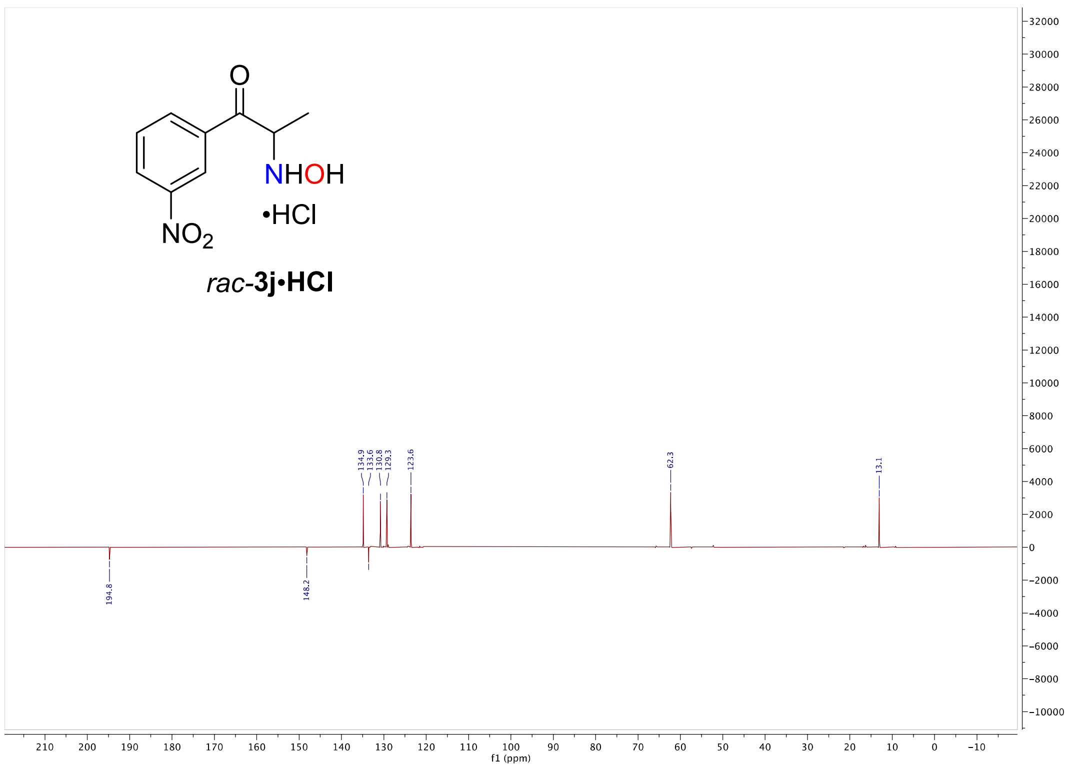

Figure S45. ^{13}C APT NMR spectrum (100.6 MHz) of 2-(hydroxyamino)-1-(3-nitrophenyl)propan-1-one hydrochloride (*rac*-**3j•HCl**) in D_2O.

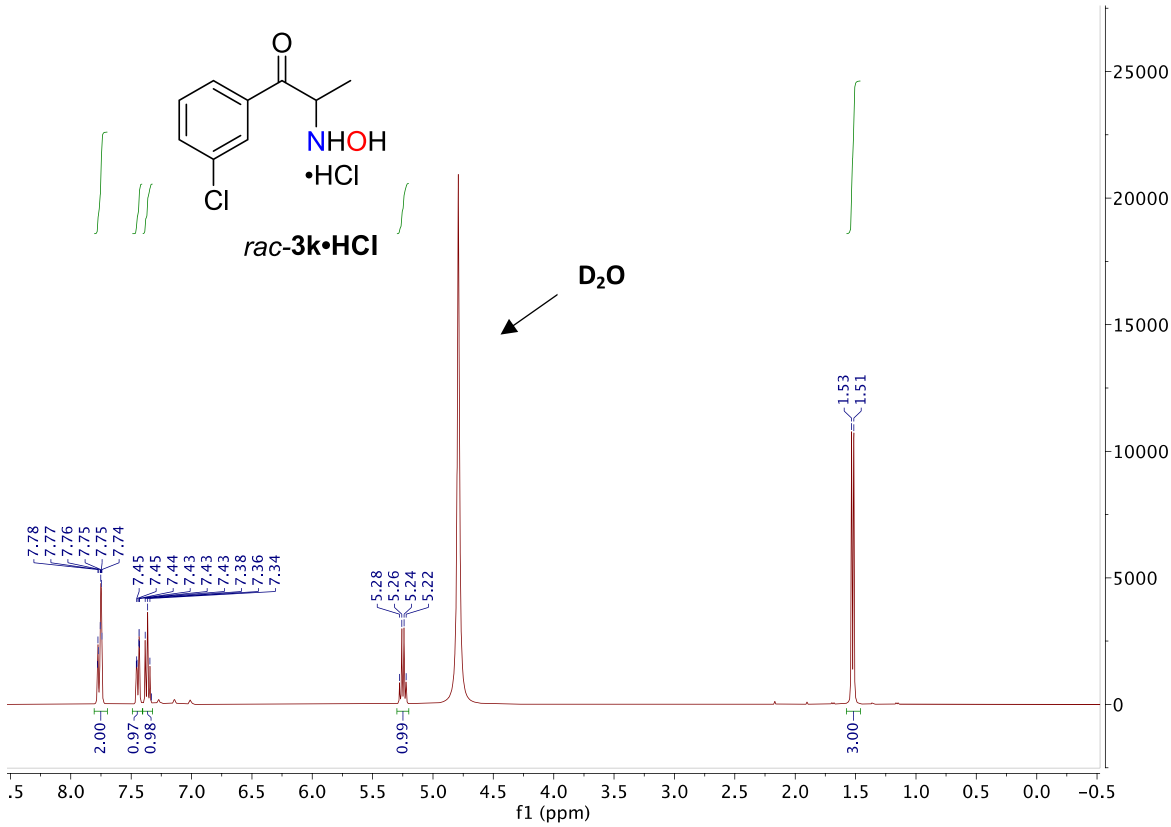

Figure S46. ^{1}H NMR spectrum (400 MHz) of 1-(3-chlorophenyl)-2-(hydroxyamino)propan-1-one hydrochloride (*rac*-**3k•HCl**) in D_2O.

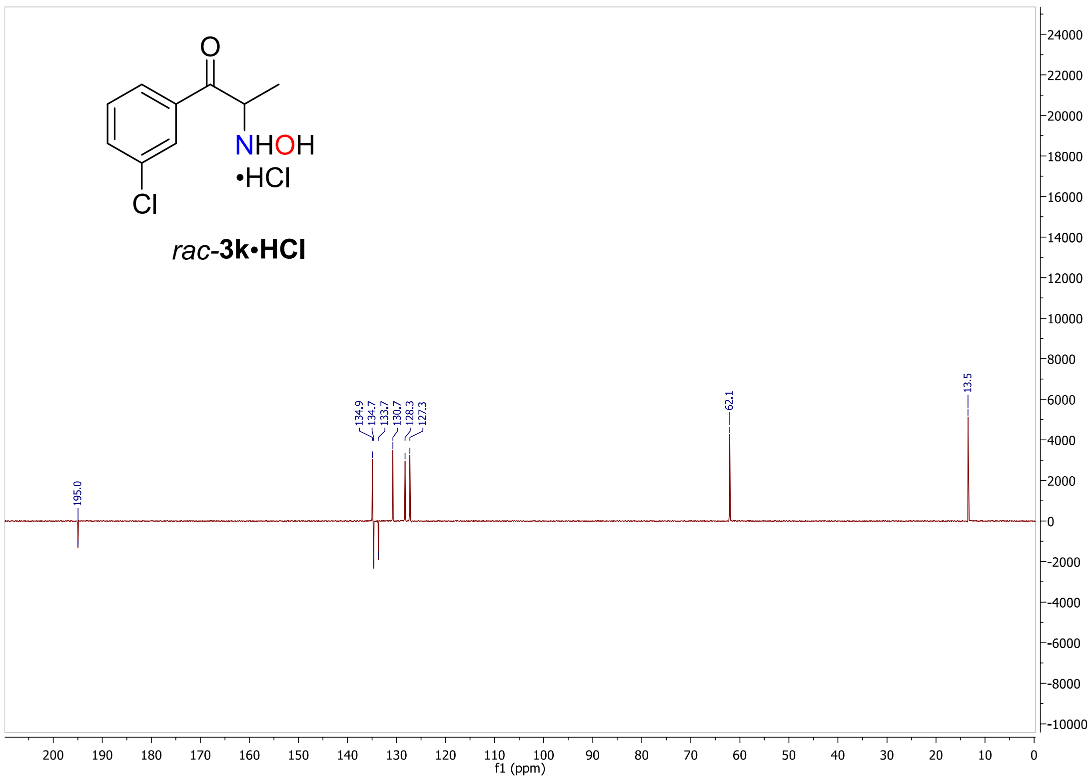

Figure S47. ^{13}C APT NMR spectrum (100.6 MHz) of 1-(3-chlorophenyl)-2-(hydroxyamino)propan-1-one hydrochloride (*rac*-**3k•HCl**) in D_2O.

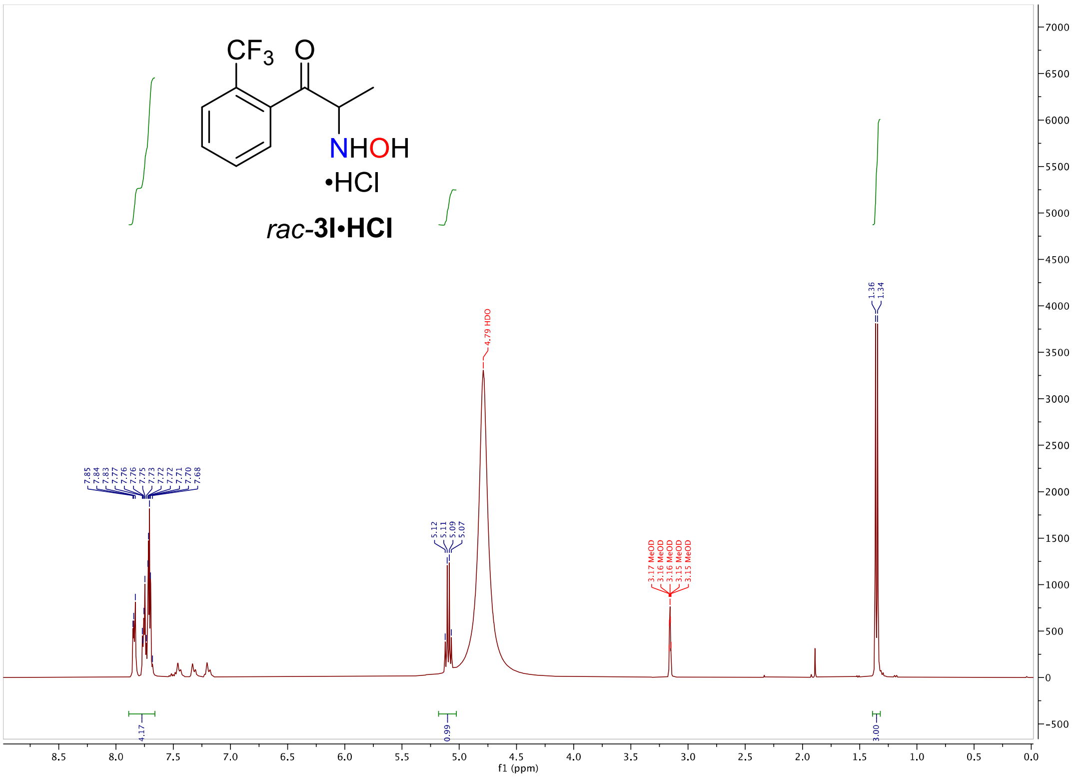

Figure S48. ^{1}H NMR spectrum (400 MHz) of 2-(hydroxyamino)-1-(2-(trifluoromethyl)phenyl)propan-1-one hydrochloride (*rac*-**3l•HCl**) in MeOD/D_2O.

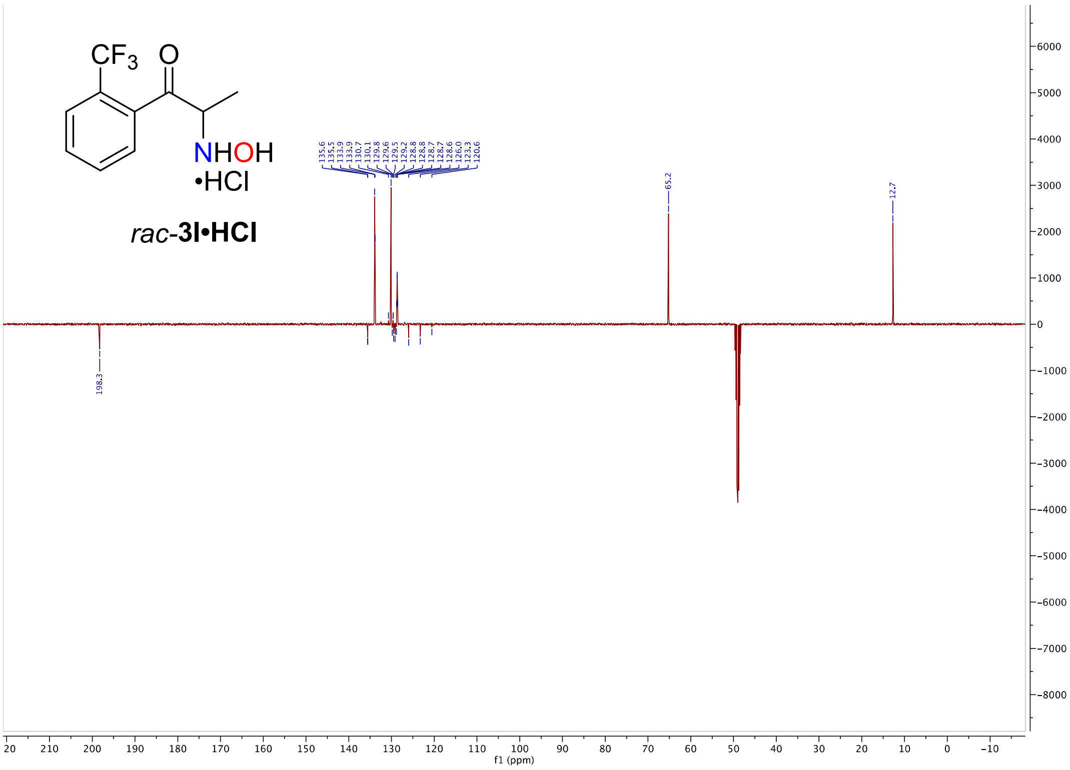

Figure S49. ^{13}C APT NMR spectrum (100.6 MHz) of 2-(hydroxyamino)-1-(2-(trifluoromethyl)phenyl)propan-1-one hydrochloride (*rac*-**3l•HCl**) in MeOD/D_2O.

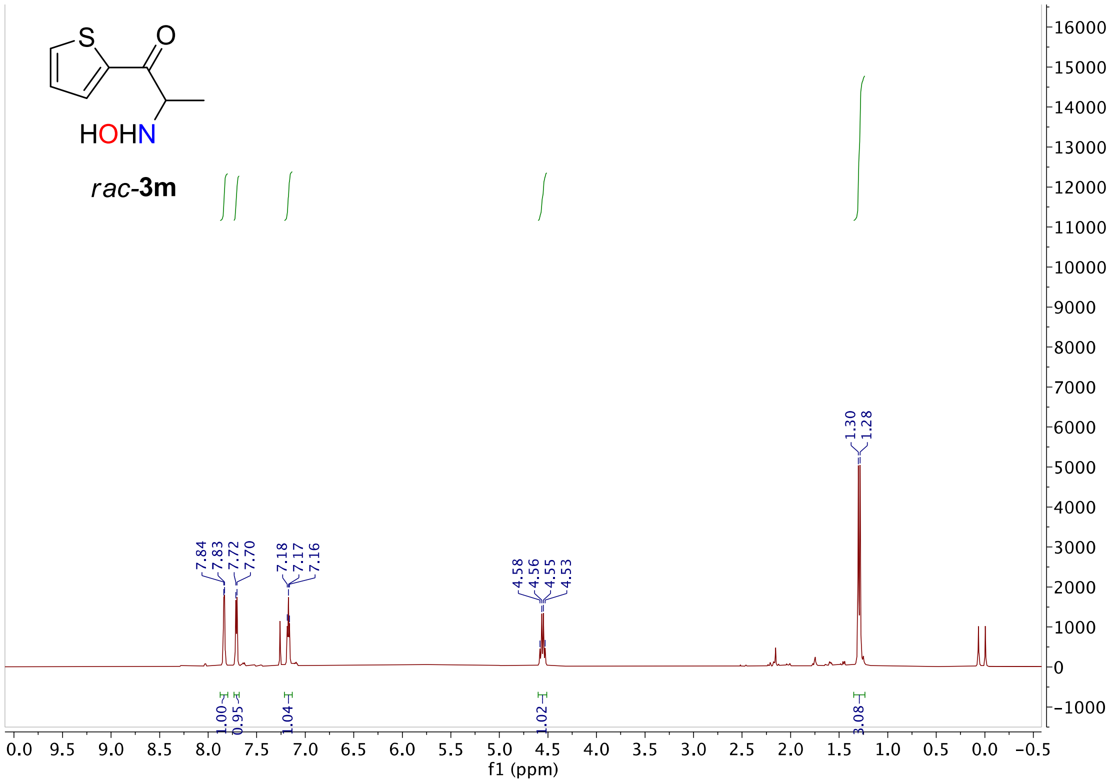

Figure S50. ^{1}H NMR spectrum (400 MHz) of 2-(hydroxyamino)-1-(thiophen-2-yl)propan-1-one (*rac*-**3m**) in $CDCl_3$.

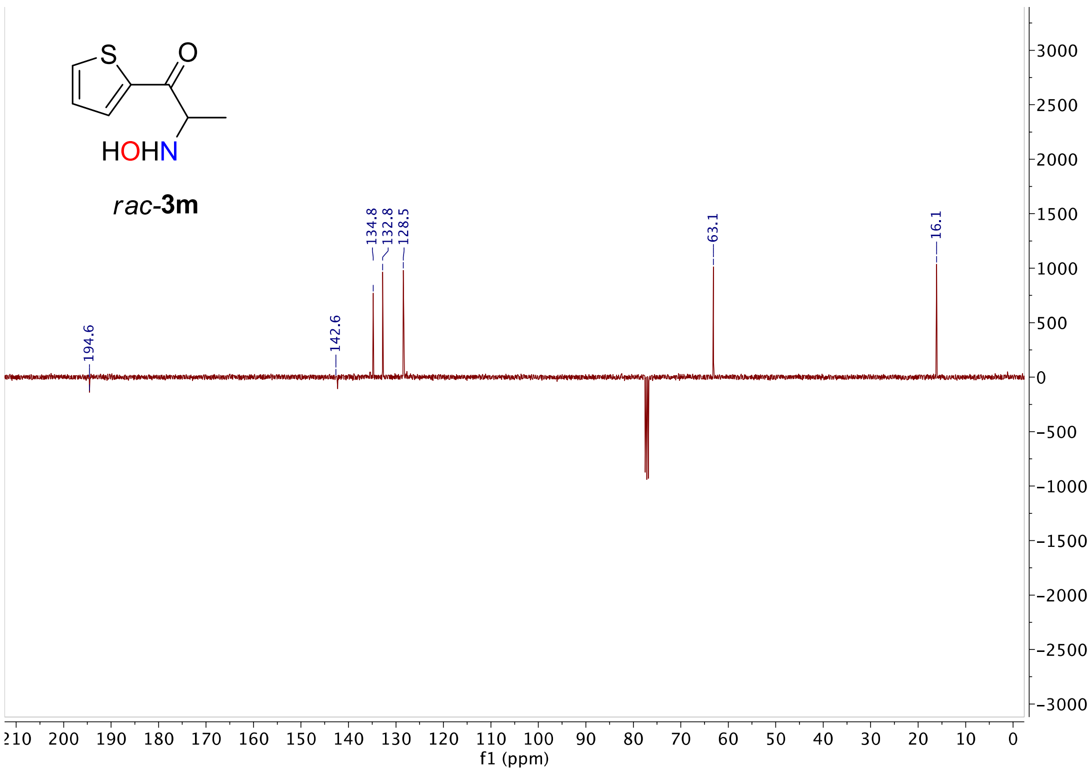

Figure S51. ^{13}C APT NMR spectrum (100.6 MHz) of 2-(hydroxyamino)-1-(thiophen-2-yl)propan-1-one (*rac*-**3m**) in $CDCl_3$.

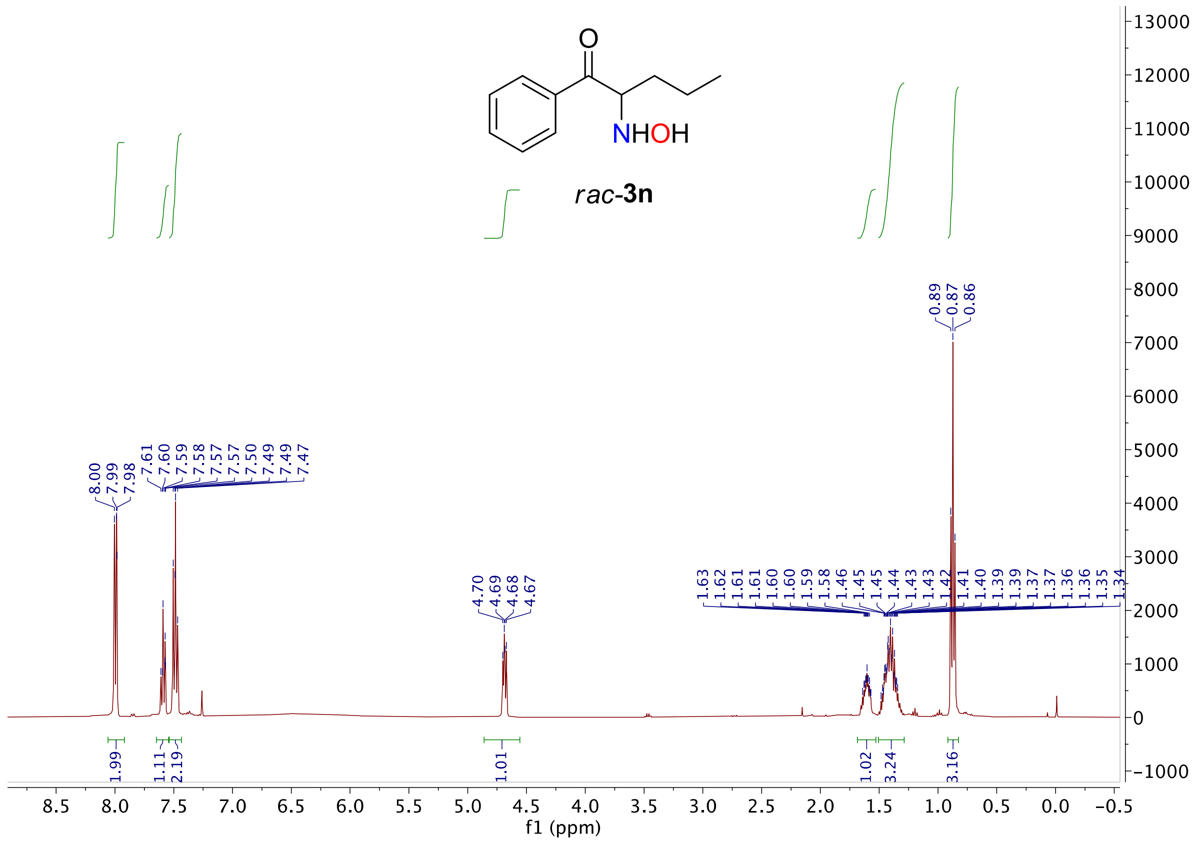

Figure S52. [1]H NMR spectrum (400 MHz) of 2-(hydroxyamino)-1-phenylpentan-1-one (*rac*-**3n**) in $CDCl_3$.

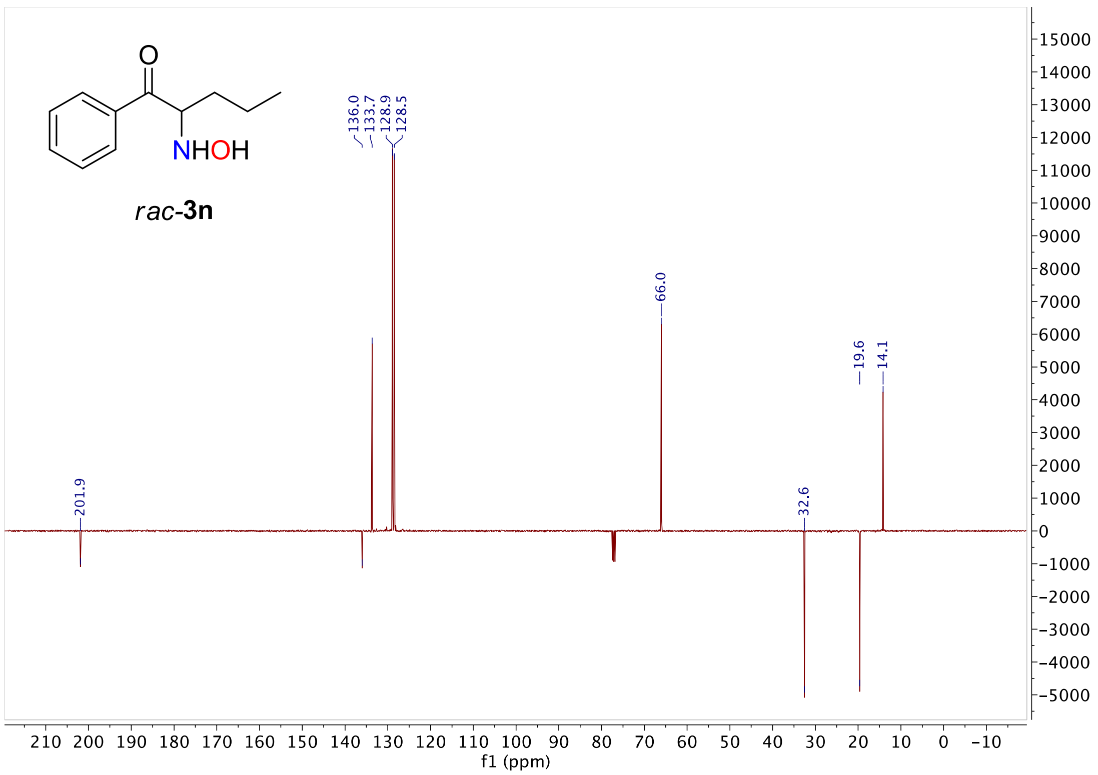

Figure S53. [13]C APT NMR spectrum (100.6 MHz) of 2-(hydroxyamino)-1-phenylpentan-1-one (*rac*-**3n**) in $CDCl_3$.

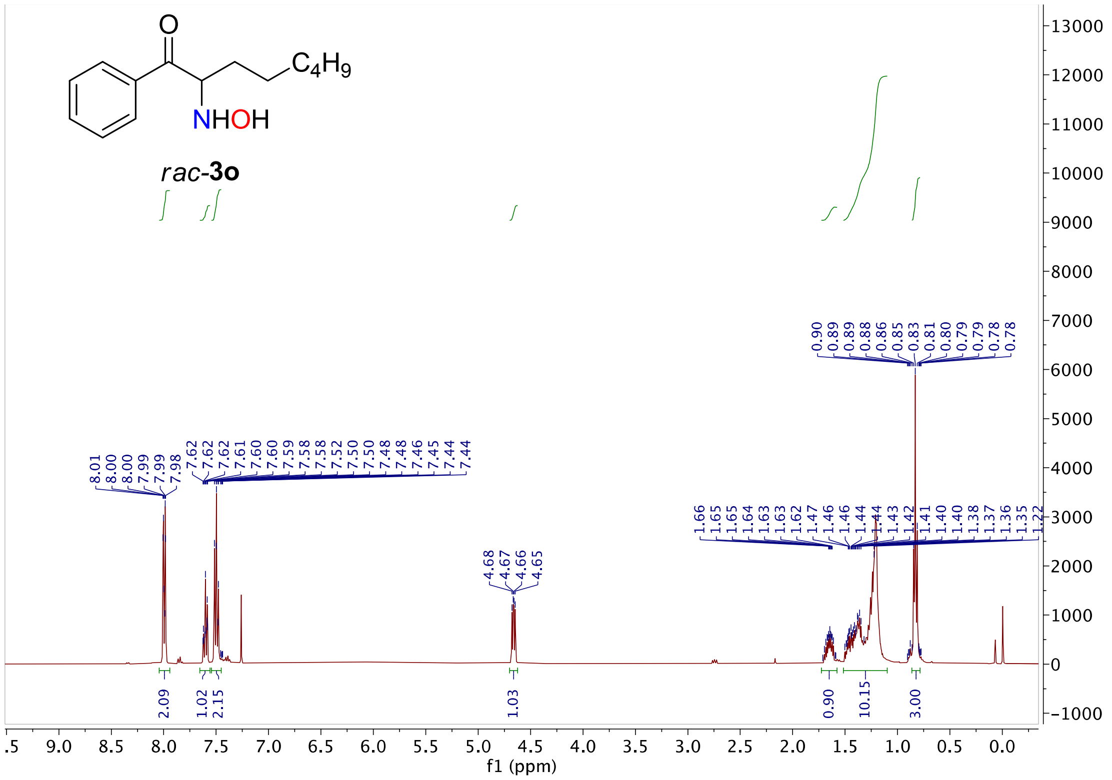

Figure S54. ^{1}H NMR spectrum (400 MHz) of 2-(hydroxyamino)-1-phenyloctan-1-one (*rac*-**3o**) in $CDCl_3$.

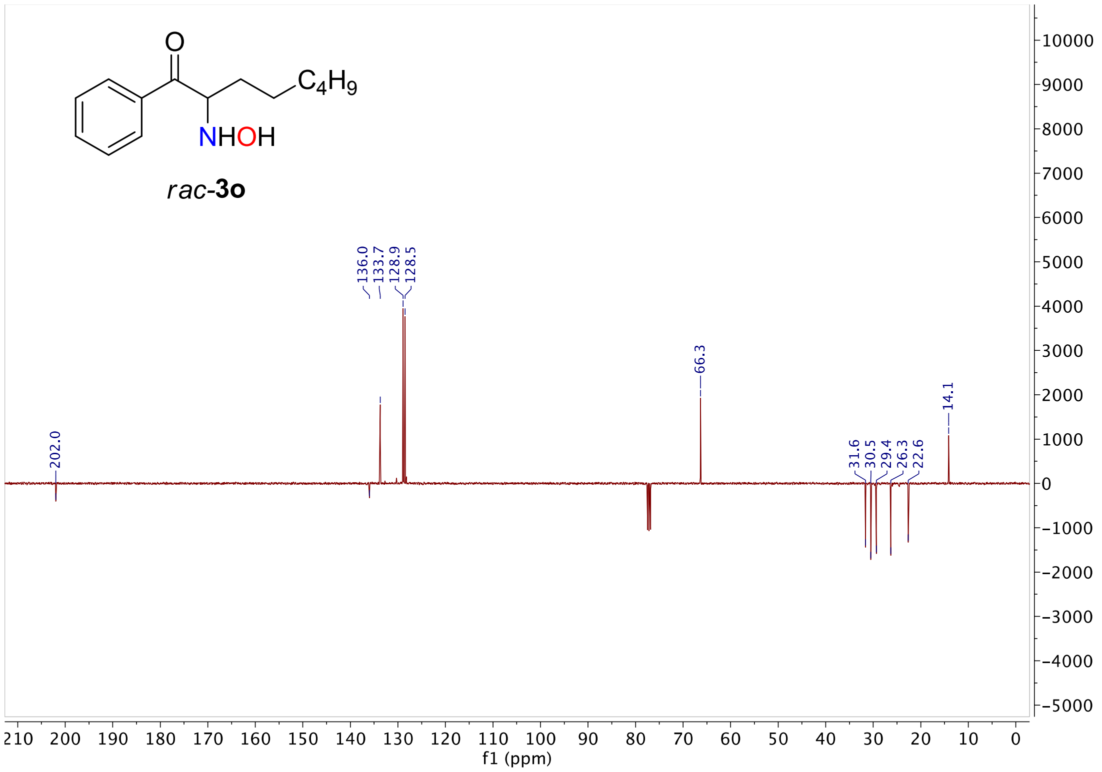

Figure S55. ^{13}C APT NMR spectrum (100.6 MHz) of 2-(hydroxyamino)-1-phenyloctan-1-one (*rac*-**3o**) in $CDCl_3$.

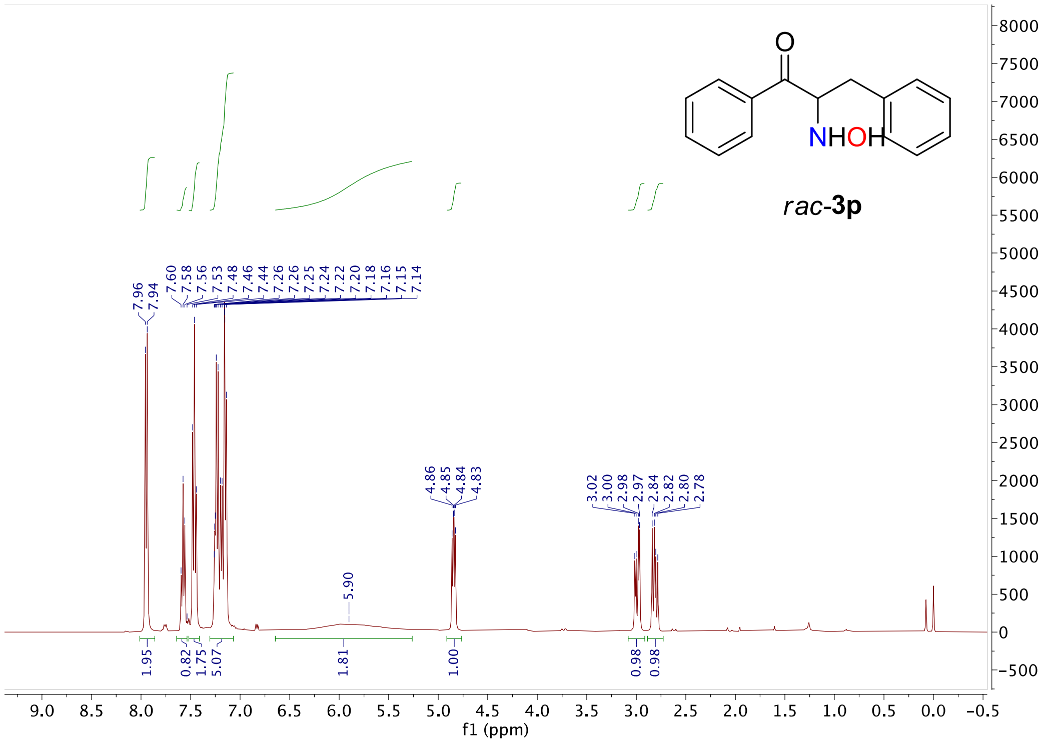

Figure S56. ^{1}H NMR spectrum (400 MHz) of 2-(hydroxyamino)-1,3-diphenylpropan-1-one (*rac*-**3p**) in $CDCl_3$.

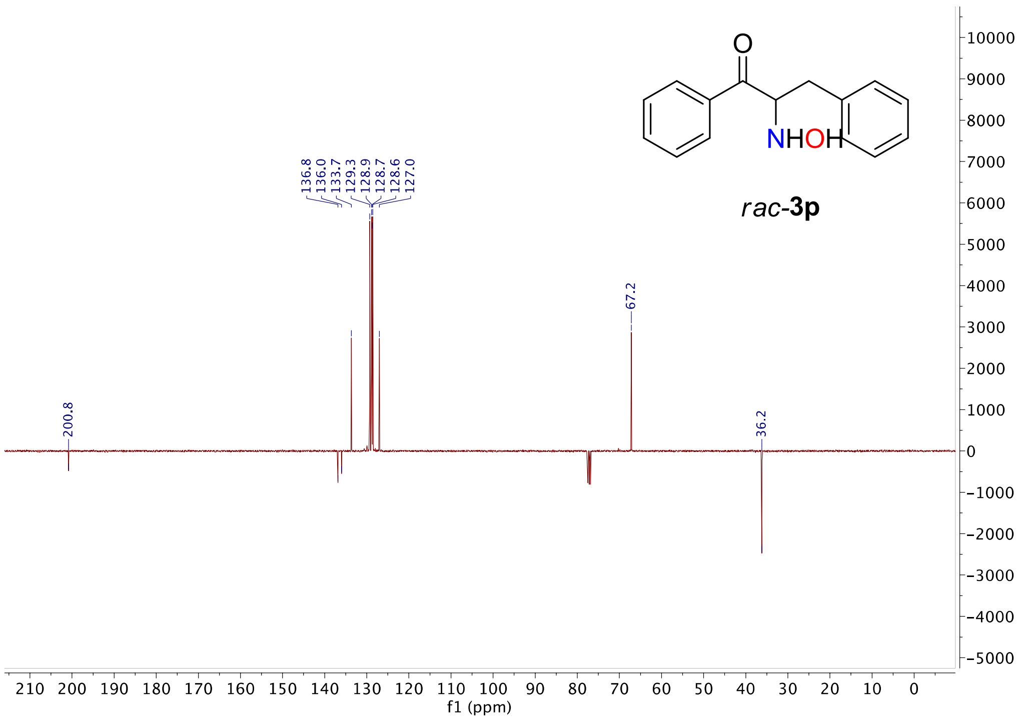

Figure S57. ^{13}C APT NMR spectrum (100.6 MHz) of 2-(hydroxyamino)-1,3-diphenylpropan-1-one (*rac*-**3p**) in $CDCl_3$.

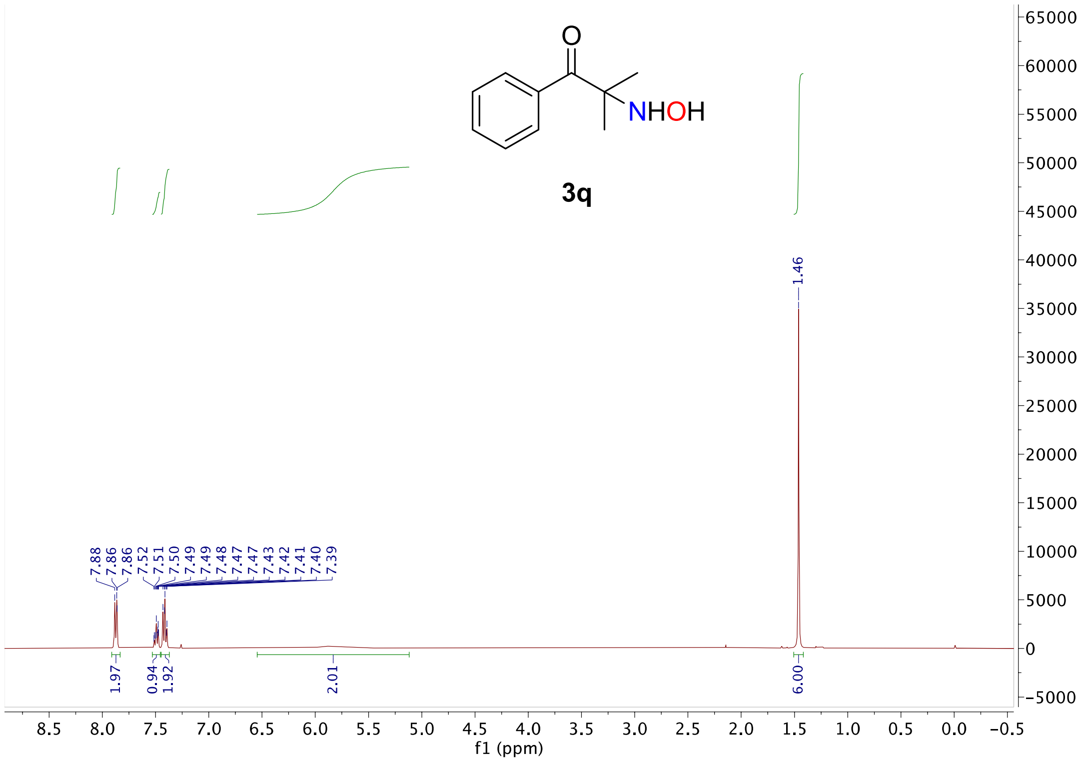

Figure S58. ^{1}H NMR spectrum (400 MHz) of 2-(hydroxyamino)-2-methyl-1-phenylpropan-1-one (**3q**) in $CDCl_3$.

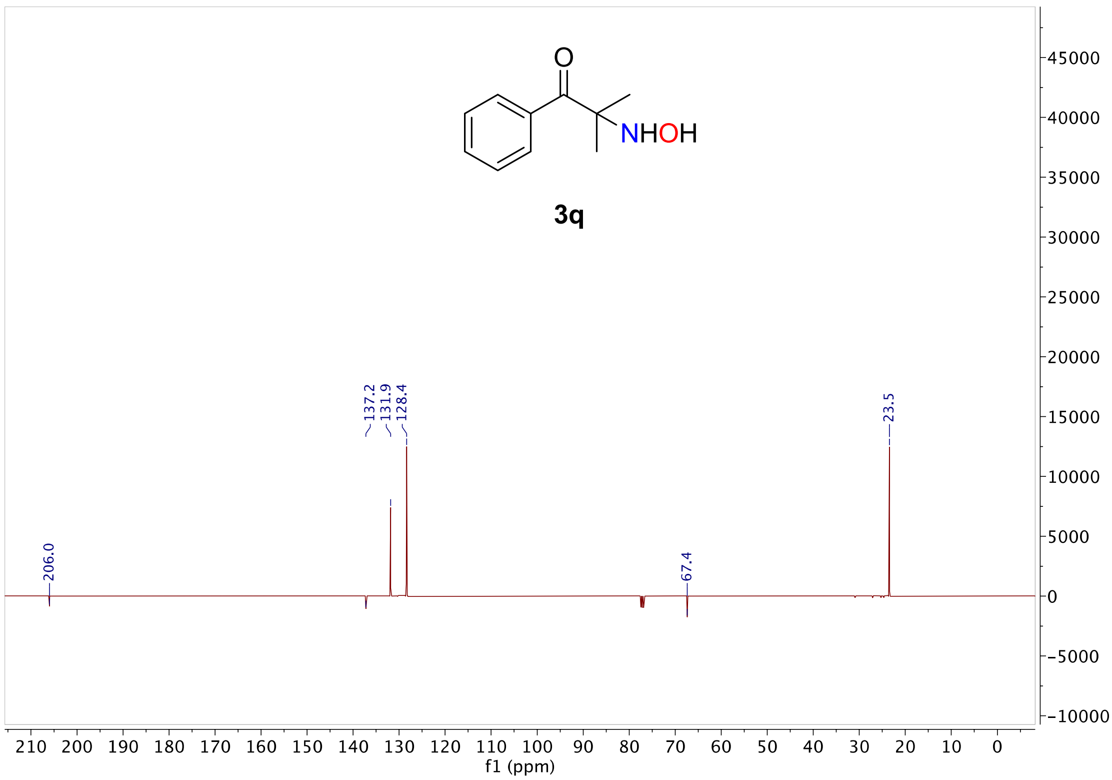

Figure S59. ^{13}C APT NMR spectrum (100.6 MHz) of 2-(hydroxyamino)-2-methyl-1-phenylpropan-1-one (**3q**) in $CDCl_3$.

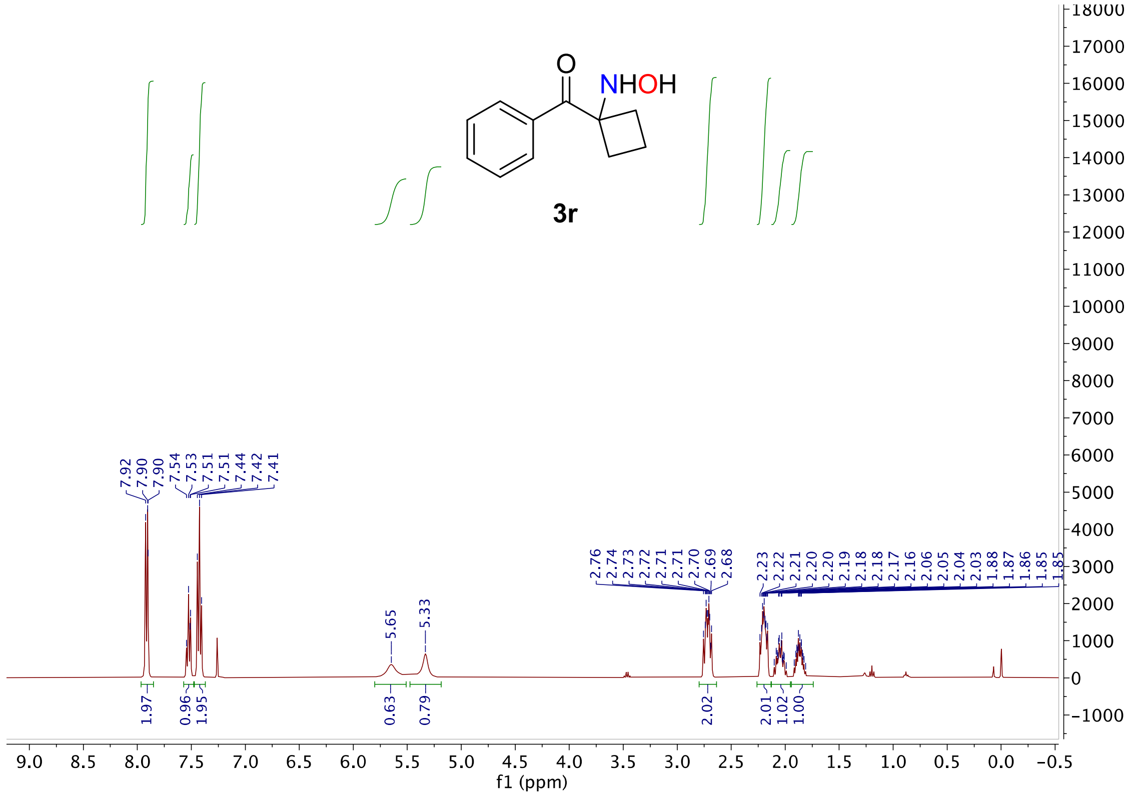

Figure S60. ^{1}H NMR spectrum (400 MHz) of (1-(hydroxyamino)cyclobutyl)(phenyl)methanone (**3r**) in $CDCl_3$.

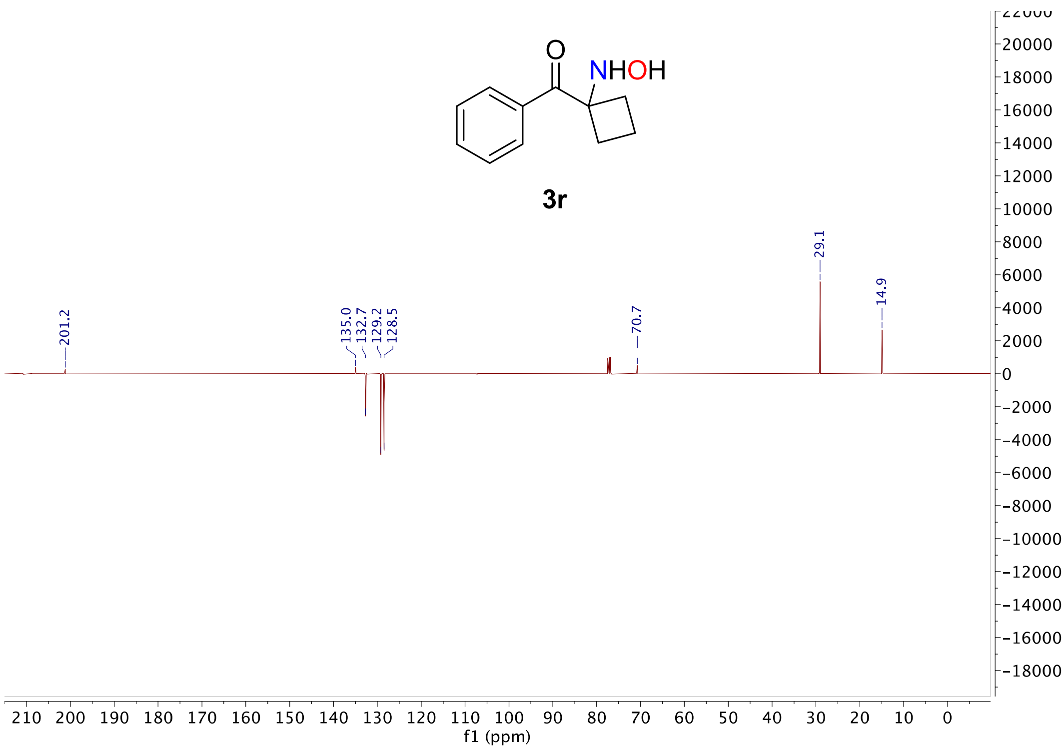

Figure S61. ^{13}C APT NMR spectrum (100.6 MHz) of (1-(hydroxyamino)cyclobutyl)(phenyl)methanone (**3r**) in $CDCl_3$.

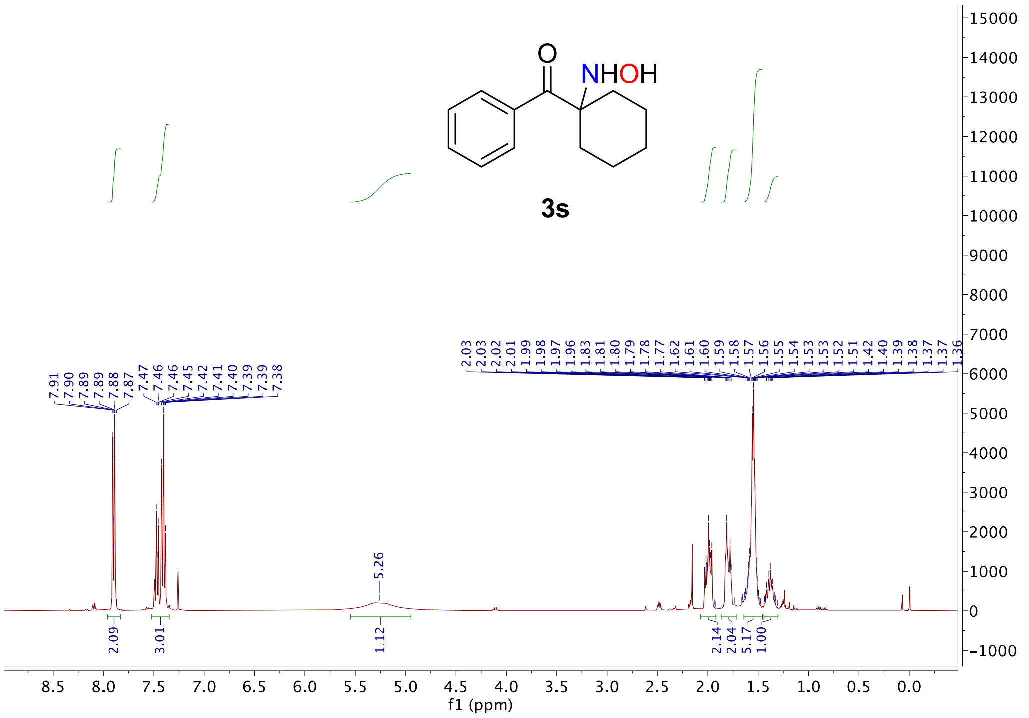

Figure S62. ^{1}H NMR spectrum (400 MHz) of (1-(hydroxyamino)cyclohexyl)(phenyl)methanone (**3s**) in $CDCl_3$.

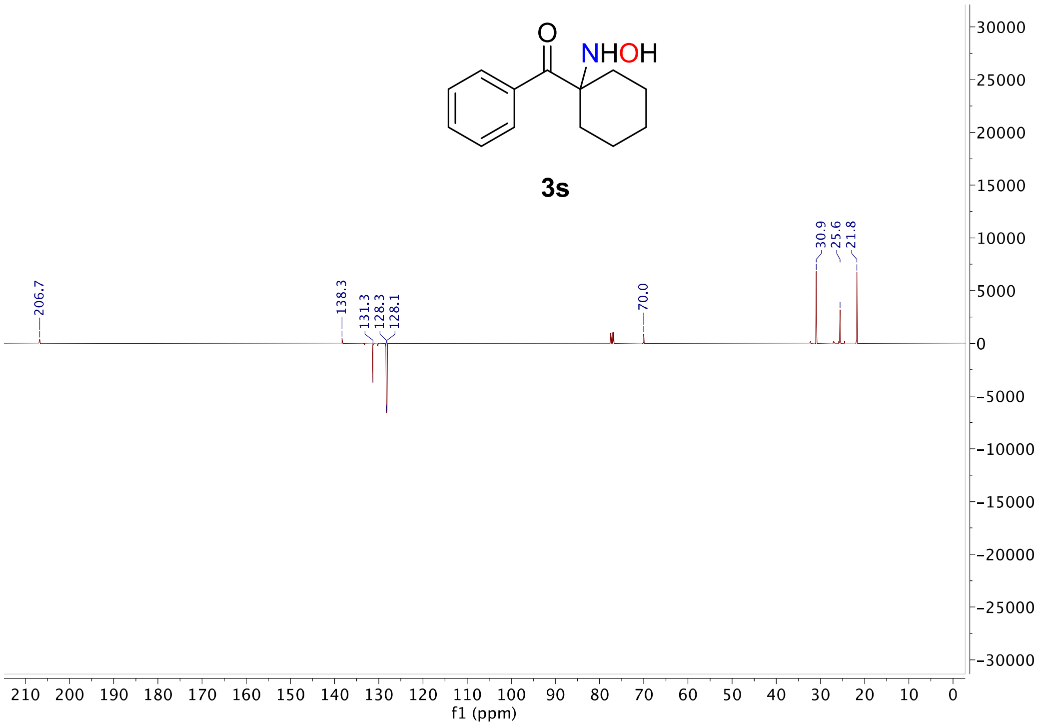

Figure S63. ^{13}C APT NMR spectrum (100.6 MHz) of (1-(hydroxyamino)cyclohexyl)(phenyl)methanone (**3s**) in $CDCl_3$.

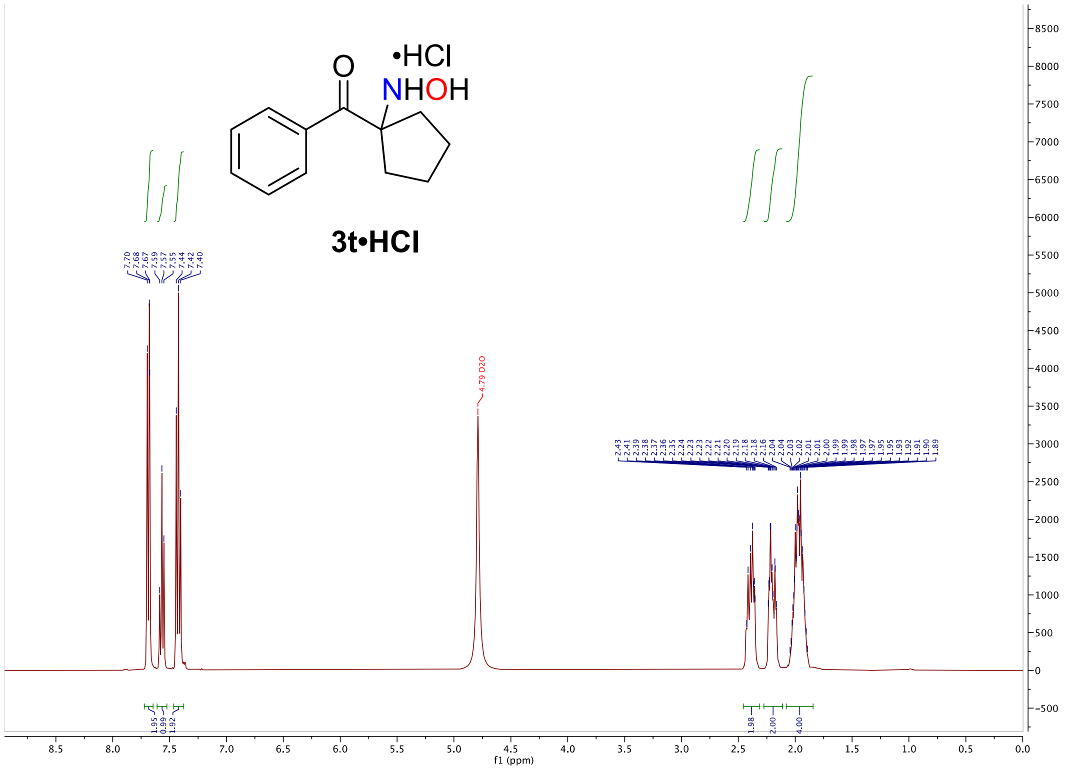

Figure S64. ^{1}H NMR spectrum (400 MHz) of (1-(hydroxyamino)cyclopentyl)(phenyl)methanone hydrochloride (**3t•HCl**) in D_2O.

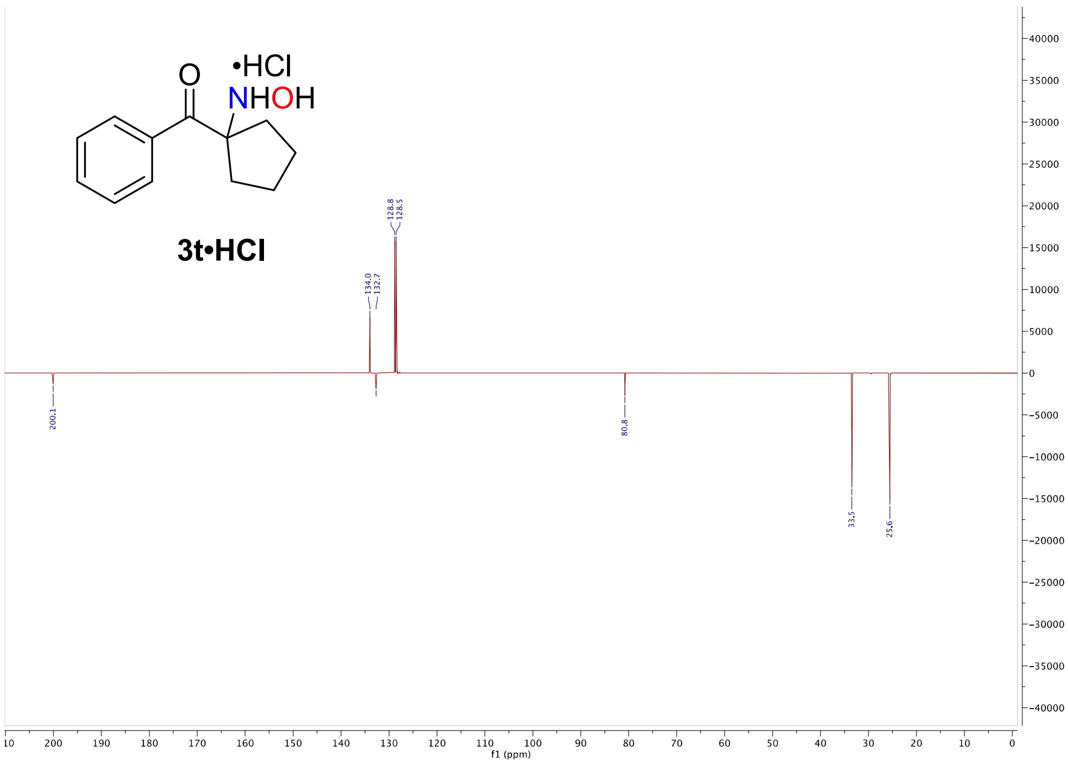

Figure S65. ^{13}C APT NMR spectrum (100.6 MHz) of (1-(hydroxyamino)cyclopentyl)(phenyl)methanone hydrochloride (**3t•HCl**) in D_2O.

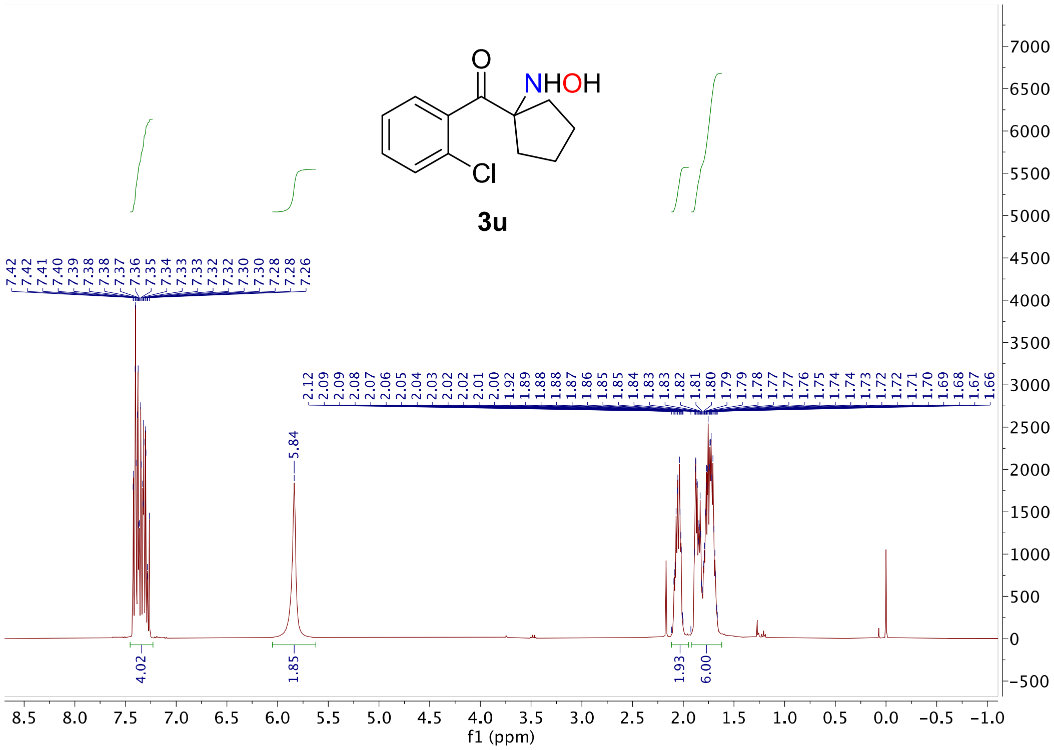

Figure S66. ^{1}H NMR spectrum (400 MHz) of (2-chlorophenyl)(1-(hydroxyamino)cyclopentyl)methanone (**3u**) in $CDCl_3$.

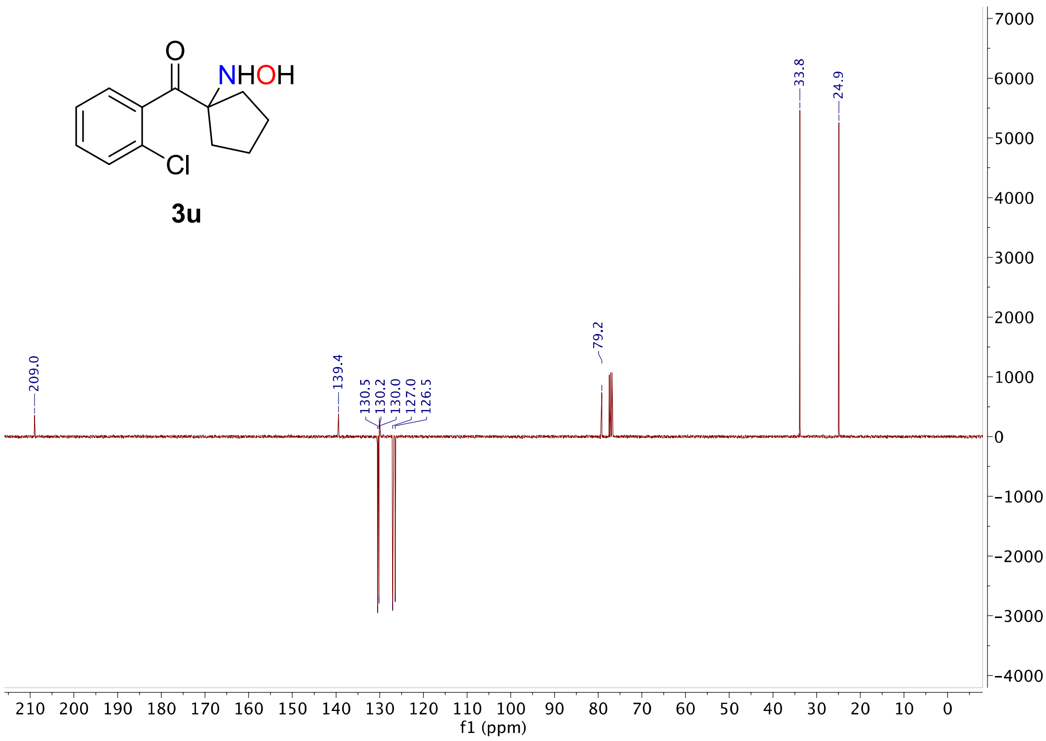

Figure S67. ^{13}C APT NMR spectrum (100.6 MHz) of (2-chlorophenyl)(1-(hydroxyamino)cyclopentyl)methanone (**3u**) in $CDCl_3$.

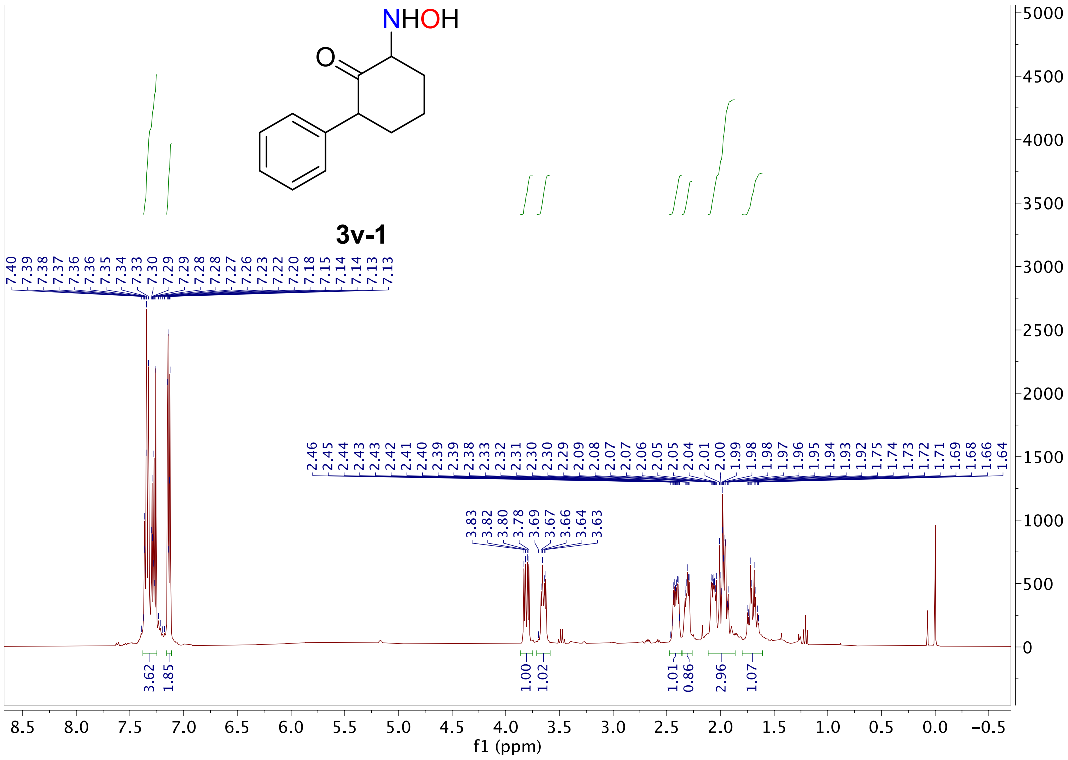

Figure S68. ^{1}H NMR spectrum (400 MHz) of 2-(hydroxyamino)-6-phenylcyclohexan-1-one (**3v-1**) in $CDCl_3$.

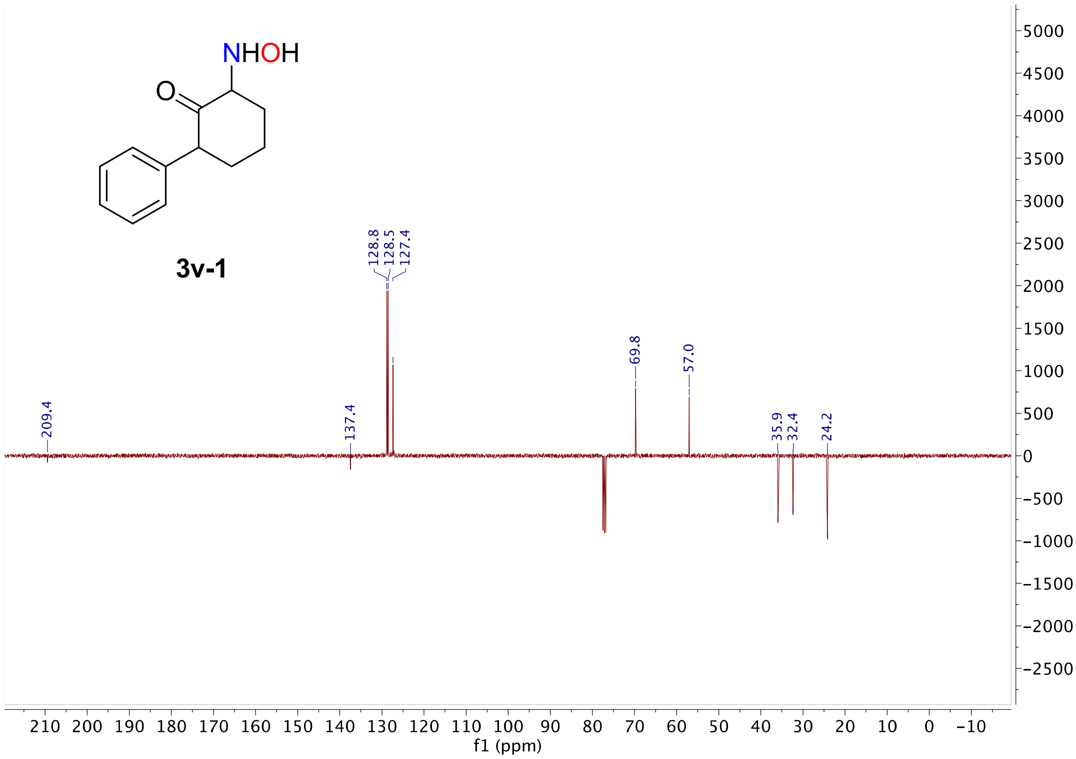

Figure S69. ^{13}C APT NMR spectrum (100.6 MHz) of 2-(hydroxyamino)-6-phenylcyclohexan-1-one (**3v-1**) in $CDCl_3$.

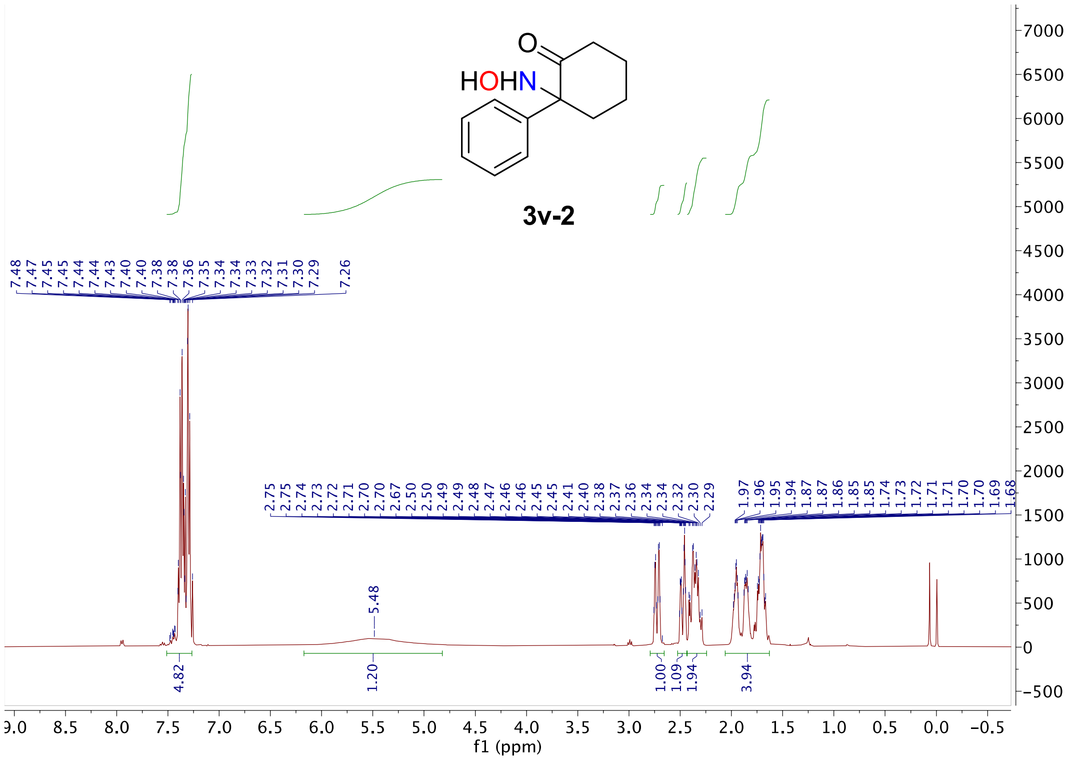

Figure S70. ^{1}H NMR spectrum (400 MHz) of 2-(hydroxyamino)-2-phenylcyclohexan-1-one (**3v-2**) in $CDCl_3$.

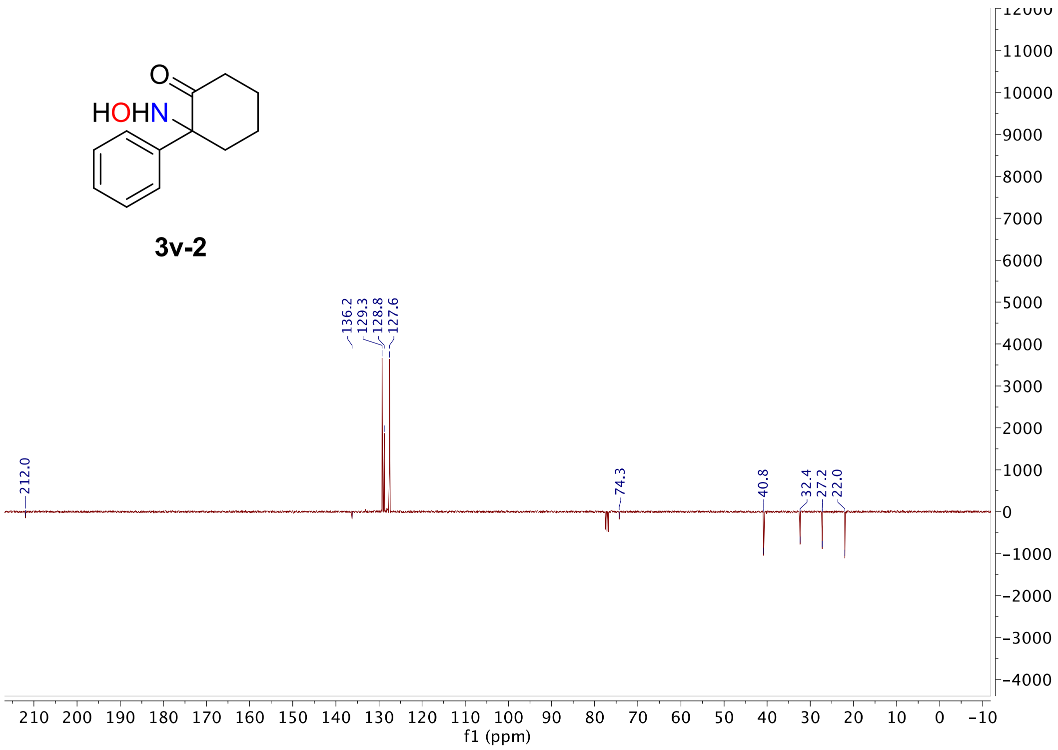

Figure S71. ^{13}C APT NMR spectrum (100.6 MHz) of 2-(hydroxyamino)-2-phenylcyclohexan-1-one (**3v-2**) in $CDCl_3$.

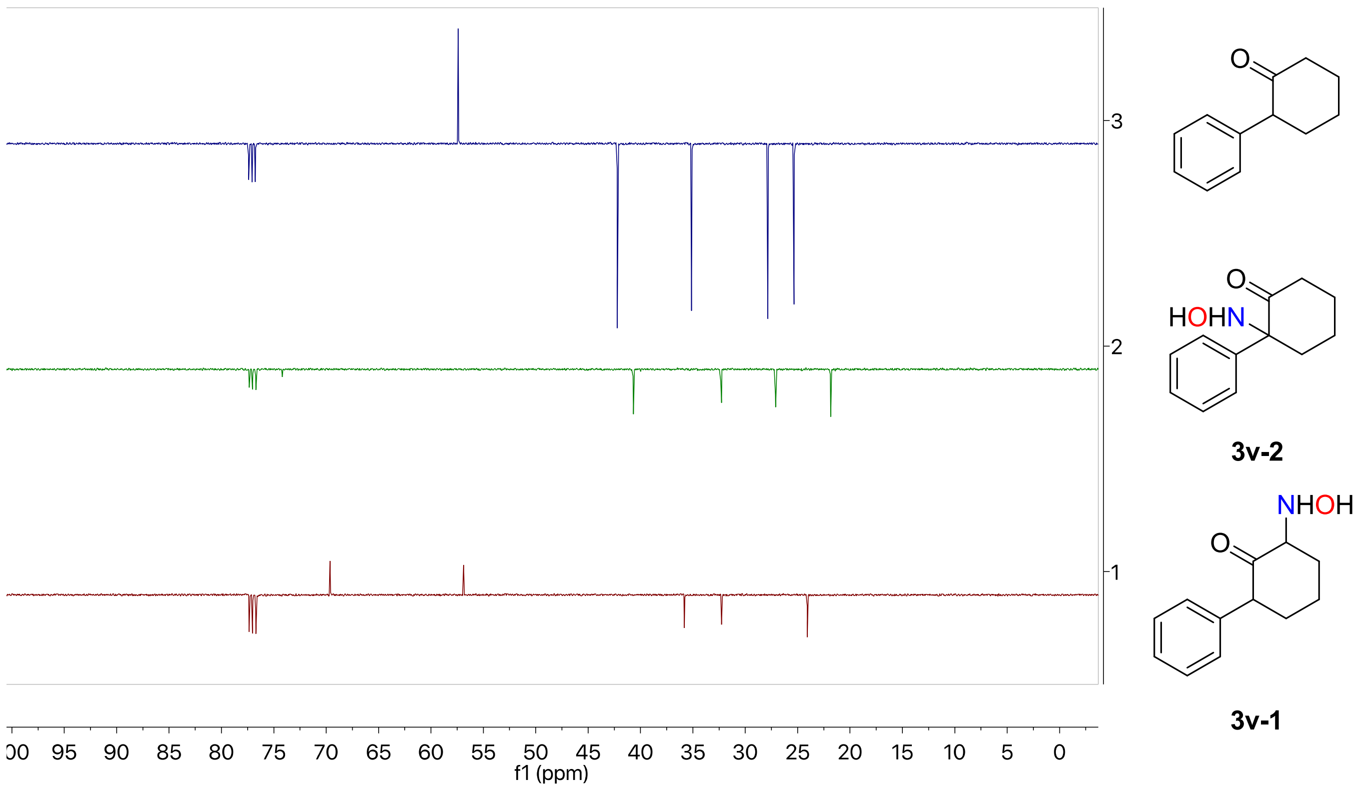

Figure S72. ^{13}C APT NMR spectrum (100.6 MHz) (aliphatic peaks only) stacked of 2-phenylcyclohexan-1-one (blue); 2-(hydroxyamino)-2-phenylcyclohexan-1-one (**3v-2**, green); 2-(hydroxyamino)-6-phenylcyclohexan-1-one (**3v-1**, red) in $CDCl_3$.

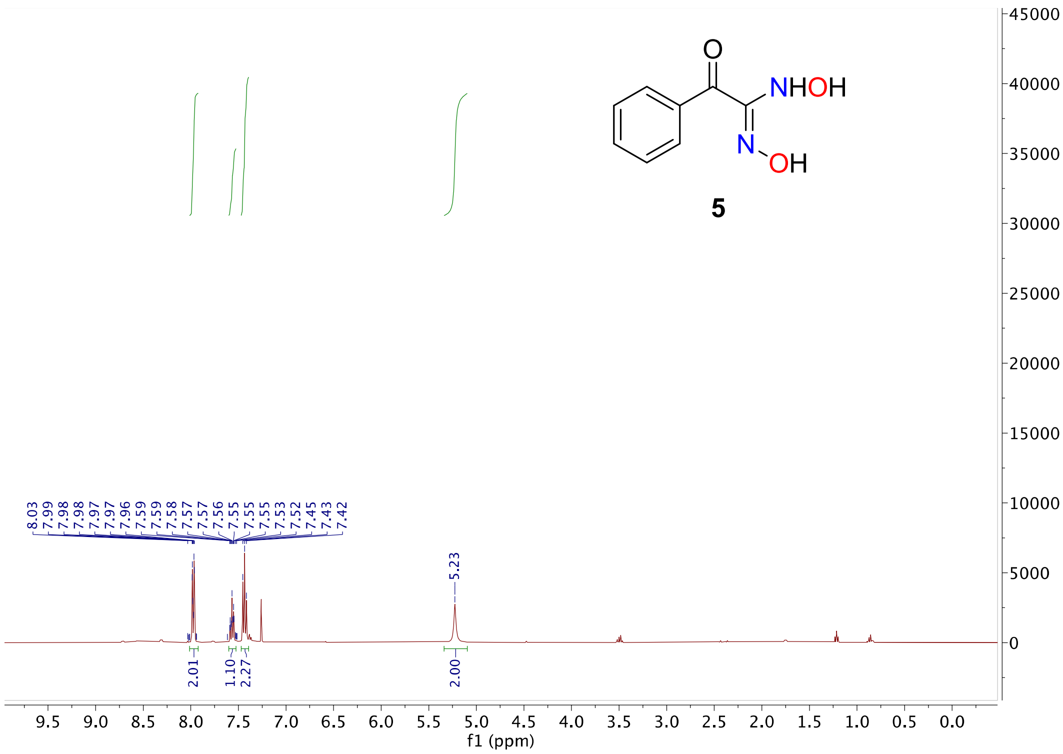

Figure S73. ^{1}H NMR spectrum (400 MHz) of (*Z*)-*N*,*N*'-dihydroxy-2-oxo-2-phenylacetimidamide (**5**) in $CDCl_3$.

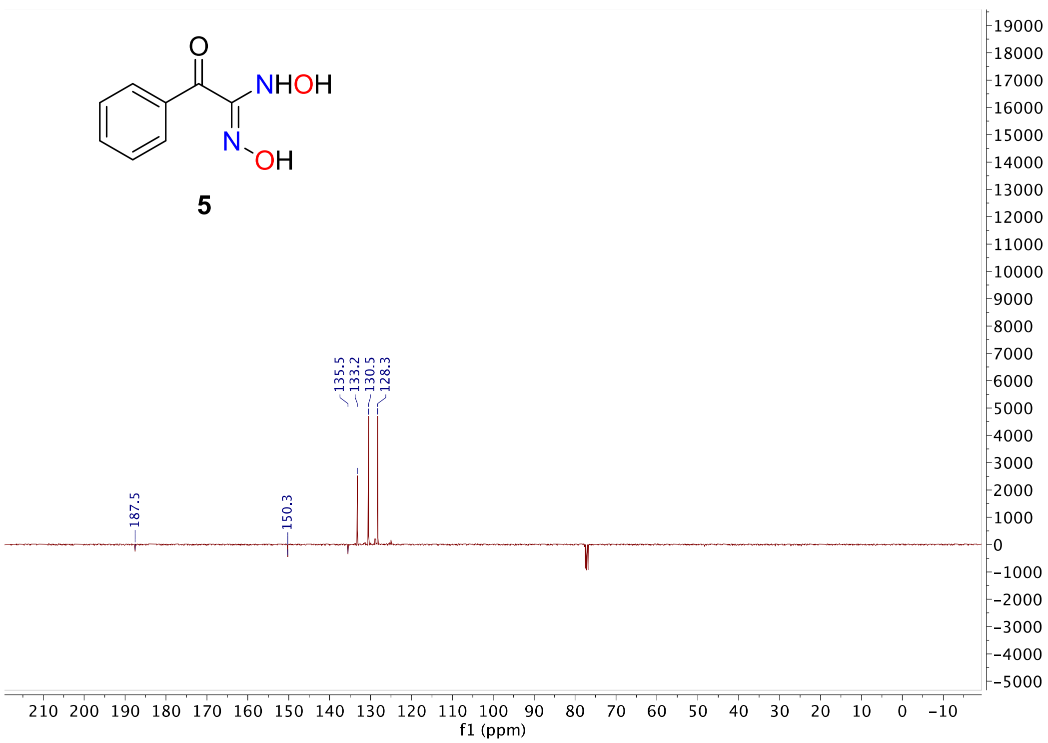

Figure S74. ^{13}C APT NMR spectrum (100.6 MHz) of (*Z*)-*N*,*N*'-dihydroxy-2-oxo-2-phenylacetimidamide (**5**) in $CDCl_3$.

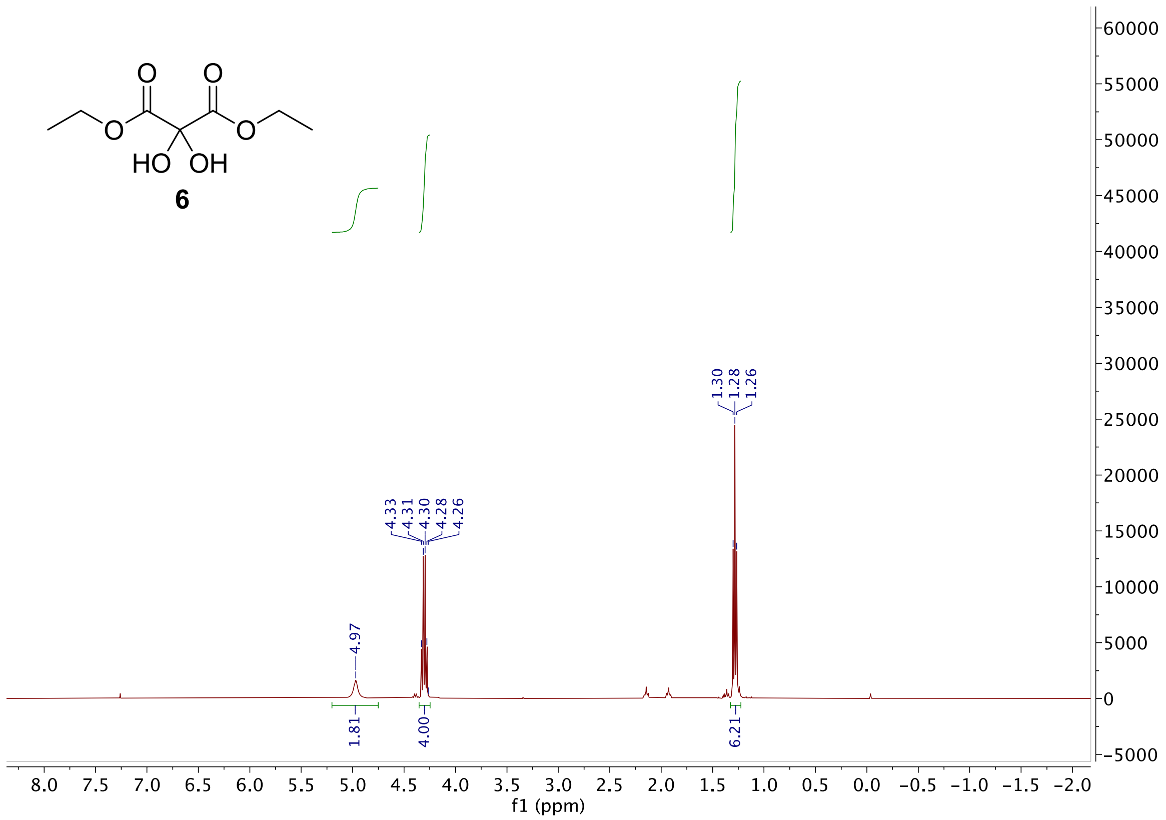

Figure S75. ^{1}H NMR spectrum (400 MHz) of diethyl 2,2-dihydroxymalonate (**6**) in $CDCl_3$.

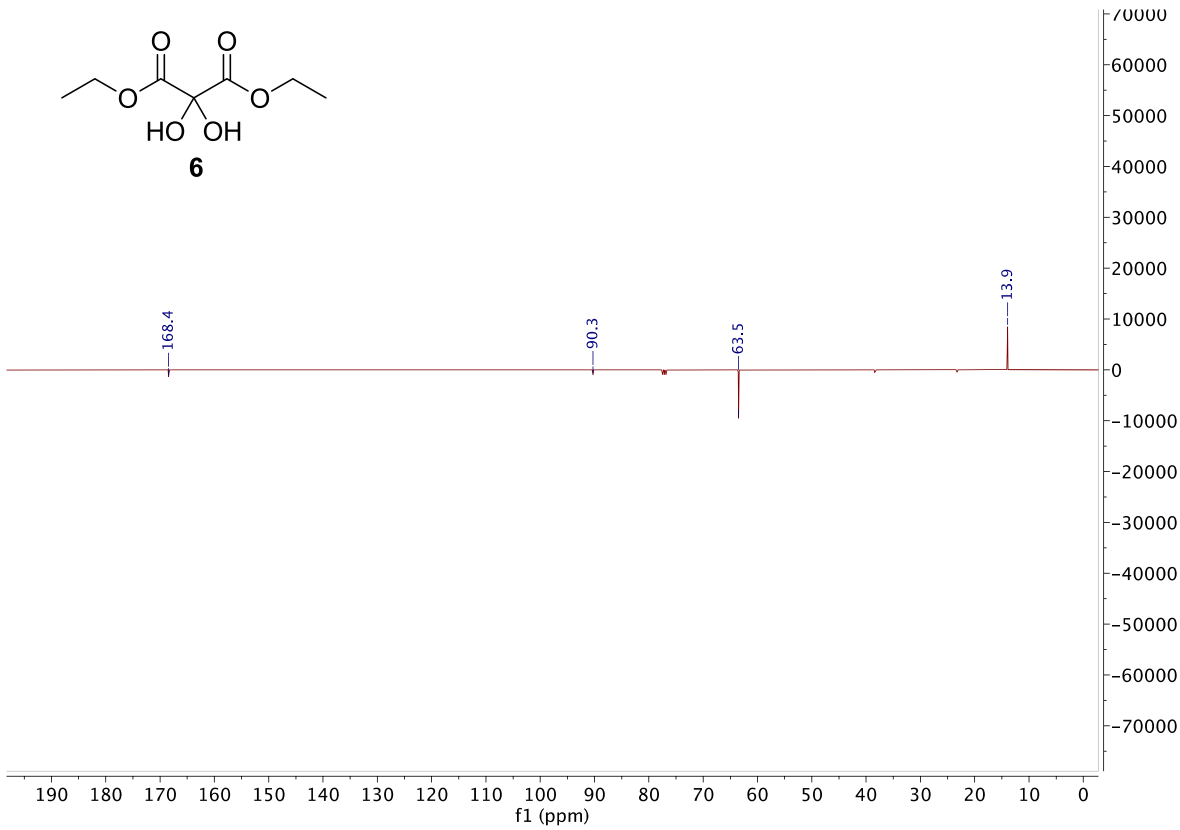

Figure S76. ^{13}C APT NMR spectrum (100.6 MHz) of diethyl 2,2-dihydroxymalonate (**6**) in $CDCl_3$.

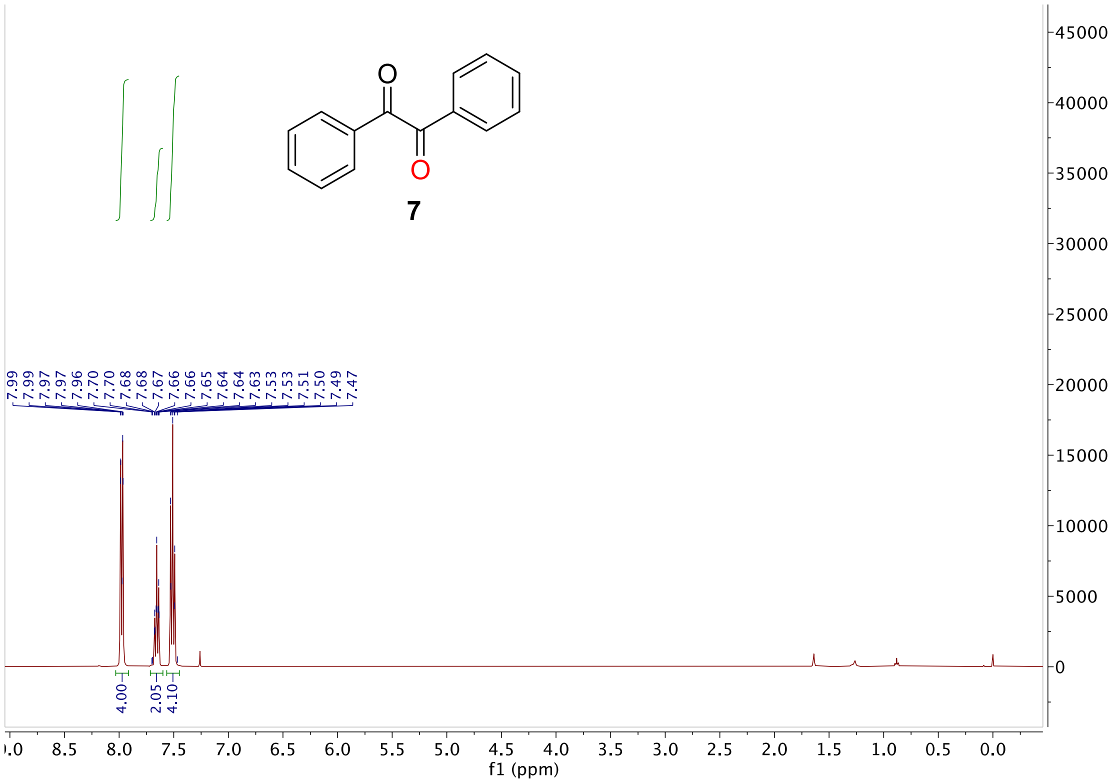

Figure S77. ^{1}H NMR spectrum (400 MHz) of benzil (**7**) in $CDCl_3$.

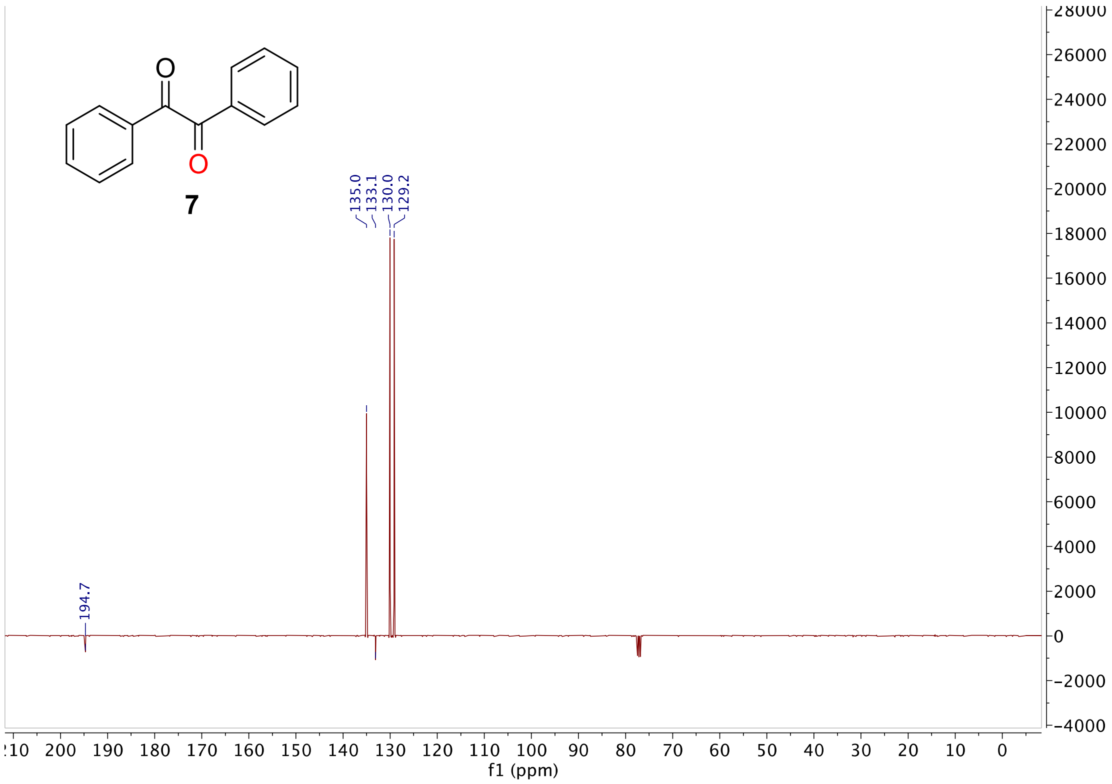

Figure S78. ^{13}C APT NMR spectrum (100.6 MHz) of benzil (**7**) in $CDCl_3$.

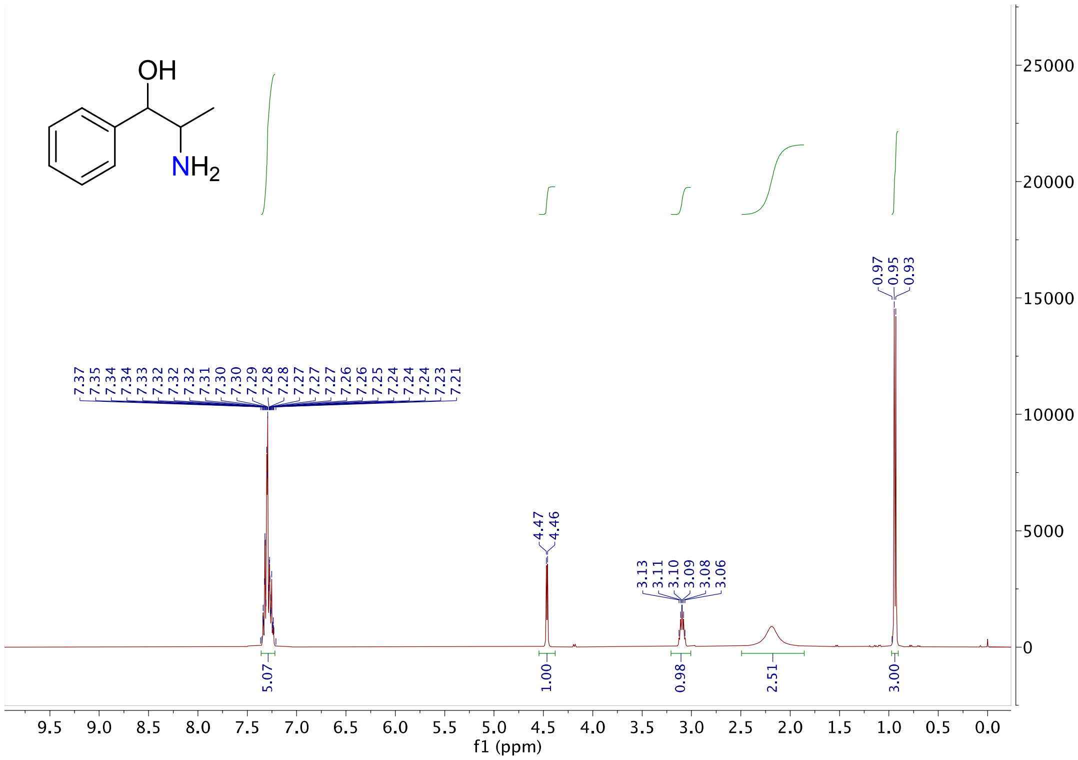

Figure S79. ^{1}H NMR spectrum (400 MHz) of 2-amino-1-phenylpropan-1-ol in $CDCl_3$.

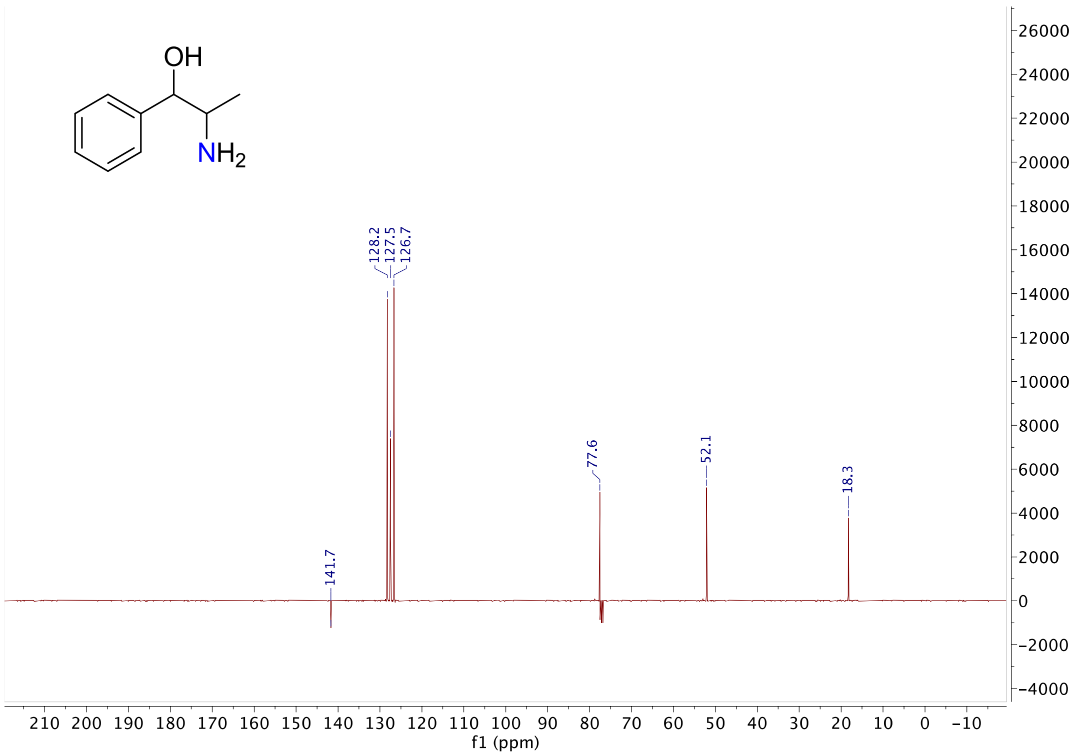

Figure S80. ^{13}C APT NMR spectrum (100.6 MHz) of 2-amino-1-phenylpropan-1-ol in $CDCl_3$.

2.6 Molecular structure by single crystal X-ray diffraction analysis of compounds *rac*-3g·HCl, 3q, 3r, 3t·HCl, 3t, 5, 6 and 7

For the structures of *rac*-**3g·HCl**, **3q**, **3r**, **3t·HCl**, **3t**, **5**, **6** and **7**, X-ray intensity data were collected at 100 K, on a Rigaku Oxford Diffraction Supernova Dual Source (Cu at zero) diffractometer equipped with an Atlas CCD detector using ω scans and CuKα (λ = 1.54184 Å) radiation. For **3t·HCl**, MoKα (λ = 0.71073 Å) radiation was used. The images were interpreted and integrated with the program CrysAlisPro.[S3] Using Olex2,[S4] the structures were solved by direct methods using the ShelXS/T structure solution programs and refined by full-matrix least-squares on F^2 using the ShelXL program package.[S5-S7] Non-hydrogen atoms were anisotropically refined and the hydrogen atoms in the riding mode with isotropic temperature factors fixed at 1.2 times U(eq) of the parent atoms (1.5 times for methyl and hydroxyl groups). When possible, amine and hydroxyl hydrogen atoms were located from a difference Fourier electron density map.

*Crystal data for compound rac-***3g·HCl**. $C_{10}H_{11}ClF_3NO_2$, M = 269.65, triclinic, space group P-1 (No. 2), a = 5.6416(2) Å, b = 5.8788(2) Å, c = 18.0049(8) Å, α = 95.374(3)°, β = 95.693(4)°, γ = 96.475(3)°, V = 587.08(4) Å^3, Z = 2, T = 100 K, ρ_{calc} = 1.525 g cm^{-3}, μ(Cu-Kα) = 3.209 mm^{-1}, F(000) = 276, 17106 reflections measured, 2262 unique (R_{int} = 0.0738) which were used in all calculations. The final R1 was 0.0724 ($I > 2\sigma(I)$) and wR2 was 0.1917 (all data). The structure was refined as a 2-component twin, with a refined twin fraction of 0.0062.

*Crystal data for compound **3q***. $C_{10}H_{13}NO_2$, M = 179.21, monoclinic, space group $P2_1/c$ (No. 14), a = 5.7769(3) Å, b = 7.6286(5) Å, c = 21.5338(10) Å, β = 96.167(5)°, V = 943.50(9) Å^3, Z = 4, T = 100 K, ρ_{calc} = 1.262 g cm^{-3}, μ(Cu-Kα) = 0.716 mm^{-1}, F(000) = 384, 9351 reflections measured, 1859 unique (R_{int} = 0.0592) which were used in all calculations. The final R1 was 0.0432 ($I > 2\sigma(I)$) and wR2 was 0.1245 (all data).

*Crystal data for compound **3r***. $C_{11}H_{13}NO_2$, M = 191.22, monoclinic, space group $P2_1/c$ (No. 14), a = 9.0379(3) Å, b = 10.0440(3) Å, c = 11.0835(3) Å, β = 99.123(3)°, V = 993.40(5) Å^3, Z = 4, T = 100 K, ρ_{calc} = 1.279 g cm^{-3}, μ(Cu-Kα) = 0.716 mm^{-1}, F(000) = 408, 18075 reflections measured, 2033 unique (R_{int} = 0.0860) which were used in all calculations. The final R1 was 0.0447 ($I > 2\sigma(I)$) and wR2 was 0.1220 (all data).

*Crystal data for compound **3t·HCl***. $C_{12}H_{16}ClNO_2$, M = 241.71, monoclinic, space group $P2_1/c$ (No. 14), a = 6.09900(10) Å, b = 7.70410(10) Å, c = 25.2722(4) Å, β = 94.075(2)°, V = 1184.47(3) Å^3, Z = 4, T = 100 K, ρ_{calc} = 1.355 g cm^{-3}, μ(Mo-Kα) = 0.308 mm^{-1}, F(000) = 512, 25529 reflections measured, 3178 unique (R_{int} = 0.0313) which were used in all calculations. The final R1 was 0.0341 ($I > 2\sigma(I)$) and wR2 was 0.0884 (all data). The cyclopentyl moiety was found to be disordered and was refined in two parts with occupancy factors of 0.645(17) and 0.355(17).

*Crystal data for compound **3t***. $C_{12}H_{14}ClNO_2$, M = 239.69, triclinic, space group P-1 (No. 2), a = 5.7548(3) Å, b = 10.5744(5) Å, c = 10.5916(6) Å, α = 110.243(5)°, β = 102.912(5)°, γ = 100.879(5)°, V = 563.94(6) Å^3, Z = 2, T = 100 K, ρ_{calc} = 1.412 g cm^{-3}, μ(Cu-Kα) = 2.876 mm^{-1}, F(000) = 252, 10603 reflections measured, 2285 unique (R_{int} = 0.0571) which were used in all calculations. The final R1 was 0.0377 ($I > 2\sigma(I)$) and wR2 was 0.1015 (all data). The cyclopentyl moiety was found to be disordered and was refined in two parts with occupancy factors of 0.792(7) and 0.208(7).

*Crystal data for compound **5***. $C_8H_8N_2O_2$, M = 164.16, monoclinic, space group $C2/c$ (No. 15), a = 18.9356(3) Å, b = 3.81317(10) Å, c = 21.6720(5) Å, β = 101.7022(19)°, V = 1532.30(6) Å^3, Z = 8, T = 100 K, ρ_{calc} = 1.423 g cm^{-3}, μ(Cu-Kα) = 0.876 mm^{-1}, F(000) = 688, 38369 reflections measured, 1577 unique (R_{int} = 0.0497) which were used in all calculations. The final $R1$ was 0.0378 ($I > 2\sigma(I)$) and $wR2$ was 0.1050 (all data).

*Crystal data for compound **6***. $C_7H_{12}O_6$, M = 192.17, triclinic, space group P-1 (No. 2), a = 7.6334(2) Å, b = 8.7609(3) Å, c = 14.2366(3) Å, α = 81.705(2)°, β = 88.677(2)°, γ = 73.562(3)°, V = 903.45(5) Å^3, Z = 4, T = 100 K, ρ_{calc} = 1.413 g cm^{-3}, μ(Cu-Kα) = 1.090 mm^{-1}, F(000) = 408, 32011 reflections measured, 3680 unique (R_{int} = 0.0829) which were used in all calculations. The final $R1$ was 0.0419 ($I > 2\sigma(I)$) and $wR2$ was 0.1176 (all data).

*Crystal data for compound **7***. $C_{14}H_{10}O_2$, M = 210.22, trigonal, space group $P3_221$ (No. 154), a = 8.3441(3) Å, b = 8.3441(3) Å, c = 13.3783(5) Å, V = 806.66(8) Å^3, Z = 3, T = 100 K, ρ_{calc} = 1.298 g cm^{-3}, μ(Cu-Kα) = 0.697 mm^{-1}, F(000) = 330, 15607 reflections measured, 1122 unique (R_{int} = 0.0621) which were used in all calculations. The final $R1$ was 0.0377 ($I > 2\sigma(I)$) and $wR2$ was 0.1028 (all data). This structure has previously been reported (CSD refcodes BENZIL and BENZIL01-05).[S8-S11]

CCDC 2046130-2046136 (respectively for *rac*-**3g·HCl**, **3q**, **3r**, **3t·HCl**, **3t**, **5**, **6**) contain the supplementary crystallographic data for this paper. These data can be obtained free of charge from The Cambridge Crystallographic Data Centre via www.ccdc.cam.ac.uk/structures.

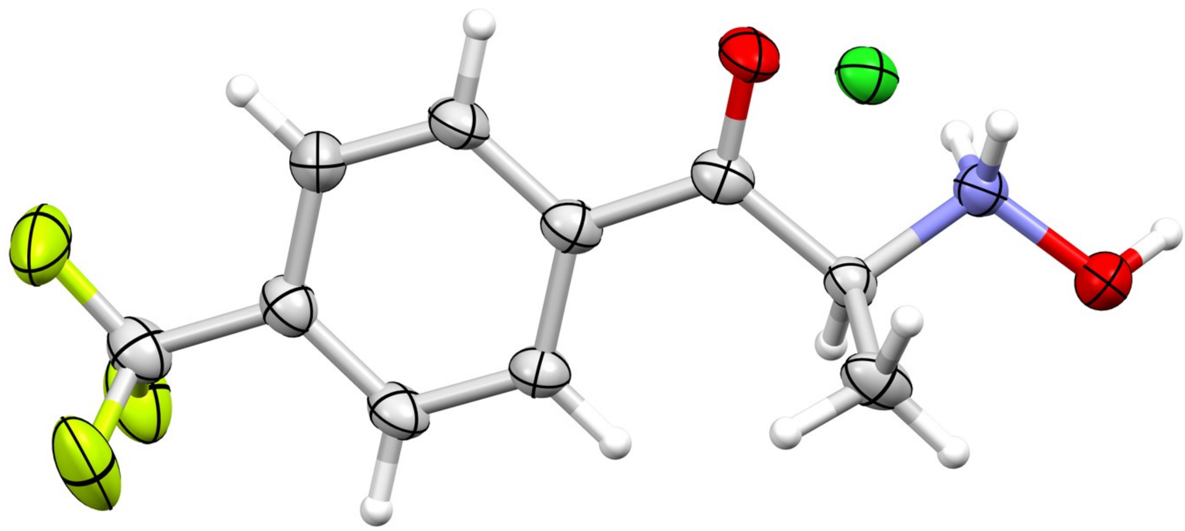

Figure S81. Asymmetric unit of the crystal structure of *rac*-**3g·HCl**, showing thermal displacement ellipsoids at the 50% probability level.

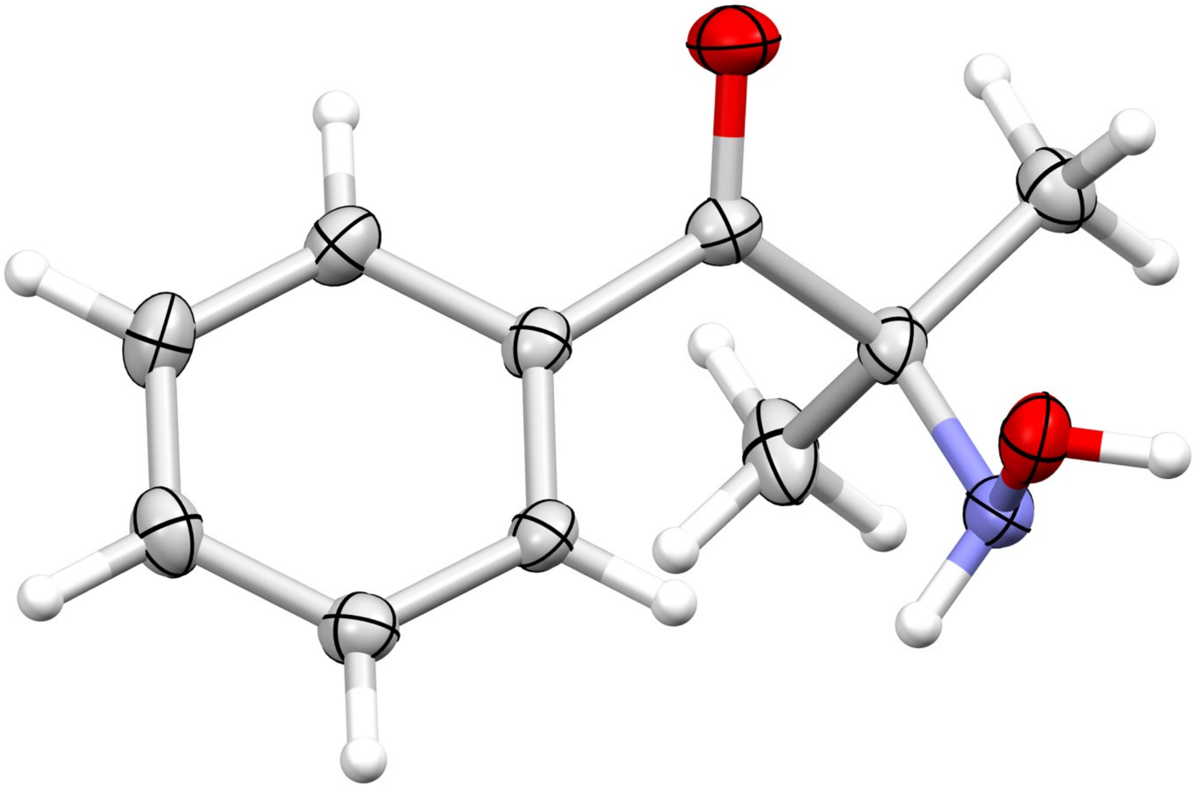

Figure S82. Asymmetric unit of the crystal structure of **3q**, showing thermal displacement ellipsoids at the 50% probability level.

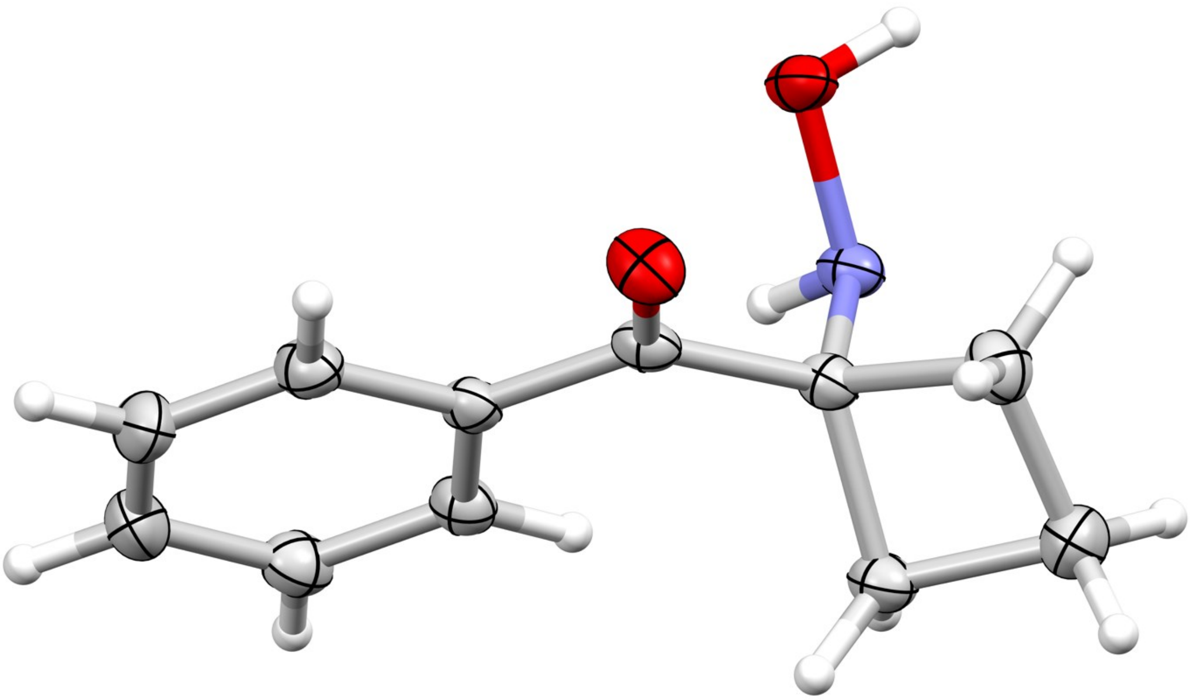

Figure S83. Asymmetric unit of the crystal structure of **3r**, showing thermal displacement ellipsoids at the 50% probability level.

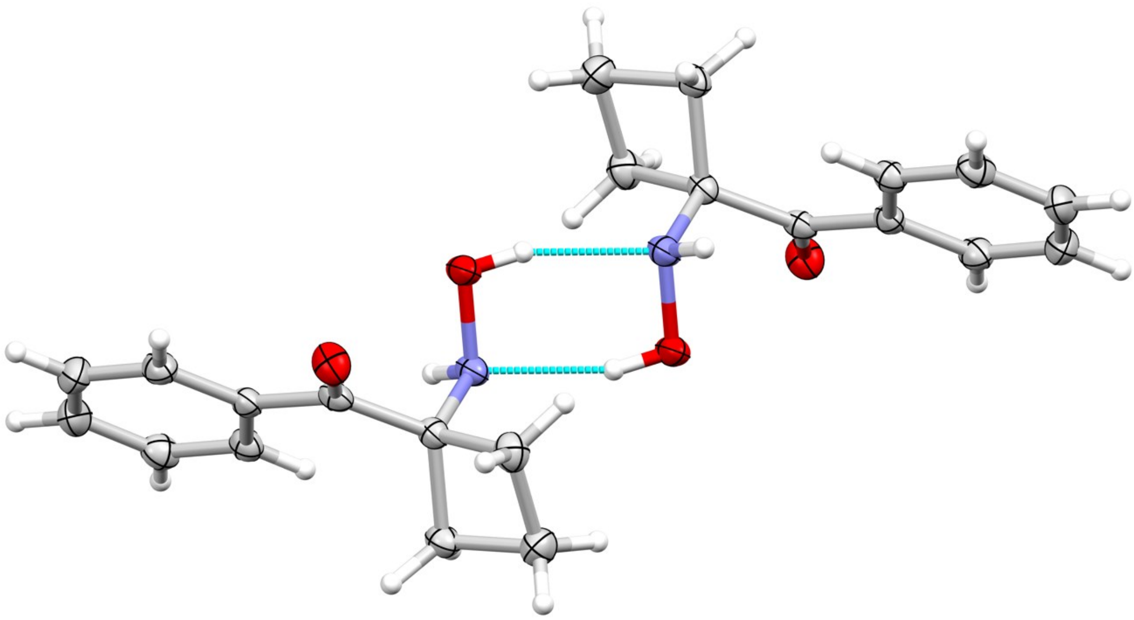

Figure S84. Dimer formation in the crystal structure of **3r**, by intermolecular hydrogen bonds, showing thermal displacement ellipsoids at the 50% probability level.

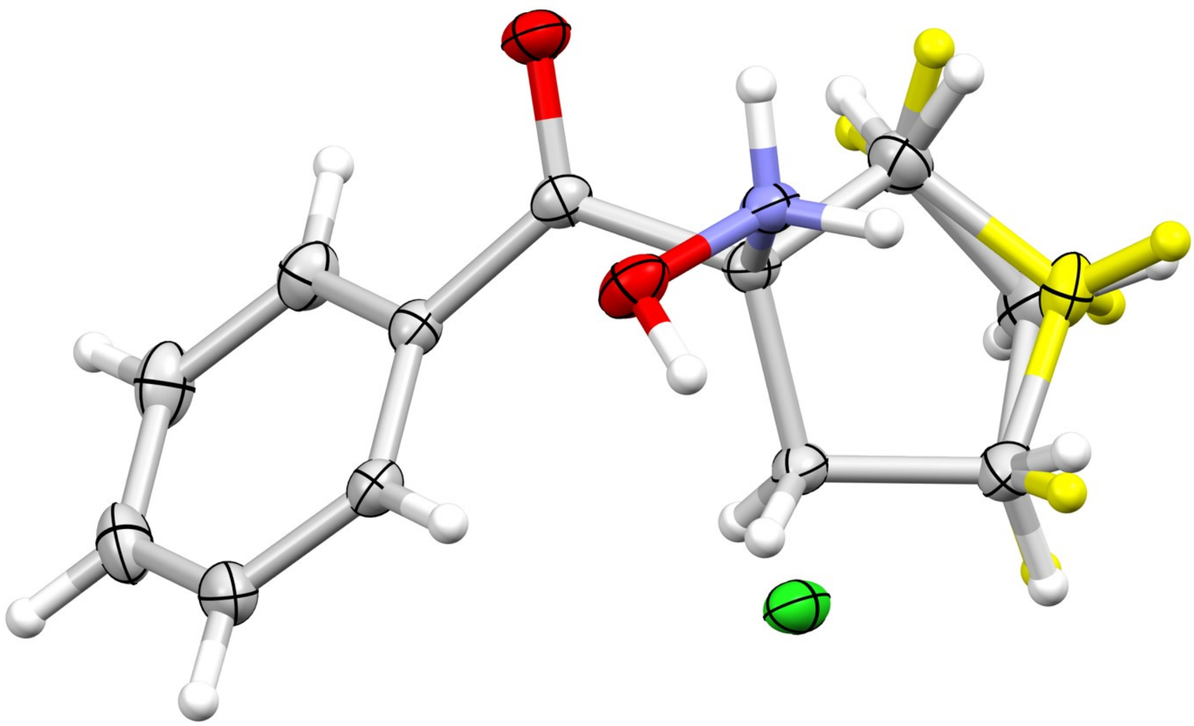

Figure S85. Asymmetric unit of the crystal structure of **3t·HCl**, showing thermal displacement ellipsoids at the 50% probability level. Disorder of the cyclopentyl moiety is shown in yellow.

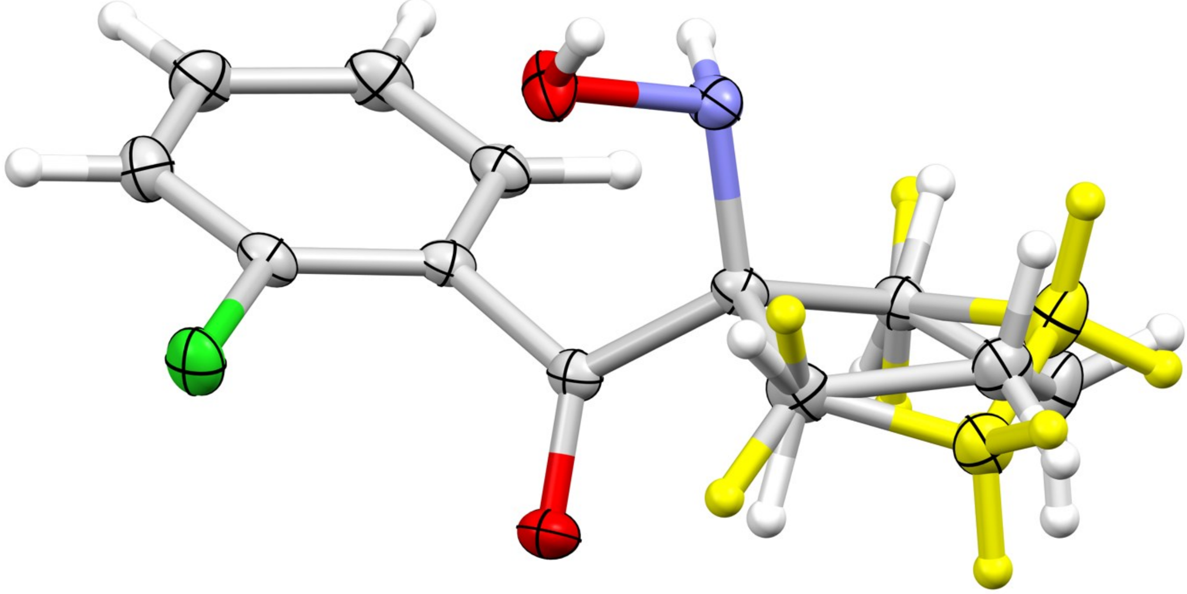

Figure S86. Asymmetric unit of the crystal structure of **3t**, showing thermal displacement ellipsoids at the 50% probability level. Disorder of the cyclopentyl moiety is shown in yellow.

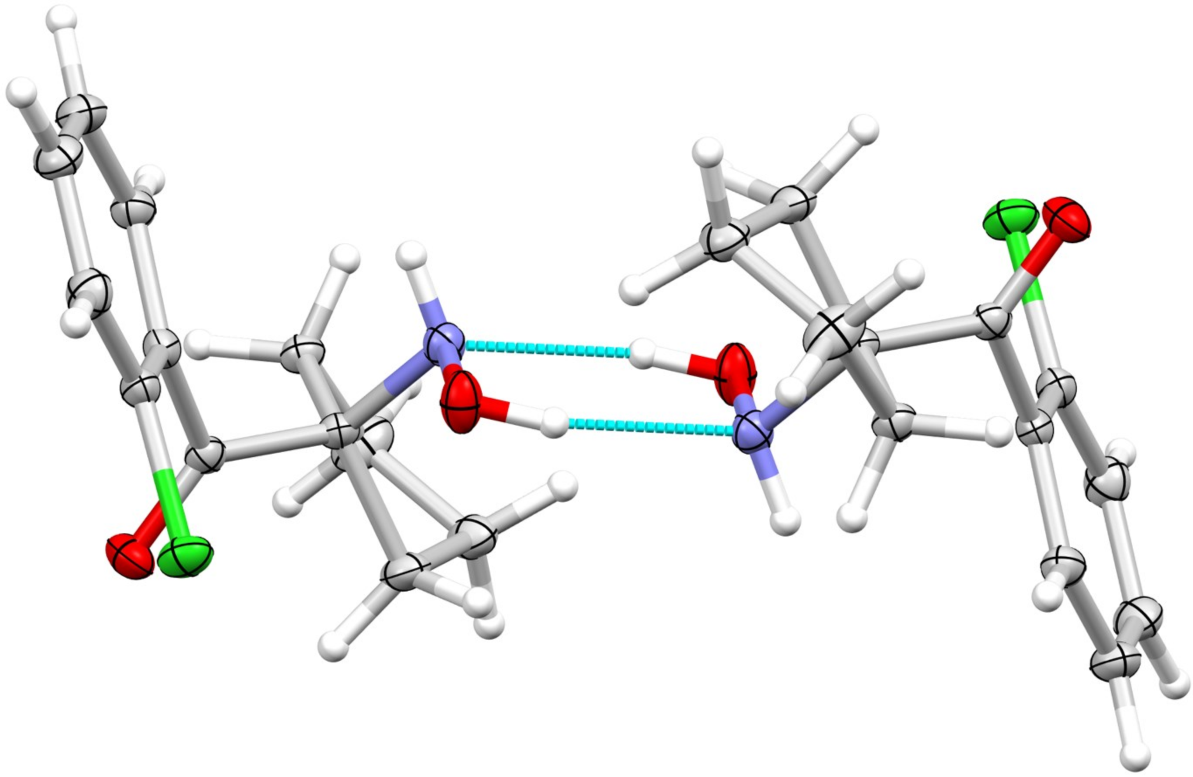

Figure S87. Dimer formation in the crystal structure of **3t**, by intermolecular hydrogen bonds, showing thermal displacement ellipsoids at the 50% probability level. Disorder of the cyclopenty moiety is omitted.

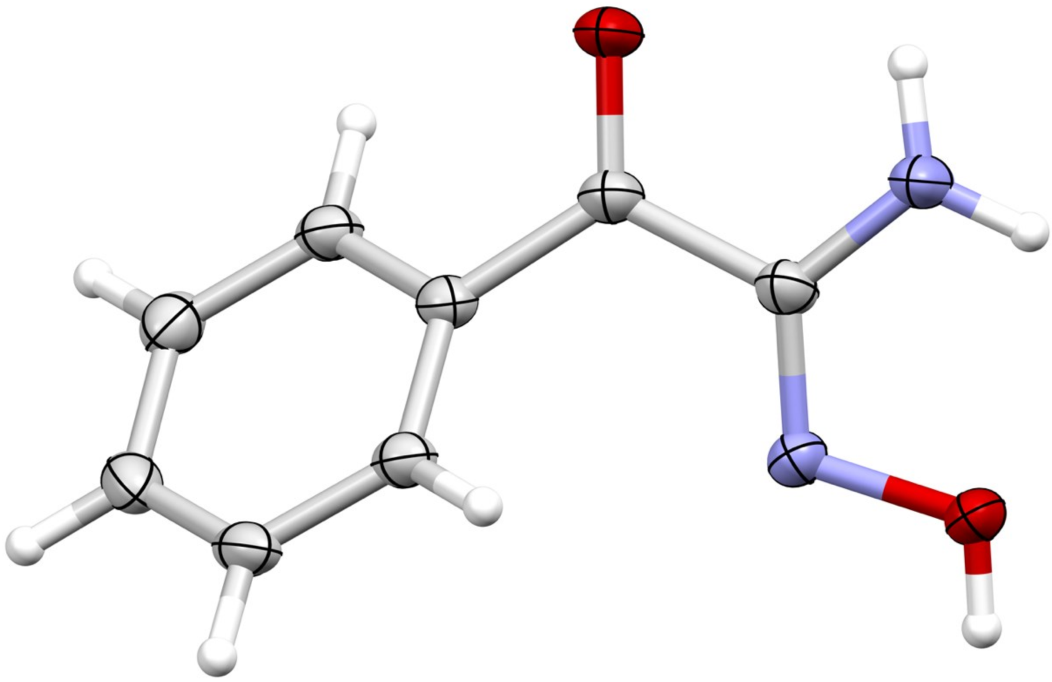

Figure S88. Asymmetric unit of the crystal structure of **5**, showing thermal displacement ellipsoids at the 50% probability level.

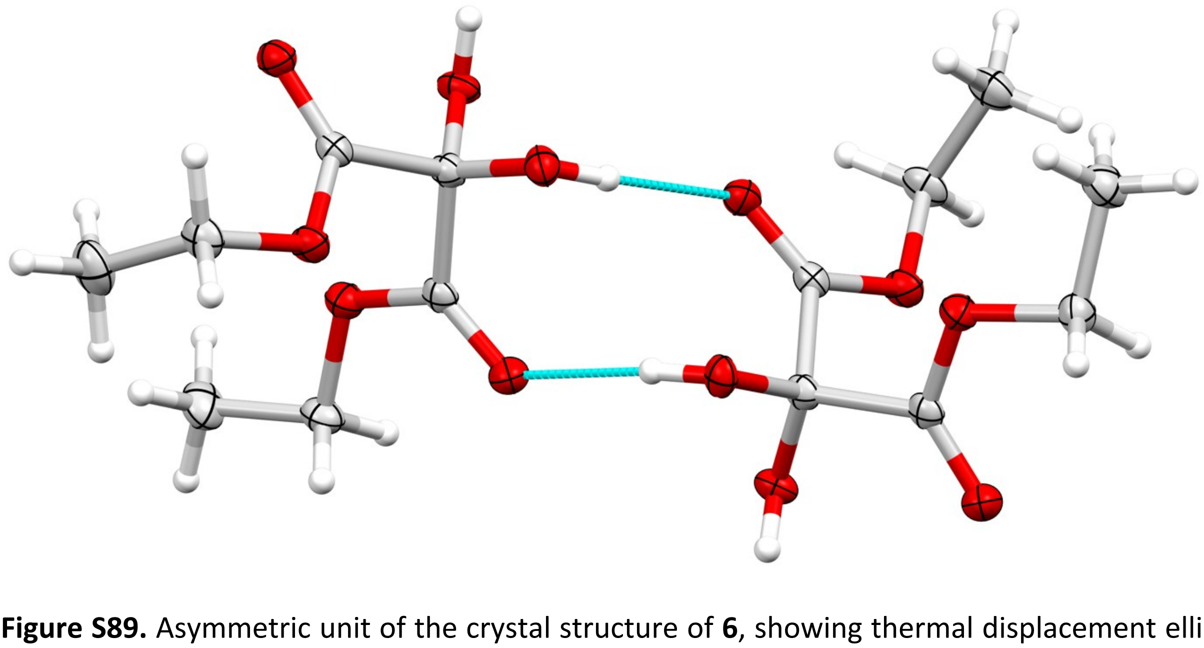

Figure S89. Asymmetric unit of the crystal structure of **6**, showing thermal displacement ellipsoids at the 50% probability level and dimer formation by intermolecular hydrogen bonds.

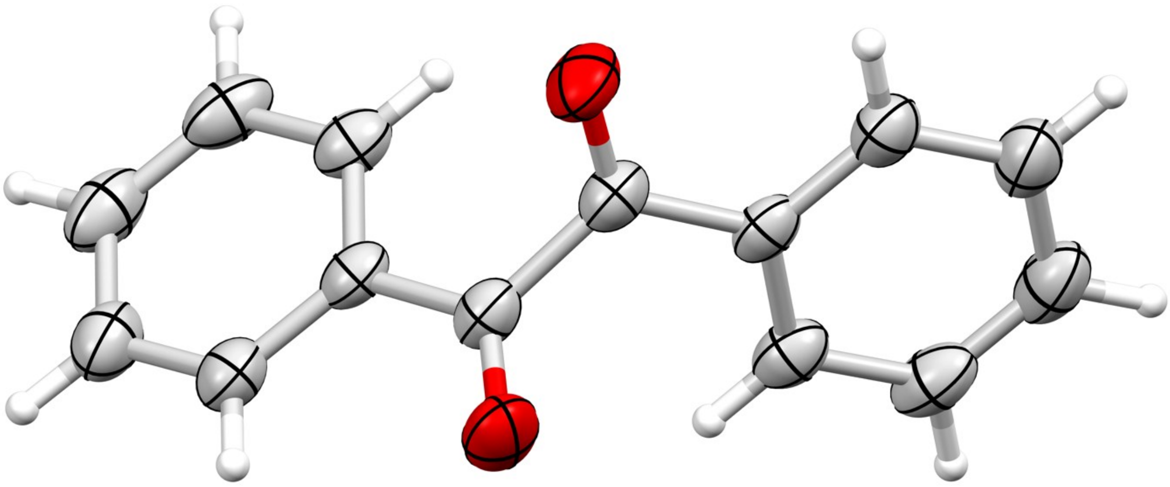

Figure S90. Asymmetric unit of the crystal structure of **7**, showing thermal displacement ellipsoids at the 50% probability level. This structure has previously been reported (CSD refcodes BENZIL and BENZIL01-05).[S8-S11]

3 Sustainability metrics

3.1 Environmental Factor

3.1.1 Preparation of α-chloronitroso derivative **1a**

Table S11. Calculated environmental factors (E-factors) for the preparation of **1a**

Entry	Oxime	Oxime mol	MM (g/mol) oximes	Mass (g)	Reagents & solvents	Ketone molarity in solvent (M)	Solvent Density (g/mL)	Reagents & solvents equivalents	MM (g/mol) Reagents & solvents	Mass (g) Reagents & solvents	**1** derivatives	Product(s) yield (%)	**Mol of product(s)**	MM (g/mol) product(s)	Mass (g) product(s)	Recovered valued by-products	Mol of recovered valued by-product	Mass (g) of recovered valued by-products	E-Factor	Ref.
1	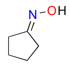	1	99,13	99,13	*t* BuOCl MTBE	1	 0.74	1,00 8,39	108,56 88,14	108,56 740,00	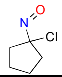	99	0,99	133,57	132,23		0	0	6	this work
2	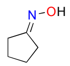	1	99,13	99,13	34% aqueous HCl 37% aqueous H2O2 Dichloromethane	0,4	 1,12 1,33	5 5 39,15	112,5 52 84,93	562,5 136 3325	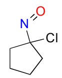	94	0,94	133,57	125,56		0	0	32	1
3	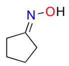	1	99,13	99,13	Dichloromethane 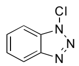	1	1,33	15,66 1	84,93 153,56	1330 153,56	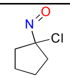	99	0,99	133,57	132,23		0	0	11	2
4	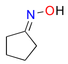	1	99,13	99,13	Acetonitrile 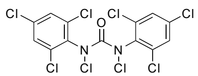	0,66	0,8	29,23 0,5	41,05 487,78	1200 243,89	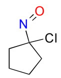	92	0,92	133,57	122,88		0	0	12	3

References	Scale	Sector
1 Terent'ev, A. O.; Krylov, I. B.; Ogibin, Y. N.; Nikishin, G. I., Synthesis (Stuttg). 2006, No. 22, 3819–3824.	<0.1	Oil refining
2 Monbaliu, J. C. M.; Beagle, L. K.; Kovacs, J.; Zeller, M.; Stevens, C. V.; Katritzky, A. R., RSC Adv. 2012, 2 (24), 8941–8945.	<1 - 5	Bulk chemicals
3 Gupta, A. K.; Acharya, J.; Pardasani, D.; Dubey, D. K., Tetrahedron Lett. 2007, 48 (5), 767–770.	5 - 50	Fine chemicals
	25 - 100	Pharmaceuticals

3.1.2 Electrophilic amination on **2b**

Table S12. Calculated environmental factors (E-factors) for the electrophilic amination step on **2b** or derivatives.

Entry	Propiophenone or alike	Propiophenone or alike mol	MM (g/mol) ketone	Mass (g)	Reagents & solvents	Ketone molarity in solvent (M)	Solvent Density (g/mL)	Reagents & solvents equivalents	MM (g/mol) Reagents & solvents	Mass (g) Reagents & solvents	Aminated products	Product(s) yield (%)	**Mol of product(s)**	MM (g/mol) product(s)	Mass (g) product(s)	Recovered valued by-products	Mol of recovered valued by-product	Mass (g) of recovered valued by-products	E-Factor	Ref.
1	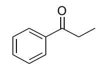	1	134,17	134,17	LiHMDS THF MTBE 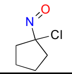	0.5	 0.89 0.74	1,01 24,68 8,405 1	167,32 72,1 88,14 133,57	168,99 1779,43 740,82 133,57	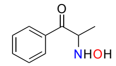	98	0,98	165,19	161,89	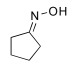	0,83	82,17	11	this work
2	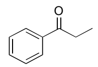	1	134,17	134,17	LDA Ti(OiPr)4 THF 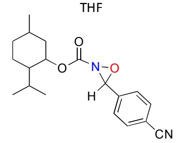	0.5	 0.89	1 1 41,14 1	107,12 284,21 72,1 328,17	107,12 284,21 2966,66 328,17	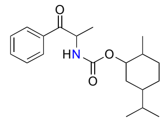	62	0,62	331,45	205,50		0	0	18	1
3	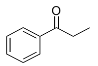	1	134,17	134,17	L-proline Triethylamine 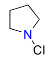	neat		0,3 2 1	115,13 101,19 105,1	34,54 202,38 105,1	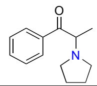	22	0,22	203,28	44,72		0	0	10	2
3	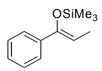	1	206,36	206,36	AgOTf CH2Cl2 HF-THF 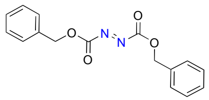	0,2	 1,33	0,1 76,53 76,53 1,1	256,93 84,93 75 298,29	25,69 6500 5739,75 328,12	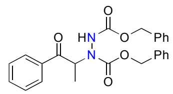	84	0,84	432,47	363,27		0	0	34	3
4	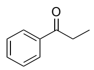	1	206,36	206,36	LiHMDS ZnCl2 Et2O THF 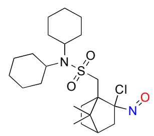	0,07	 0,714 0.89	1,1 2 15,13 158,7 1	167,32 136,28 74,12 72,1 445,05	184,05 272,56 1122 11442 445,05	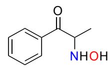	98	0,98	165,19	161,89	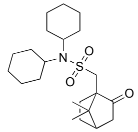	0,85	336,26	26	4

References	Scale	Sector
1 Armstrong, A.; Atkin, M. A.; Swallow, S. Tetrahedron Asymmetry 2001, 12 (4), 535–538.	<0.1	Oil refining
2 Scarpino Schietroma, D. M.; Monaco, M. R.; Bucalossi, V.; Walter, P. E.; Gentili, P.; Bella, M., Org. Biomol. Chem. 2012, 10 (24), 4692–4695.	<1 - 5	Bulk chemicals
3 Yamashita, Y.; Ishitani, H.; Kobayashi, S., Can. J. Chem. 2000, 78 (6), 666–672.	5 - 50	Fine chemicals
4 Oppolzer, W.; Tamura, O.; Sundarababu, G.; Signer, M., J. Am. Chem. Soc. 1992, 114 (14), 5900–5902.	25 - 100	Pharmaceuticals

3.2 EcoScale (EcoSynth)

Data were generated from the EcoScale web-based calculator (http://ecoscale.cheminfo.org/calculator)

3.2.1 Preparation of *t*BuOCl

Reagents

Link

	identifier*	name	MF*	MW	density	purity*	ml	g	mmoles	equiv.
1		tert-Butanol	C4H10O	74.1228	0.78	100%	95.029231	74.1228	1000	1
2		Acetic acid	C2H4O2	60.05256	1.048	100%	57.302061	60.05256	1000	1
3		Hypochlorite salts	H10O6ClNa	164.51857		100%	0	246.77785	1500	1.5

Products

identifier*:	name:	MF*:	MW:	g:	mmoles:	g theor:	yield:
	2-chlorosyl-2-methylpropane	C4H9OCl	108.56786	108.45929	999	108.56786	99.9

Conditions

Reagents

Name	mmoles	eq.	Bp	Hazard	Price
tert-Butanol	10.81	1	83		
Acetic acid	10.81	1	117		
Hypochlorite salts	16.22	1.5	51		

Yield	99		-0.5
Price / availability			-3
Safety			-5
Technical setup	Possible items: Instruments for controlled addition of chemicals; Unconventional activation technique; Pressure equipment, > 1 atm; Any additional special glassware	Selected items: Instruments for controlled addition of chemicals; Pressure equipment, > 1 atm	-4
Temperature / time	Possible items: Heating, < 1h; Heating, > 1h; Cooling to 0°C; Cooling, < 0°C	Selected items: Cooling to 0°C	-4

Workup and purification	Possible items Distillation Sublimation Liquid - liquid extraction or washing Classical chromatography	Selected items Liquid - liquid extraction or washing	-3
EcoScale			80.5

^

3.2.2 Preparation of α-chloronitroso derivative **1a**

Ecoscale calculator

Reagents

☑ Link

	identifier*	name	MF*	MW	density	purity*	ml	g	mmoles	equiv.
1		Cyclopentanone oxime	C5H9NO	99.13256		100%	0	99.13256	1000.0000	1
2		2-chlorosyl-2-methylpropane	C4H9OCl	108.56786		100%	0	108.56786	1000.0000	1
3		tert-Butyl methyl ether	C5H12O	88.14968		100%	0	738.69431	8380.0000	8.38

Products

identifier*:	name:	MF*:	MW:	g:	mmoles:	g theor:	yield:
	1-chloro-1-nitrosocyclopentane	C5H8ClNO	133.57	130.90167	980.02300	133.57	98.002299

Conditions

Reagents

Name	mmoles	eq.	Bp	Hazard	Price
Cyclopentanone oxime	7.63	1	218		
2-chlorosyl-2-methylpropane	7.63	1	114		
tert-Butyl methyl ether	64.01	8.38			

Yield: 100 — 0

Price / availability: -8

Safety: -5

Technical setup

Possible items: Pressure equipment, > 1 atm; Any additional special glassware; (Inert) gas atmosphere; Glove box

Selected items: Instruments for controlled addition of chemicals; Pressure equipment, > 1 atm

-4

Temperature / time

Possible items: Heating, < 1h; Heating, > 1h; Cooling to 0°C; Cooling, < 0°C

Selected items: Cooling to 0°C

-4

Cooling, < 0°C

Workup and purification

Possible items

- Simple filtration
- Removal of solvent with bp < 150°C
- Crystallization and filtration
- Removal of solvent with bp > 150°C

Selected items

- Liquid - liquid extraction or washing

-3

EcoScale

76

^

3.2.3 Electrophilic amination on **2b** (continuous flow)

Ecoscale calculator

Reagents

☑ Link

	identifier*	name	MF*	MW	density	purity*	ml	g	mmoles	equiv.
1		Propiophenone	C9H10O	134.1778	1	100%	134.1778	134.1778	1000.0000	1
2		Lithium bis(trimethylsilyl)amide	C6H18LiNSi2	167.32762		100%	0	169.00089	1010.0000(	1.01
3		Tetrahydrofuran	C4H8O	72.10692	0.88	100%	2022.2713	1779.5987	24680.000	24.68
4		tert-Butyl methyl ether	C5H12O	88.14968	0.7404	100%	1000.6726	740.89806	8405	8.405
5		1-chloro-1-nitrosocyclopentane	C5H8ClNO	133.57		100%	0	133.57	1000.0000	1

Products

identifier*:	name:	MF*:	MW:	g:	mmoles:	g theor:	yield:
	2-(hydroxyamino)-1-phenylpropan-1-one	C9H11NO2	165.19	161.89	980.02300	165.19	98.002299

Conditions

Reagents

Name	mmoles	eq.	Bp	Hazard	Price
Propiophenone	6.17	1	218		
Lithium bis(trimethylsilyl)amide	6.23	1.01	114		
Tetrahydrofuran	152.44	24.68	66		
tert-Butyl methyl ether	51.91	8.4	54		
1-chloro-1-nitrosocyclopentane	6.17	1			

Yield 98 -1

Price / availability -11

Safety -15

	Possible items	Selected items	
Technical setup	Pressure equipment, > 1 atm Any additional special glassware (Inert) gas atmosphere Glove box	Instruments for controlled addition of chemicals Pressure equipment, > 1 atm	-4
Temperature / time	Heating, < 1h Heating, > 1h Cooling to 0°C Cooling, < 0°C	Heating, < 1h Cooling to 0°C	-6
Workup and purification	Simple filtration Removal of solvent with bp < 150°C Crystallization and filtration Removal of solvent with bp > 150°C	Liquid - liquid extraction or washing Removal of solvent with bp < 150°C	-3
EcoScale			60

3.2.4 Electrophilic amination on **2b** (adaptation of Oppolzer's procedure in batch)

Ecoscale calculator

Reagents

☑ Link

	identifier*	name	MF*	MW	density	purity*	ml	g	mmoles	equiv.
1		Propiophenone	C9H10O	134.1778	1	100%	134.1778	134.1778	1000.0000	1
2		Lithium bis(trimethylsilyl)amide	C6H18LiNSi2l	167.32762		100%	0	169.00089	1010.0000(	1.01
3		Zinc chloride	Cl2Zn	136.286	0.95	100%	286.91789!	272.572	2000.0000	2
4		Tetrahydrofuran	C4H8O	72.10692	0.88	100%	2022.2713-	1779.5987ł	24680.000	24.68
5		tert-Butyl methyl ether	C5H12O	88.14968	0.7404	100%	1000.6726!	740.89806	8405	8.405
6		1-chloro-1-nitrosocylopentane	C5H8ClNO	133.57		100%	0	133.57	1000.0000	1

Products

identifier*:	name:	MF*:	MW:	g:	mmoles:	g theor:	yield:
	2-(hydroxyamino)-1-phenylpropan-1-one	C9H11NO2	165.19	161.89	980.02300	165.19	98.002299

Conditions

Reagents

Name	mmoles	eq.	Bp	Hazard	Price
Propiophenone	6.17	1	218		
Lithium bis(trimethylsilyl)amide	6.23	1.01	114		
Zinc chloride	12.35	2			
Tetrahydrofuran	152.44	24.68	66		
tert-Butyl methyl ether	51.91	8.4	54		
1-chloro-1-nitrosocylopentane	6.17	1			

Yield	98	-1
Price / availability		-11
Safety		-35

	Possible items	Selected items	
Technical setup	Unconventional activation technique Pressure equipment, > 1 atm Any additional special glassware (Inert) gas atmosphere	(Inert) gas atmosphere Common set-up	-1
Temperature / time	Room temperature, < 1h Room temperature, < 24h Heating, < 1h Heating, > 1h	Cooling, < 0°C Room temperature, < 24h	-6
Workup and purification	Distillation Sublimation Liquid - liquid extraction or washing Classical chromatography	Liquid - liquid extraction or washing Removal of solvent with bp < 150°C	-3
EcoScale			43

4 Computational study

4.1 Model reaction

We began our investigation by exploring the model reaction between nitroso **1-model** and the enolate of acetone (**en-2-model**) (Scheme S1).

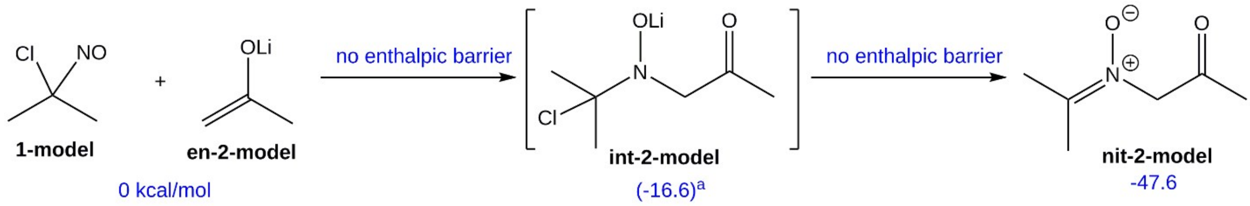

Scheme S1. Model reaction (free energy relative to reactant in kcal mol^{-1}).

Both steps, addition of enolate **en-2-model** onto **1-model** and chloride elimination, are predicted to be exergonic. Unexpectedly, no transition state could be found on the potential energy surface; both steps proceeding consecutively without enthalpic barrier. Indeed, a set of constrained geometry optimization at successively smaller values of the C-N distance showed that the interaction between reactants is uniformly attractive in solution (Figure S91).[a]

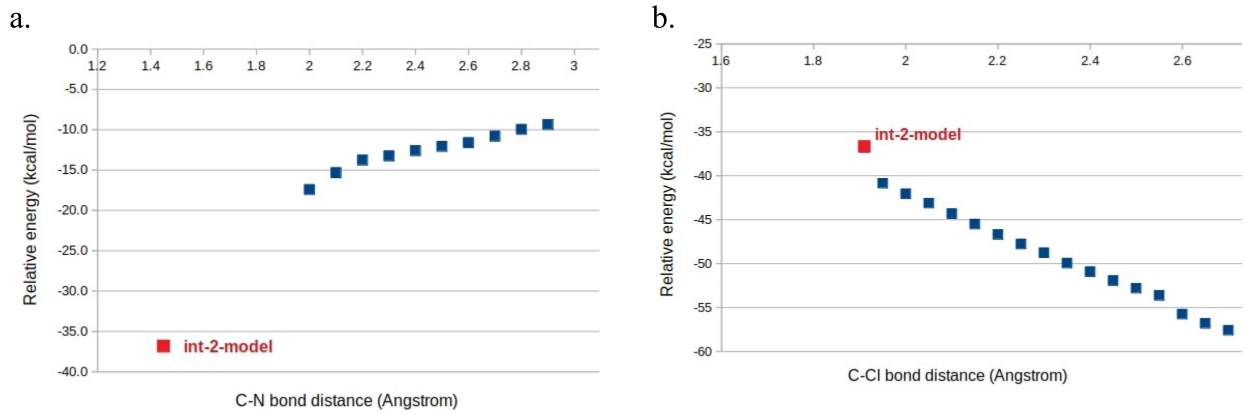

Figure S91. a. Set of constrained geometry optimization at successively smaller values of the C-N distance between **en-2-model** and **1-model**. **b.** Set of constrained geometry optimization at successively larger values of the C-Cl distance in **int-2-model**.

Test calculations with $ZnCl_2$ gave very similar results; the reactions were just slightly more exothermic than without $ZnCl_2$.[b] This support the fact that $ZnCl_2$-catalysis is not mandatory.

a Reactions proceeding without a barrier on the potential energy surface are assumed to be diffusion-controlled, with rate constants in solution given by the approximate expression $k = 8k_BT/3\eta$, where k_B is Boltzmann's constant, T is temperature, and η dis the solvent viscosity.

b Calculations with $ZnCl_2$ were carried out using the 6-31+G(tm)* basis set as incorporated in Jaguar.

4.2 Full system

4.2.1 First amination

Our results on the full systems are very similar to those obtained on the model reaction. Indeed, here also, both steps are computed to be highly exergonic and involve no enthalpic barrier (Scheme S2, Figure S92).[c] The rate of the reaction of **1a** with **en-2a** and **en-2b** is thus predicted to be limited only by diffusion.[a]

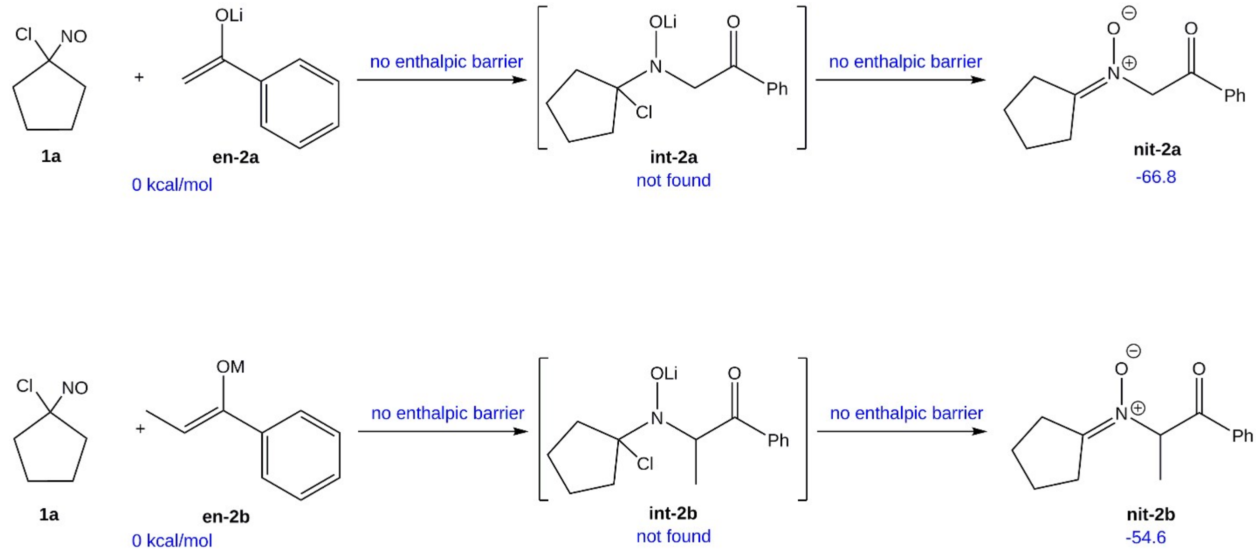

Scheme S2. Realistic systems (free energy relative to reactant in kcal mol^{-1}).

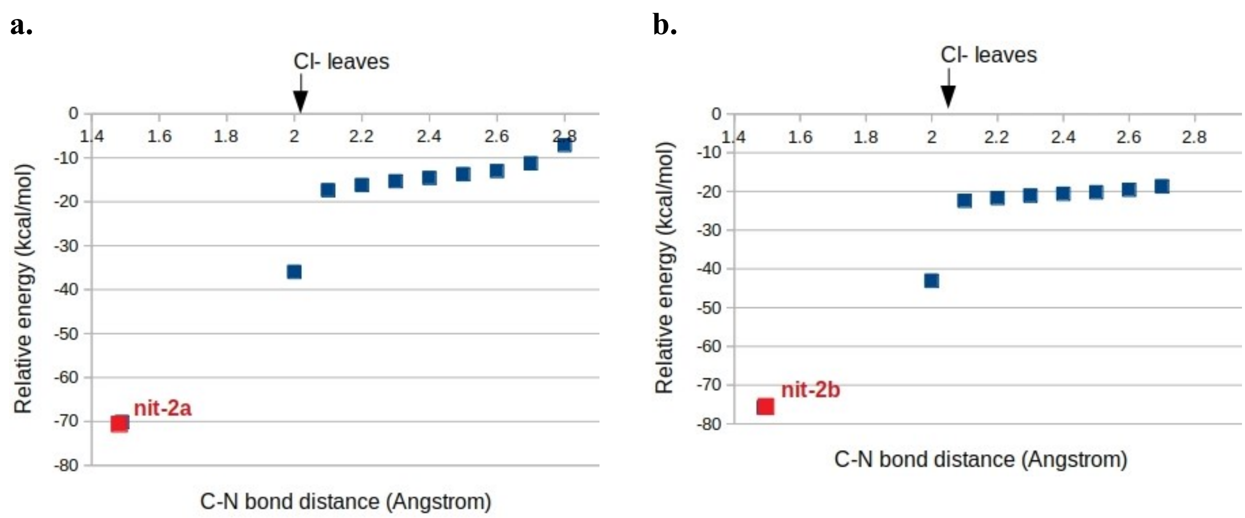

Figure S92. a. Set of constrained geometry optimization at successively smaller values of the C-N distance between **en-2a** and **1a**. **b.** Set of constrained geometry optimization at successively smaller values of the C-N distance between **en-2b** and **1a**.

---

[c] Every attempt to optimize **int-2a** and **int-2b** led to **nit-2a** and **nit-2b**, respectively.

4.2.2 Second amination

Experimentally, a second amination is observed in the case of **en-2a**, but not for **en-2b**. We thus investigated computationally this transformation in order to understand its mechanism and why it is observed for **en-2a** and not in the case of **en-2b**.

Our hypothesis is that this second electrophilic amination involves first the deprotonation of **nit-2** to form corresponding enolates (**en-nit-2a** and **en-nit-2b**), followed by addition of these latter onto nitroso **1a** and elimination of the chloride. Our computational investigation of these steps indicates that the acid-base equilibrium involves a low free energy barrier (3.7 and 9.4 kcal mol^{-1} for **nit-2a** and **nit-2b**, respectively) and is highly displaced toward the formation of **en-nit-2** (ΔG = -22.8 and -19.7 kcal mol^{-1} for **en-nit-2a** and **en-nit-2a**, respectively). Subsequent addition onto **1a** occurs in these cases with an enthalpic barrier which means that a transition state could be obtained; corresponding free energy barrier to addition is 11.4 and 19.5 kcal mol^{-1} for **en-nit-2a** and **en-nit-2b**, respectively.

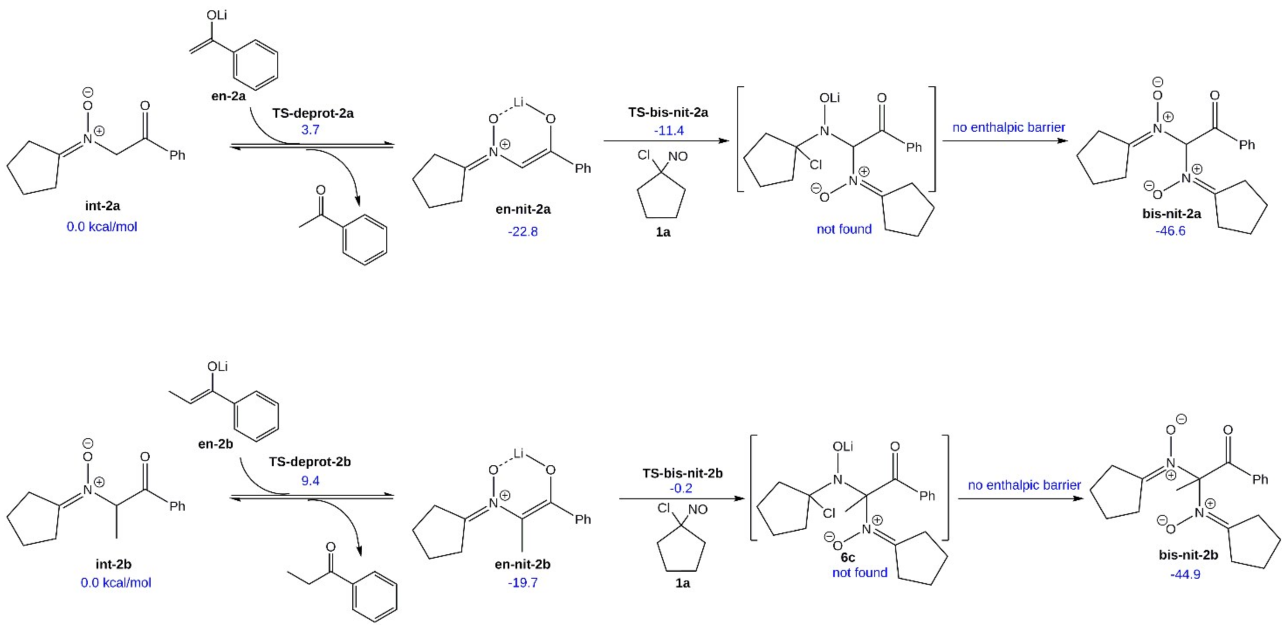

Scheme S3. Pathway for second amination (free energy relative to reactants in kcal mol^{-1})

Obtained free energy profiles indicate that, in both cases, deprotonation of **nit-2** by the enolate (**en-2**) should be non-reversible. This means that the first amination/second amination selectivity is determined by the competition between the addition onto **1a** and the deprotonation of **nit-2**. In both cases, **en-2a** and **en-2b**, addition onto **1a** (first amination) is diffusion-controlled (see above). Concerning deprotonation, for **en-2a**, it involves a very low free energy barrier (3.7 kcal mol^{-1}) which means that the rate of this step (k ~ 6.10^9 M^{-1} s^{-1}) is also at, or very close to, the diffusion limit. In the case of **en-2b**, the free energy barrier is higher (9.4 kcal mol^{-1}) and the rate significantly lower than the diffusion limit (k ~ 2.10^5 M^{-1} s^{-1}).

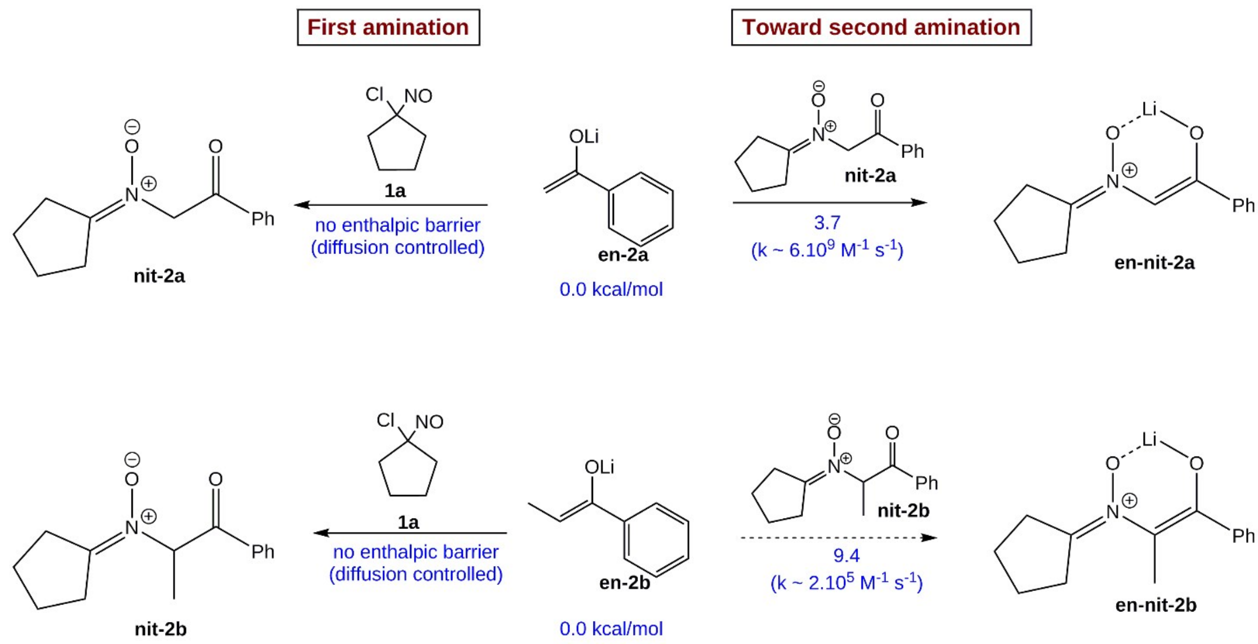

Scheme S4. Competition between first amination and second amination for **en-2a** and **en-2b**.

Thus, our results indicate that the observation of a second amination for **en-2a** and not for **en-2b** can be explained by a fast (diffusion-controlled) non-reversible deprotonation of **nit-2a** by **en-2a** (which is competitive with the, also diffusion-controlled, addition of **en-2a** onto **1a**) whereas in the case of **en-2b**, due to steric factors, deprotonation of **nit-2b** is too slow to compete with addition of **en-2b** onto **1a**.

4.3 Structures and energies

1-model	
C1 -0.6436648350 0.4138225586 6.5065145714 H2 -1.2479065804 1.0018022202 7.2029808621 H3 -1.3058955065 -0.1689676123 5.8606598347 H4 -0.0156698672 -0.2785975432 7.0777159394 C5 0.2362067466 1.3440992275 5.6966000086 Cl6 -0.8003901670 2.4568462776 4.6721186043 C7 1.2235686221 2.1740993836 6.5063954957 H8 1.8387144715 2.7952710451 5.8486515276 H9 0.6787175136 2.8201368035 7.2020728553 H10 1.8762316697 1.5062997161 7.0830937010 N11 1.0651361301 0.6500959794 4.6107654919 O12 0.9567967402 -0.5505467559 4.6056874012	E(B3LYP-D3/6-31+G*) = -708.04510002621 E(B3LYP-D3/6-31+G*)(mtbe) = -708.04828483791 E(B3LYP-D3/6-311+G**) = -708.13698937512 G(mtbe) = -708.0800462507
en-2-model	
C1 -2.9196902144 2.0342526319 9.0387224328 C2 -2.1716279222 1.5585015599 8.0010490707 H3 -2.4465157696 2.3989647794 9.9482982577 H4 -4.0066024748 2.0617796380 8.9926831703 C5 -0.6500745191 1.5626513144 8.1342592231 H6 -0.1947707253 2.2124401553 7.3741422355 H7 -0.3231023020 1.9176659121 9.1198465670 H8 -0.2447854081 0.5529900213 7.9839302618 O9 -2.6558246748 1.0875309560 6.8589907979 Li10 -3.7854889942 0.4267272648 5.6299626837	E(B3LYP-D3/6-31+G*) = -200.10822138634 E(B3LYP-D3/6-31+G*)(mtbe) = -200.15434666395 E(B3LYP-D3/6-311+G**) = -200.16300654757 G(mtbe) = -200.1637147681
Int-2-model	
C1 1.6811351940 5.0387876504 4.4594833117 H2 1.2710012417 5.6088437937 5.2983764271	E(B3LYP-D3/6-31+G*) = -908.23188526701 E(B3LYP-D3/6-31+G*)(mtbe) = -908.26130912626

H3 2.7561047246 5.2279684819 4.3897192586 H4 1.2015681357 5.3569649214 3.5305952996 C5 1.4168058213 3.5554723226 4.6676299250 Cl6 2.1738869098 3.1297453320 6.3637506497 C7 -0.0795593496 3.2516940413 4.7899797711 H8 -0.2707496822 2.2347901390 5.1437080640 H9 -0.5547751405 3.9447849780 5.4913139049 H10 -0.5355966971 3.3748053441 3.8003599094 N11 2.1642075826 2.7517463395 3.6887950824 C12 1.8329699705 1.3373685485 3.7463455616 H13 1.7514808570 0.9936284293 4.7869419173 H14 0.8654304080 1.1168063352 3.2570186499 C15 2.8757127542 0.4708753133 3.0755799185 O16 3.8023871023 0.9408774337 2.4140050583 C17 2.7241720815 -1.0153183536 3.3039309291 H18 3.2407429021 -1.5926352398 2.5333971982 H19 3.1662031079 -1.2592959175 4.2817301671 H20 1.6672460973 -1.3039193436 3.3529979713 O21 1.8879709942 3.2315981227 2.3571086412 Li22 3.7030716759 3.0200722932 2.0054639415	E(B3LYP-D3/6-311+G**) = -908.37603869832 G(mtbe) = -908.27324037857
nit-2-model	
C1 0.4450569858 4.6699357941 5.7817511946 H2 -0.3573750241 4.9441420724 6.4710649335 H3 1.4000181965 4.6583079944 6.3238460896 H4 0.5435631046 5.4357097148 5.0040805790 C5 0.1824848166 3.3250153164 5.1792406148 Cl6 5.8773256923 3.4836611859 3.1787765755 C7 -1.0151332073 2.5523580810 5.6502148335 H8 -0.9856189194 2.4683565160 6.7443155009 H9 -1.9228285420 3.1208103633 5.4029596634 H10 -1.1205553892 1.5492747572 5.2368984349 N11 1.0141871184 2.9111026429 4.2572226746 C12 0.9628577495 1.5880079757 3.5883469308 H13 -0.0020249078 1.1052049944 3.7244769416 H14 1.1252534518 1.7792217169 2.5239175571 C15 2.1225840300 0.7357519251 4.1399760482 O16 3.2726032902 1.0679127152 3.8913321013 C17 1.7781006565 -0.4580346853 4.9847728371 H18 2.6814664591 -0.9101806877 5.4013740783 H19 1.0958633964 -0.1643730682 5.7943530295 H20 1.2423844955 -1.1954710400 4.3692363522 O21 2.0305589991 3.6539534541 3.8627901267 Li22 3.7271360656 2.9718635910 3.2223301957	E(B3LYP-D3/6-31+G*) = -908.27024336594 E(B3LYP-D3/6-31+G*)(mtbe) = -908.30623543281 E(B3LYP-D3/6-311+G**) = -908.41437550613 G(mtbe) = -908.32263803656
1a	
C1 -0.7145464640 0.5466249575 6.5278200331 H2 -1.6483996564 1.0872719939 6.7136791325 H3 -0.9606588772 -0.4146207233 6.0685943952 C4 0.1677691080 1.4017305128 5.6167364715 Cl5 -0.7779456412 2.3524729706 4.3890049176 C6 1.0662219371 2.2799588331 6.5303618034 H7 2.1209258808 2.0637034849 6.3090250814 H8 0.9128816291 3.3432247363 6.3298667170 N9 1.1286552417 0.6218885984 4.7128364474 O10 1.1293075217 -0.5693911922 4.8961774237 C11 0.6929853556 1.8627513041 7.9718036362 H12 1.5511127607 1.9070715731 8.6494052775 H13 -0.0756448072 2.5394627029 8.3654387289 C14 0.1063396787 0.4460019442 7.8244940778 H15 -0.5054928683 0.1448619527 8.6811440368 H16 0.9082474140 -0.2942072504 7.7089202421	E(B3LYP-D3/6-31+G*) = -785.46425406415 E(B3LYP-D3/6-31+G*)(mtbe) = -785.46688726125 E(B3LYP-D3/6-311+G**) = -785.57244416031 G(mtbe) = -785.48044451702
en-2a	
C1 -2.9286898435 1.7635204357 9.0925517093 C2 -2.1655745709 1.5269965290 7.9833526344 H3 -2.4849506374 1.9513214391 10.0657099633 H4 -4.0141687471 1.7262280546 9.0406286775 O5 -2.6559042183 1.2214857434 6.7892084202	E(B3LYP-D3/6-31+G*) = -391.85944348654 E(B3LYP-D3/6-31+G*)(mtbe) = -391.90678698608 E(B3LYP-D3/6-311+G**) = -391.95187893996 G(mtbe) = -391.90474984478

Li6 -3.9410127649 0.8978718077 5.5539247080 C7 2.1690756099 1.5232471118 8.4192373331 C8 1.5436531707 0.7601062696 7.4284267433 C9 0.1519599446 0.7914432853 7.2816354649 C10 -0.6566807500 1.5705784266 8.1262436527 C11 -0.0065791293 2.3496183684 9.1083035115 C12 1.3831066962 2.3242628757 9.2559545178 H13 3.2513573202 1.5011344808 8.5349542383 H14 2.1421450084 0.1342737353 6.7689636823 H15 -0.3283732439 0.1947731808 6.5119154972 H16 -0.5878002091 2.9956043167 9.7606136964 H17 1.8563382350 2.9363822859 10.0225526806	
nit-2a	
C1 0.7997517878 4.6287480716 5.8544565305 H2 1.8903626409 4.6931837950 5.9427251278 H3 0.4860768649 5.5039550486 5.2652237754 C4 0.3836707715 3.3725165297 5.1459322794 Cl5 5.5546164178 2.9744492604 2.1351925549 C6 -0.7597547879 2.6852940635 5.8579670935 H7 -0.3926722348 1.7952420271 6.3898056526 H8 -1.5510492419 2.3521555148 5.1765765436 N9 0.9625322512 2.9558135258 4.0573833939 C10 0.6522108623 1.6380867461 3.4431795949 H11 -0.3444179207 1.3157977912 3.7311368755 H12 0.6990294572 1.7754585320 2.3607504784 C13 1.7830694381 0.7061841910 3.9133394540 O14 2.9057684041 0.9097936776 3.4517409200 O15 1.9314182744 3.6198612399 3.4595005245 Li16 3.4053707181 2.7075885086 2.5800569029 C17 1.1355568820 -2.1359329938 7.0536634385 C18 0.0607551712 -1.7521762978 6.2443915482 C19 0.2541770754 -0.8206057679 5.2245144876 C20 1.5345577655 -0.2861564034 4.9841666321 C21 2.6162841442 -0.6929904546 5.7921886932 C22 2.4115614421 -1.6016930964 6.8290511649 H23 0.9792973244 -2.8519750412 7.8574617370 H24 -0.9266016972 -2.1768508654 6.4073437327 H25 -0.5893975850 -0.5449087882 4.5987065517 H26 3.6027089119 -0.2764710217 5.6083023470 H27 3.2436973346 -1.8961246362 7.4639700279 C28 -1.2378951059 3.7614448163 6.8590999947 H29 -1.7271207052 3.3237421585 7.7350841242 H30 -1.9634244734 4.4226277463 6.3675219982 C31 0.0431722822 4.5461931678 7.2007803187 H32 0.6415443708 3.9850274802 7.9309758045 H33 -0.1618253950 5.5313056201 7.6306233210	E(B3LYP-D3/6-31+G*) = -1177.44985533962 E(B3LYP-D3/6-31+G*)(mtbe) = -1177.48546885585 E(B3LYP-D3/6-311+G**) = -1177.64741814822 G(mtbe) = -1177.46889968996
en-2b	
C1 -2.8836200027 1.6704413769 9.1357648624 C2 -2.1535494191 1.6180662472 7.9830383990 O3 -2.6809361200 1.5751823382 6.7554695537 Li4 -3.8473220047 1.5887435794 5.3883996599 C5 2.1598245596 1.4128650324 8.4457505871 C6 1.4744433801 0.4184589677 7.7367720070 C7 0.0903887390 0.5073079941 7.5519882751 C8 -0.6447958654 1.5791576961 8.0857946326 C9 0.0604790715 2.5762854126 8.7840554046 C10 1.4463658850 2.4984239825 8.9631433402 H11 3.2354202920 1.3395700894 8.5970774295 H12 2.0205648827 -0.4357098318 7.3405448979 H13 -0.4353967172 -0.2803223740 7.0169191201 H14 -0.4880009909 3.4126506838 9.2108465669 H15 1.9672178334 3.2793284793 9.5151955773 H16 -3.9688556685 1.7032895166 9.0222327361 C17 -2.3677664807 1.6373845120 10.5608035472 H18 -2.9844324453 0.9769048468 11.1881519155 H19 -1.3383041758 1.2690171120 10.6260818855 H20 -2.3787133848 2.6243554254 11.0526224147	E(B3LYP-D3/6-31+G*) = -431.17343740794 E(B3LYP-D3/6-31+G*)(mtbe) = -431.21931749169 E(B3LYP-D3/6-311+G**) = -431.27545393717 G(mtbe) = -0.04588008375

nit-2b	
C1 0.6247758276 5.0463192340 5.1820057289 H2 1.7054685345 5.2131981964 5.1165156418 H3 0.1715361388 5.6724776993 4.3979310718 C4 0.2799665899 3.6099094880 4.9217207724 Cl5 5.4605377653 3.8432742472 3.2722423891 C6 -0.7176998712 3.0846059700 5.9303629201 H7 -0.2074389001 2.4270319525 6.6507209157 H8 -1.5330499897 2.5066135198 5.4802516083 N9 0.8267868959 2.9479907328 3.9458849238 C10 0.5881895720 1.4951605550 3.7284998340 H11 -0.3026480958 1.2341172727 4.2965963033 C12 1.8025550728 0.7136931760 4.2724707496 O13 2.9325863879 1.1939546327 4.1604189109 O14 1.6839956937 3.5233188014 3.1199116126 Li15 3.4720423408 2.9067251765 3.2858342417 C16 1.3210507186 -3.1342493319 6.0974240941 C17 0.2202875985 -2.5343342258 5.4756591038 C18 0.3510092495 -1.2772270027 4.8851369996 C19 1.5939985472 -0.6129794187 4.8987473322 C20 2.6995351798 -1.2324158121 5.5166195736 C21 2.5601939978 -2.4802026303 6.1185261134 H22 1.2140420402 -4.1108372288 6.5641371941 H23 -0.7391750633 -3.0449427178 5.4520888649 H24 -0.5180750889 -0.8378085463 4.4043291384 H25 3.6571651024 -0.7199440737 5.5220386449 H26 3.4152837005 -2.9461767509 6.6018862192 C27 -1.2095865596 4.3750120356 6.6277850355 H28 -1.5650602079 4.1861427733 7.6455259780 H29 -2.0438701177 4.8023982115 6.0564366416 C30 0.0061422610 5.3202502684 6.5692346324 H31 0.7263586729 5.0546168514 7.3542782621 H32 -0.2632701656 6.3712885348 6.7093591560 C33 0.3626172510 1.1882049754 2.2417462820 H34 -0.4896644403 1.7643800011 1.8670066607 H35 1.2464494051 1.4467803744 1.6551495053 H36 0.1513015191 0.1212244089 2.1168949436	E(B3LYP-D3/6-31+G*) = -1216.77782302060 E(B3LYP-D3/6-31+G*)(mtbe) = -1216.80900766572 E(B3LYP-D3/6-311+G**) = -1216.98456424307 G(mtbe) = -1216.77251498002
acetophenone	
C1 -2.1272356709 1.4657301729 7.9900217281 H2 -2.8172850471 1.9108898721 9.9930062646 H3 -4.0519953530 2.0632635154 8.7106369661 O4 -2.6363983465 0.7843659237 7.1022518540 C5 2.1643864750 1.6555397961 8.3175550193 C6 1.5574508606 0.8903141092 7.3129668626 C7 0.1675202390 0.8378862257 7.2194508334 C8 -0.6367394539 1.5495022468 8.1284234884 C9 -0.0189938693 2.3153542354 9.1334006606 C10 1.3743483220 2.3672826530 9.2265522832 H11 3.2489681547 1.6971294445 8.3903377988 H12 2.1695108843 0.3368244830 6.6045216710 H13 -0.3141363530 0.2481511120 6.4448653724 H14 -0.6155092336 2.8744457104 9.8484061994 H15 1.8422173129 2.9622744650 10.0073559349 C16 -3.0026930495 2.2341418377 8.9606728130 H17 -2.7882966929 3.3095761994 8.9121453388	E(B3LYP-D3/6-31+G*) = -384.92262419963 E(B3LYP-D3/6-31+G*)(mtbe) = -384.92911290080 E(B3LYP-D3/6-311+G**) = -385.01203018252 G(mtbe) = -384.9126620404
TS-deprot-2a	
C1 -1.9908952933 -0.2271028009 6.6660427338 C2 -0.6141323893 0.2159130911 6.8033580199 H3 -0.0897244609 -0.1364347373 7.6845661787 C4 1.0116515107 1.9499220601 6.6953408553 C5 1.4999890831 3.3415419995 6.4349828379 H6 1.5469041723 3.5060607820 5.3488185297 H7 0.8100256088 4.0926064384 6.8354985778 C8 2.1068406029 1.0644919883 7.2421508799 H9 1.9689875120 0.9115491377 8.3258712528 H10 2.1315831677 0.0751911863 6.7735133240	E(B3LYP-D3/6-31+G*) = -1101.51763561445 E(B3LYP-D3/6-31+G*)(mtbe) = -1101.54121395422 E(B3LYP-D3/6-311+G**) = -1101.77569284028 G(mtbe) = -1101.46785687615

O11	-1.1102393544	2.4146524494	5.9637568627	
N12	-0.2212235866	1.5828183840	6.4839043153	
C13	-2.9205766153	-3.7087641965	9.0364486629	
C14	-2.1566583080	-2.6786174811	9.5954085764	
C15	-1.8710379281	-1.5357779102	8.8461675668	
C16	-2.3536082942	-1.3995089869	7.5297844334	
C17	-3.1447768450	-2.4276473213	6.9897873445	
C18	-3.4177360675	-3.5774680000	7.7343294472	
H19	-3.1279138514	-4.6074318875	9.6136139801	
H20	-1.7803434297	-2.7662791925	10.6124263796	
H21	-1.2900066257	-0.7385077517	9.3021995281	
H22	-3.5187663591	-2.3248561572	5.9750916217	
H23	-4.0103031118	-4.3776936656	7.2972031250	
C24	2.9086768184	3.3560592993	7.0714383905	
H25	2.8384461870	3.6546074847	8.1262700366	
H26	3.5882247305	4.0557041918	6.5741941313	
C27	3.3819386782	1.8926901595	6.9690867877	
H28	4.1932873771	1.6504296066	7.6641506100	
H29	3.7359856329	1.6850563647	5.9533419266	
O30	-2.7491524392	0.1509077365	5.7413516579	
Li31	-2.0820255058	1.5718180469	4.4204132675	
C32	0.4710654344	0.2083391291	3.7274226839	
O33	-0.4799120049	0.9778709225	3.3560326272	
C34	0.2286467465	-1.0075071217	4.4150046896	
H35	1.0327269174	-1.7190715339	4.5821924166	
H36	-0.1101239474	-0.4596027269	5.7895963011	
H37	-0.7519530649	-1.4562809307	4.2548140253	
C38	4.5204340010	1.6598600666	3.1706156073	
C39	4.3096272955	0.3307217142	3.5542215204	
C40	3.0117827685	-0.1528094315	3.7306408124	
C41	1.8931096922	0.6813504789	3.5347311709	
C42	2.1213178092	2.0072057285	3.1306538832	
C43	3.4188315501	2.4945797500	2.9559245574	
H44	5.5318870494	2.0373351870	3.0358207953	
H45	5.1572781811	-0.3331590672	3.7126889726	
H46	2.8813313456	-1.1926164561	4.0125906844	
H47	1.2614159758	2.6479321858	2.9627057431	
H48	3.5713951334	3.5276798617	2.6515257563	
en-nit-2a				
C1	-0.2899791136	-0.3943134968	6.7946429165	E(B3LYP-D3/6-31+G*) = -709.60209547901
C2	1.7529673131	2.0580529830	6.6477060181	E(B3LYP-D3/6-31+G*)(mtbe) = -709.61609722968
C3	2.1017263073	3.3664652183	6.0038515822	E(B3LYP-D3/6-311+G**) = -709.76815206223
H4	1.4428253695	3.5229769741	5.1354418315	G(mtbe) = -709.56593219548
H5	1.9209766860	4.2110544078	6.6789291810	
C6	2.8373799100	1.0255512294	6.4522470636	
H7	3.4207272918	0.9070944996	7.3799220433	
H8	2.4513343463	0.0402840492	6.1737434517	
O9	-0.2956255460	2.8050352806	7.3733873317	
N10	0.6229792918	1.8772636828	7.2643806140	
C11	-2.1115185361	-4.0712206180	8.0738929245	
C12	-1.5873649439	-3.1993687253	9.0342262035	
C13	-0.9967684853	-1.9963583801	8.6404426235	
C14	-0.9217790630	-1.6575210309	7.2769703077	
C15	-1.4494304942	-2.5428161215	6.3185413527	
C16	-2.0420997174	-3.7400765396	6.7141984149	
H17	-2.5737388066	-5.0057993184	8.3835874740	
H18	-1.6407368094	-3.4542421651	10.0898121101	
H19	-0.6003476489	-1.3342398477	9.4048055941	
H20	-1.3877233083	-2.2745272771	5.2680105974	
H21	-2.4503566311	-4.4154383417	5.9661190539	
C22	3.5771097150	3.1804860456	5.5866021710	
H23	4.2369885226	3.4855189745	6.4099846800	
H24	3.8477405155	3.7765905755	4.7091812843	
C25	3.7099046796	1.6623625960	5.3451122376	
H26	4.7456871912	1.3082488594	5.3730669889	
H27	3.2948011629	1.4027190459	4.3627656354	
O28	-0.1795119334	-0.1398825363	5.6033441576	
C29	0.2650198954	0.5753344988	7.8507666119	

H30 -0.4816335502 0.7908127386 8.6174137767 H31 1.1387464078 0.1211442443 8.3333269002	
TS-bis-nit-2a	
Li1 -0.3219576518 0.2557462176 4.2588442841 C2 -1.2112159549 -0.5708967052 6.7945199835 O3 -1.6140732846 -0.6231638793 5.6056263004 C4 -0.1462931436 0.2775109614 7.2608411331 H5 0.1131099091 0.2020438643 8.3025323665 C6 2.3980793614 -1.1285761881 7.0752992672 Cl7 3.3700945067 0.4967652604 7.1124199762 C8 3.3565365084 -2.2126217655 6.5387024505 H9 2.7405337035 -3.0773982154 6.2554678478 H10 3.8979368794 -1.8740932505 5.6522032021 C11 2.0918989436 -1.5710826822 8.5188364512 H12 1.9644676211 -0.7193990604 9.1898379922 H13 1.1432862182 -2.1186853822 8.4977458189 O14 1.3820058073 -0.5680338540 5.0685652489 N15 1.2058301261 -1.0778892589 6.2195955811 C16 -2.4727021209 -3.5174764803 9.6864315970 C17 -2.2008479466 -2.2118026690 10.1074042173 C18 -1.8109364121 -1.2461715708 9.1769324639 C19 -1.6955464930 -1.5680531944 7.8115587562 C20 -1.9987236796 -2.8741041365 7.3965480745 C21 -2.3755213627 -3.8438731498 8.3284522613 H22 -2.7608713500 -4.2751272809 10.4123793410 H23 -2.2889566092 -1.9462200891 11.1589806940 H24 -1.6138310394 -0.2333934706 9.5191746174 H25 -1.9110610062 -3.1220803949 6.3427041383 H26 -2.5866707750 -4.8584640058 7.9986823619 C27 4.2352777083 -2.5589231524 7.7485295221 H28 5.0306826299 -1.8127109353 7.8520234262 H29 4.7124172055 -3.5394948879 7.6440342236 C30 3.2684959067 -2.4906624893 8.9580044628 H31 3.7697423322 -2.1085756776 9.8537753176 H32 2.8902416635 -3.4892862774 9.2063030795 N33 0.1125279353 1.5717617739 6.7336676790 O34 -0.1550057719 1.8003127961 5.4518625866 C35 0.6173387626 2.5124771663 7.4961177494 C36 0.9391839763 2.3787052626 8.9679965570 C37 1.7170050418 3.6764460905 9.2776535158 C38 1.1440410357 4.7047283006 8.2845093138 C39 0.9195409511 3.8893586884 6.9906785387 H40 1.5299724820 1.4886999720 9.2023425582 H41 0.0100616522 2.3262595261 9.5594015969 H42 1.6187593786 3.9822942425 10.3250167125 H43 2.7841896505 3.5151788627 9.0768104520 H44 0.1822135663 5.0831710355 8.6563008175 H45 1.8028100130 5.5663357330 8.1357012624 H46 1.8314586676 3.8579805674 6.3725175374 H47 0.1200677838 4.2729727425 6.3474007841	E(B3LYP-D3/6-31+G*) = -1502.08313269125 E(B3LYP-D3/6-31+G*)(mtbe) = -1502.10834907626 E(B3LYP-D3/6-311+G**) = -1502.3591648459 G(mtbe) = -1502.05969344821
bis-nit-2a	
C1 -1.1145576855 -1.0090325040 7.5926447821 O2 -2.1427315640 -0.6795367101 7.0267873661 C3 0.2270658792 -0.3323659351 7.1779344734 H4 0.7522416369 0.0272362323 8.0631594023 C5 2.3389652708 -1.0759587695 6.2481478742 C6 3.2101494189 -2.0534031352 5.5186805764 H7 3.1170353383 -3.0637702803 5.9347449766 H8 2.8697874797 -2.1268658715 4.4735125545 C9 3.0899014288 0.1736072032 6.6386445282 H10 2.5228660525 1.0989167939 6.5006065452 H11 3.3616967042 0.1243181255 7.7062138490 O12 0.4889231878 -2.4366310205 6.1095851345 N13 1.0794707510 -1.3287616853 6.4719825410 C14 -1.1520622785 -3.7544829101 10.8883404983 C15 0.0736569678 -3.2642218328 10.4243983857 C16 0.1094198917 -2.3729290425 9.3514645023	E(B3LYP-D3/6-31+G*) = -1034.28446060494 E(B3LYP-D3/6-31+G*)(mtbe) = -1034.29971620232 E(B3LYP-D3/6-311+G**) = -1034.52703989398 G(mtbe) = -1034.21600864678

C17 -1.0840043784 -1.9655510087 8.7294136684 C18 -2.3111386341 -2.4666546367 9.1995425051 C19 -2.3445962607 -3.3542470802 10.2731412572 H20 -1.1776352333 -4.4471764790 11.7263834729 H21 1.0014260357 -3.5784903698 10.8962581663 H22 1.0737781583 -2.0218004294 8.9975256190 H23 -3.2287392712 -2.1485734969 8.7137785402 H24 -3.2981446889 -3.7341034970 10.6317425642 C25 4.6205629046 -1.4327968654 5.6302328727 H26 5.2613949760 -1.6858737788 4.7798766724 H27 5.1162014274 -1.8014998874 6.5378403303 C28 4.3568529133 0.0821594158 5.7561246236 H29 4.1436574347 0.5094784624 4.7669809075 H30 5.2014041168 0.6339046461 6.1807538435 N31 -0.0096207106 0.9045121786 6.3964712836 O32 0.0879649959 1.9926813966 7.1276940210 C33 -0.3343190775 0.9230272522 5.1361811490 C34 -0.5967658620 2.2284359089 4.4444149871 C35 -0.7884589372 1.8264698872 2.9663052998 C36 -1.3235079967 0.3827110331 3.0433530920 C37 -0.5307532060 -0.2496207884 4.2090750514 H38 0.2086425293 2.9500524602 4.6274241899 H39 -1.5056812955 2.6771023330 4.8745008474 H40 -1.4580838403 2.5047739242 2.4280479324 H41 0.1802760016 1.8378443937 2.4482758631 H42 -2.3928442599 0.3913842973 3.2921850357 H43 -1.2030087327 -0.1750897322 2.1088486668 H44 0.4459662839 -0.6120049796 3.8527367559 H45 -1.0291732451 -1.0982174027 4.6798782452	
Propiophenone	
C1 -2.1466361472 1.6312609386 7.9215936286 O2 -2.6595800333 1.5622999245 6.8071252138 C3 2.1520266908 1.6473887659 8.2533705952 C4 1.3749174965 1.7293083359 9.4136619164 C5 -0.0195202886 1.7235165252 9.3250163067 C6 -0.6527354425 1.6355851351 8.0719978906 C7 0.1389250048 1.5548288203 6.9120558971 C8 1.5303183521 1.5598615635 7.0011299386 H9 3.2375071381 1.6533523967 8.3240070174 H10 1.8541522155 1.7995646349 10.3873809709 H11 -0.6036596905 1.7903997752 10.2379484716 H12 -0.3540470640 1.4902303219 5.9464668901 H13 2.1313819497 1.4977616160 6.0968667394 C14 -4.5108097360 1.6897510161 8.8799300301 H15 -5.0791956844 1.7502354101 9.8149821888 H16 -4.7990211149 2.5329444682 8.2434871687 H17 -4.7970876881 0.7706362131 8.3583210744 C18 -3.0111362970 1.7112146614 9.1729378247 H19 -2.7325723533 0.8768238132 9.8327384109 H20 -2.7370774172 2.6249669093 9.7196932592	E(B3LYP-D3/6-31+G*) = -424.24014424448 E(B3LYP-D3/6-31+G*)(mtbe) = -424.24593990252 E(B3LYP-D3/6-311+G**) = -424.3392215461 G(mtbe) = -424.21246126353
TS-deprot-2b	
C1 -1.8612618991 -0.3992296370 6.6820378127 C2 -0.4267715418 -0.1086300082 6.8820273719 C3 1.1907747936 1.7500850733 6.7880629659 C4 1.4708172526 3.2171767775 6.6176523884 H5 1.3018264571 3.4873681544 5.5652632674 H6 0.7749742713 3.8262628357 7.2051360229 C7 2.4773440877 0.9870091162 7.0327764022 H8 2.5766809721 0.7248341082 8.0948929319 H9 2.5426054673 0.0642706757 6.4506455711 O10 -0.9867764304 2.1767114505 6.3449910767 N11 -0.0365041869 1.3087377428 6.6818815731 C12 -3.6930676807 -3.3863801106 9.2047611734 C13 -3.1959614725 -2.2047402984 9.7667321999 C14 -2.6016849814 -1.2388417529 8.9517080448 C15 -2.5121793748 -1.4350573316 7.5641324256 C16 -3.0544987733 -2.5998182446 7.0024634339	E(B3LYP-D3/6-31+G*) = -1180.14313107785 E(B3LYP-D3/6-31+G*)(mtbe) = -1180.16506924370 E(B3LYP-D3/6-311+G**) = -1180.42028772136 G(mtbe) = -1180.05555673038

C17 -3.6256564809 -3.5793038139 7.8207900004 H18 -4.1305563772 -4.1515164867 9.8425223691 H19 -3.2579085499 -2.0424784187 10.8406912138 H20 -2.1927290919 -0.3338430111 9.3946524745 H21 -3.0107801870 -2.7443845159 5.9269044802 H22 -4.0141868040 -4.4940793904 7.3786397093 C23 2.9536166411 3.3692681335 7.0117453938 H24 3.0379329098 3.5440284910 8.0929199029 H25 3.4416330206 4.2064449688 6.5021726691 C26 3.5694274880 2.0077596342 6.6474084280 H27 4.5159640310 1.8061905332 7.1611725714 H28 3.7555968288 1.9573653684 5.5712470299 O29 -2.5426584497 0.0787153763 5.7478531866 Li30 -1.8785861345 1.5954978059 4.6348800233 C31 0.5860561771 0.2130229808 3.7621352183 O32 -0.4618262880 0.8889877193 3.4795655226 C33 0.5359970688 -1.0573769941 4.4084661229 H34 1.4937479057 -1.5478364369 4.5773094302 H35 0.1020138922 -0.6078680180 5.7414888083 C36 4.3904834497 2.0908609659 2.8662643305 C37 4.3457213576 0.7208127958 3.1458577647 C38 3.1289885033 0.1030275978 3.4424112361 C39 1.9282056685 0.8400598112 3.4749057519 C40 1.9901361556 2.2129398049 3.1796555737 C41 3.2046143280 2.8336669297 2.8815700931 H42 5.3385151324 2.5716972197 2.6347153754 H43 5.2587518279 0.1289029204 3.1266833474 H44 3.1218454190 -0.9666503822 3.6262704773 H45 1.0658400141 2.7814345616 3.1832460096 H46 3.2274209398 3.8988807520 2.6623259527 C47 0.3009566841 -0.8089689380 8.0298514554 H48 1.3316253476 -1.0533137116 7.7709898062 H49 0.3128949126 -0.2135551549 8.9520095141 H50 -0.1840801291 -1.7602432498 8.2492677196 C51 -0.6045324330 -2.0265674895 4.1562754090 H52 -0.8596527422 -2.5861054453 5.0670572412 H53 -1.5042948427 -1.4985419575 3.8315676606 H54 -0.3353374030 -2.7657763729 3.3885400617	
en-nit-2b	
C1 -0.51800 -1.53000 7.20600 O2 -0.34000 -2.16600 6.17800 C3 0.36500 -0.26600 7.48000 C4 2.54400 -1.33100 6.80400 C5 3.76900 -1.38300 5.93400 C6 2.50200 -2.51000 7.74700 O7 1.82700 0.55400 5.74500 N8 1.66200 -0.39200 6.64500 C9 -3.45600 -2.89900 10.02100 C10 -3.25600 -1.52200 9.86800 C11 -2.29900 -1.04500 8.97000 C12 -1.54500 -1.95100 8.20300 C13 -1.77200 -3.33300 8.34100 C14 -2.71300 -3.80500 9.25600 C15 4.54400 -2.61600 6.44800 C16 3.45200 -3.51500 7.05900 N17 -0.44800 0.82600 6.99200 O18 0.17000 2.09800 7.20500 C19 0.76600 -0.04700 8.94500 H20 3.45000 -1.49600 4.88800 H21 4.33000 -0.44100 5.97700 H22 2.92200 -2.21700 8.72200 H23 1.50300 -2.91400 7.92700 H24 -4.19500 -3.26500 10.73100 H25 -3.84900 -0.81700 10.44600 H26 -2.16700 0.02300 8.82900 H27 -1.20100 -4.02700 7.72900 H28 -2.87000 -4.87500 9.36800 H29 5.25500 -2.31400 7.22900	E(B3LYP-D3/6-31+G*) = -748.91953604919 E(B3LYP-D3/6-31+G*)(mtbe) = -748.93240285596 E(B3LYP-D3/6-311+G**) = -749.09556148551 G(mtbe) = -748.86549596119

H30 5.11500 -3.11300 5.65700 H31 3.84200 -4.26200 7.75700 H32 2.91000 -4.04500 6.26400 H33 -0.58100 0.73400 5.98200 H34 0.98600 2.05300 6.65000 H35 1.59600 0.66200 8.99400 H36 -0.06700 0.36700 9.51300 H37 1.07000 -0.98500 9.41400	
TS-bis-nit-2b	
Li1 0.1868294294 0.4572473037 4.4226965894 C2 -0.6226611712 -0.8674227833 6.7451028484 O3 -0.5761907766 -1.0068060381 5.5021567582 C4 0.0596875135 0.2508086979 7.4423436558 C5 2.7234050278 -0.8799610291 7.3840908298 Cl6 3.2831322133 -0.2118811532 9.0446921880 C7 4.0086584514 -1.1548534683 6.5875681694 H8 3.6988484675 -1.3332845502 5.5540714865 H9 4.6930716698 -0.3023225077 6.5963288480 C10 2.1464559108 -2.2780693502 7.5862975070 H11 1.4049864150 -2.3282016491 8.3837650463 H12 1.6512794022 -2.5188925783 6.6380732452 O13 1.8138666951 0.0305059348 5.4750245015 N14 1.8665753123 0.2015161699 6.7744649210 C15 -2.6103619025 -4.0052642408 8.9720489542 C16 -2.9264004752 -2.6653657082 9.2179140511 C17 -2.2778592768 -1.6515035534 8.5093214329 C18 -1.3051458837 -1.9565162223 7.5414834152 C19 -1.0420612912 -3.3063874325 7.2607887135 C20 -1.6733711711 -4.3224400528 7.9819573296 H21 -3.0959719386 -4.7952938491 9.5411704562 H22 -3.6721735343 -2.4077589100 9.9670922925 H23 -2.5380304814 -0.6170130270 8.7101679457 H24 -0.3264185146 -3.5572821549 6.4842696351 H25 -1.4317691468 -5.3625833852 7.7747369185 C26 4.5874142718 -2.4383406059 7.2192738554 H27 5.2993487960 -2.1865953350 8.0120183932 H28 5.1271879739 -3.0339532246 6.4755878681 C29 3.3640400566 -3.2005347382 7.8166954864 H30 3.5082922461 -3.3785098157 8.8876482899 H31 3.2110913599 -4.1780756879 7.3465600935 N32 -0.1993904364 1.5944910297 6.8693418817 O33 -0.8020465795 1.6474716887 5.6826378589 C34 0.1460967589 2.7225011752 7.4357852824 C35 0.9973417032 2.9860566865 8.6634576213 C36 1.3726548300 4.4768135425 8.5170373280 C37 0.1489404272 5.0942807816 7.8210430396 C38 -0.2526886929 4.0218966755 6.7888222182 H39 1.8689706728 2.3309694624 8.7120010776 H40 0.4140751772 2.8493153718 9.5842021280 H41 1.6059803852 4.9360045737 9.4839502011 H42 2.2601494871 4.5754233625 7.8783531967 H43 -0.6615890093 5.2335747619 8.5501257399 H44 0.3546494580 6.0679672004 7.3650258763 H45 0.3030089637 4.1367133605 5.8453381040 H46 -1.3141982907 4.0202344512 6.5162204678 C47 0.0330118367 0.2273366934 8.9623407355 H48 0.9029068236 0.7016472885 9.3969595539 H49 -0.8603903907 0.7293177550 9.3544041758 H50 0.0310512243 -0.7980266176 9.3293368304	E(B3LYP-D3/6-31+G*) = -1541.38500052949 E(B3LYP-D3/6-31+G*)(mtbe) = -1541.40901541998 E(B3LYP-D3/6-311+G**) = -1541.66977993533 G(mtbe) = -1541.33891802767
Bis-nit-2b	
C1 -0.3126560057 -1.1581649197 7.9924023536 O2 -0.0261176374 -1.9020246390 8.9088469223 C3 0.8641935685 -0.3541884815 7.2872737632 C4 2.1841458754 -0.9274770290 5.2665515719 C5 2.4374643541 -1.8460799385 4.1058008362 H6 2.6424331774 -2.8694121704 4.4430275264 H7 1.5189510128 -1.9125784271 3.5024538465	E(B3LYP-D3/6-31+G*) = -1073.59825208799 E(B3LYP-D3/6-31+G*)(mtbe) = -1073.61222411895 E(B3LYP-D3/6-311+G**) = -1073.85171168173 G(mtbe) = -1073.5104272846

C8	3.0677744168	0.2938930097	5.2051502423	
H9	2.5900576637	1.2146601275	5.5493615772	
H10	3.9601579226	0.1341348538	5.8293768429	
O11	0.5059275757	-2.2937694206	6.0065120313	
N12	1.2355016173	-1.2063853097	6.1136424616	
C13	-4.4343316488	-0.6353370526	6.8949225734	
C14	-3.7240843013	0.4369821192	7.4431057881	
C15	-2.3738704128	0.2903195998	7.7747760330	
C16	-1.7365445513	-0.9427326045	7.5717552902	
C17	-2.4531353440	-2.0248949834	7.0410431014	
C18	-3.7961345165	-1.8653701616	6.6940320639	
H19	-5.4821835942	-0.5153673960	6.6282845143	
H20	-4.2176278508	1.3914881668	7.6118937653	
H21	-1.8238908619	1.1238933905	8.2043222838	
H22	-1.9454909268	-2.9717803799	6.8836365044	
H23	-4.3458304962	-2.7022944275	6.2694056557	
C24	3.6002733925	-1.1727816666	3.3442754627	
H25	3.5547150756	-1.3508558678	2.2653148408	
H26	4.5595581460	-1.5665334385	3.7044548190	
C27	3.4780876667	0.3192742577	3.7148016009	
H28	2.6827131041	0.7913852109	3.1220464627	
H29	4.3989508988	0.8869402067	3.5474188007	
N30	0.3788422175	1.0070351348	6.8566518732	
O31	0.5332140855	1.9226783944	7.7804369752	
C32	-0.2549984359	1.2757190776	5.7455088601	
C33	-0.7899561036	2.6647108490	5.5366713726	
C34	-1.4775310059	2.6015471403	4.1563061467	
C35	-1.8586481211	1.1160848588	4.0028510647	
C36	-0.6549779289	0.3639099547	4.6112677845	
H37	0.0030059305	3.4181382951	5.6239089413	
H38	-1.4988475746	2.8902347331	6.3476843849	
H39	-2.3373281807	3.2754468295	4.0847067739	
H40	-0.7675599552	2.8874012329	3.3685127934	
H41	-2.7575004485	0.8929794373	4.5910659507	
H42	-2.0499178216	0.8193336680	2.9662857210	
H43	0.1588349958	0.3152022714	3.8708914986	
H44	-0.8832229720	-0.6581580619	4.9166320105	
C45	2.0416037980	-0.2205342033	8.2493416126	
H46	2.8148948216	0.4278779255	7.8376265800	
H47	1.7026319346	0.2048448392	9.1933116223	
H48	2.4443080847	-1.2195047838	8.4311854720	

5 References

S1 V. Dhayalan and P. Knochel, *Synth*., 2015, **47**, 3246–3256.

S2 C.-B. Miao, Y.-H. Wang, M.-L. Xing, X.-W. Lu, X.-Q. Sun, and H.-T. Yang, *J. Org. Chem.* 2013, **78**, 11584–11589.

S3 Rigaku Oxford Diffraction, (2018), CrysAlisPro Software system, Rigaku Corporation, Oxford, UK.

S4 O. V. Dolomanov, L. J. Bourhis, R. J. Gildea, J. A. K. Howard and H. Puschmann, *J. Appl. Crystallogr*., 2009, **42**; 339-341.

S5 G.M. Sheldrick, *Acta Crystallogr. Sect. A64* 2008, 112-122.

S6 G.M. Sheldrick, *Acta Crystallogr. Sect. C71* 2015, 3-8.

S7 G.M. Sheldrick, *Acta Crystallogr. Sect. A71* 2015, 3-8.

S8 C. J. Brown, R. Sadanaga, *Acta Crystallogr.,* 1965, **18**, 158.

S9 G. Odou, M. More and V. Warin, *Acta Crystallogr., Sect. A: Cryst. Phys., Diffr., Theor. Crystallogr.* 1978, **34**, 459.

S10 E. J. Gabe, Y. Le Page, F. L. Lee and L. R. C. Barclay, *Acta Crystallogr., Sect. B: Struct. Crystallogr. Cryst. Chem.* 1981, **37**, 197.

S11 M. More, G. Odou and J. Lefebvre, *Acta Crystallogr., Sect. B: Struct. Sci.* 1987, **43**, 398.